



UNIVERSIDADE D
COIMBRA

José Miguel Lopes Antunes

**FABRICATION OF NANOMATERIAL
COMPOSITE BASED LIQUID REPELLENT
FACEMASKS**

Thesis developed within the Integrated Master's Program in Biomedical Engineering with Specialization in Biomaterials supervised by Doctor Fábio Emanuel de Sousa Ferreira and Doctor Sandra Cruz, and presented to the Department of Physics of the Faculty of Sciences and Technology of the University of Coimbra

October 2021



FACULDADE DE
CIÊNCIAS E TECNOLOGIA
UNIVERSIDADE DE
COIMBRA

FABRICATION OF NANOMATERIAL COMPOSITE BASED LIQUID REPELLENT FACEMASKS

José Miguel Lopes Antunes

Thesis developed within the Integrated Master's Program in Biomedical Engineering with Specialization in Biomaterials supervised by Doctor Fábio Emanuel de Sousa Ferreira and Doctor Sandra Cruz, and presented to the Department of Physics of the Faculty of Sciences and Technology of the University of Coimbra

Coimbra, October 2021

Esta cópia da tese é fornecida na condição de que quem a consulta reconhece que os direitos de autor são pertença do autor da tese e que nenhuma citação ou informação obtida a partir dela pode ser publicada sem a referência apropriada.

This copy of the thesis has been provided on the condition that anyone who consults it is due to recognize that its copyright rests with its author, and that no quotation from the thesis and no information derived from it may be published without proper acknowledgement.

Agradecimentos

Em primeiro lugar, quero deixar uma palavra de agradecimento ao Professor Doutor Fábio Emanuel de Sousa Ferreira e à Doutora Sandra Cruz tanto pela orientação e apoio durante a elaboração deste projeto, assim como por toda a sua disponibilidade e prontidão em esclarecer quaisquer dúvidas.

Agradeço ao Departamento de Engenharia Mecânica da Universidade de Coimbra por tornar possível a implementação desta tese, nomeadamente a disponibilização do laboratório e equipamento necessário para a realização das deposições.

Agradeço aos colaboradores do Departamento de Engenharia Química da Universidade de Coimbra, do Instituto Pedro Nunes e à Doutora Isabel Carvalho da Universidade do Minho que disponibilizaram o seu tempo para efetuar a caracterização das amostras obtidas no decorrer deste projeto, e também agradeço a sua disponibilidade para me ajudar na interpretação dos resultados sempre que foi necessário.

Agradeço ao Alireza Vahidi pela sua disponibilidade para me ajudar a entender como trabalhar com o equipamento de pulverização catódica na fase inicial do projeto.

Agradeço profundamente à minha família por todo o apoio e motivação durante o meu percurso académico, bem como o amor e dedicação ao longo de toda a minha vida.

Por fim, quero agradecer a todos os meus amigos presentes durante todo este meu percurso, que contribuíram tanto para a minha formação pessoal como académica, um muito obrigado a todos eles.

Resumo

Com o aparecimento da pandemia Covid-19, ficou ainda mais visível a necessidade da existência de superfícies antimicrobianas, especialmente em contextos hospitalares. Os têxteis médicos são das superfícies mais complicadas de modificar, uma vez que o seu uso típico envolve contacto direto com o corpo humano, e conseqüentemente, existem vários aspetos a serem melhorados, tais como o tempo de utilização, capacidade antibacteriana e antivírica ou hidrofobicidade. Com esta finalidade, várias técnicas têm sido usadas na modificação superficial de têxteis, sendo a Pulverização Catódica uma das técnicas em crescimento nos últimos anos de modo a conseguir dar capacidades hidrofóbicas e antibacterianas aos têxteis. Neste projeto foi analisado e discutido como a utilização da pulverização catódica para a aplicação de um filme de Diamond-like Carbon (DLC) dopado com nanopartículas de prata (AgNPs) em têxteis comuns (algodão, formato jersey e TNT) se comporta, tendo sido concluído que não só os revestimentos têm uma boa adesão a este tipo de tecidos, mas também é possível conferir propriedades hidrofóbicas e antibacterianas a estes tecidos, com o algodão a ter resultados especialmente positivos.

Palavras-Chave: Têxteis Médicos, Superfícies Antibacterianas, Hidrofóbico, Pulverização Catódica, Filmes de DLC/Ag

Abstract

The Covid-19 pandemic has, even more, highlighted the need for antimicrobial surfaces, especially those used in a healthcare environment. Medical textiles are one of the most difficult surfaces to modify since their typical use is in direct human body contact, and, consequently, some aspects need to be improved, such as wear time, antibacterial and anti-viral capacity, or hydrophobicity. To this end, several techniques have been used for the surface modification of textiles, being Magnetron Sputtering (MS) one of those that have been growing in the last years to meet the antimicrobial and hydrophobic objectives. In this work it was analysed and discussed how the utilization of the MS technique to apply a Diamond-like Carbon (DLC) doped with silver nanoparticles (AgNPs) coating on common textiles (cotton, jersey format and TNT) performs, being concluded that not only the coating had a good adhesion to this type of textiles, but also that it is possible to provide antibacterial and hydrophobic properties to these textiles, with especially positive results for the cotton fabric.

Keywords: Medical Textiles, Antibacterial, Hydrophobic, Magnetron Sputtering, DLC/Ag films

Table of Contents

List of Figures	1
List of Tables	4
Abbreviations List	6
1.Introduction.....	9
2.State of the Art.....	11
2.1 Infectious Diseases.....	11
2.1.1 Transmission Routes.....	12
2.1.2 Viruses Mechanisms	12
2.2 Medical Textiles	13
2.2.1 Textiles problematic	14
2.2.2 Textile Antimicrobial Enhancement	15
2.2.2.1 Antimicrobial Textile mode of action	15
2.2.3 Facial Masks	15
2.2.3.1 Types of masks	17
2.3 Antimicrobial Agents	19
2.3.1 Antimicrobial mode of action	20
2.3.1.2 Drug resistant bacteria	21
2.3.2 Silver and Silver Nanoparticles.....	21
2.3.2.1 Cytotoxic Effect	22
2.3.2.2 Silver Ions and Nanoparticles release.....	23
2.3.3 Environmental Impact.....	23
2.4 Surface Modifications of textiles	24
2.4.1 Magnetron Sputtering in textile functionalization.....	24
2.4.1 Diamond-like carbon coatings	25
2.4.2 DLC coating with Nanoparticles.....	26
3.Methods and Procedures.....	26
3.1 Materials	26
3.1.1 Fabrics	27
3.1.2 Films	27
3.1.3 Samples preparation	27
3.2 Magnetron Sputtering Process.....	28
3.3 Characterization Techniques.....	30
3.3.1 Transmission electron microscopy	30
3.3.2 X-Ray Diffraction	31
3.3.3 Scanning Electron Microscopy and Energy Dispersive Spectroscopy.....	32
3.3.4 Antibacterial Test – Zone of Inhibition Test.....	33
3.3.5 Contact Angles Analysis.....	34
4. Results and Discussion.....	35

4.1 Fabrics-Deposition Interaction.....	35
4.1.1 First Series of Depositions.....	35
4.1.1.1 Comparison between fabrics: SEM images	38
4.1.1.2 Comparison by Ag %: SEM and TEM images.....	40
4.1.1.3 Contact Angle and Antibacterial Results.....	43
4.1.2 Second Series of Depositions	45
4.1.2.1 SEM images	46
4.1.2.2 Antibacterial tests analysis	52
4.1.2.3 Contact angles analysis.....	58
4.2 Overall Discussion	59
5. Conclusion and Future Research.....	61
6. References	63
Annex I	69

List of Figures

Figure 1 - History of viruses. (a) Threat of viral diseases to humanity at various years with number of human deaths. (b) Timeline of recent highly infectious viruses such as SARS, Swine Flu, MERS, and COVID-19 [2].	11
Figure 2 - Image illustrating common transmission pathways of respiratory diseases [13].	12
Figure 3 - Structure of virus and mechanistic action. (a) Structure of a coronavirus. (b) Relative size of various pathogens. (c) Mechanism to invade a cell via a virus. (d) Surface addition of viruses via electrostatic interaction [2].	13
Figure 4 - Relative size chart of common airborne contaminants and pathogens [1].	16
Figure 5 - Representation of the basic cloth homemade masks [26].	17
Figure 6 – Typical surgical mask and respective illustration showing the function of each individual layers [1], [26].	18
Figure 7 - Schematic representation of the N95 mask with various layers [26].	19
Figure 8 - Schematic overview of the nanosilver effect on surfaces [41].	22
Figure 9 – Substrate holder prepared for the deposition process.	28
Figure 10 – Magnetron Sputtering machine scheme.	29
Figure 11 - Schematic drawing of a transmission electron microscope [73].	31
Figure 12 - Schematic representation of the Bragg equation [75].	32
Figure 13 – a) Schematic of the SEM process [77]; b) Photography of the SEM/EDS machine used to obtain the first set of images [74].	33
Figure 14 - Schematic of a typical zone of inhibition test [79].	34
Figure 15- Representation of a liquid drop on solid surface and the respective equation that connects the surfaces tensions and angles between them [74].	34
Figure 16 - EDS graphic correspondent to the series of depositions varying the power given to the Ag target.	Erro! Marcador não definido.
Figure 17 – XRD Analysis of Sample 16 with reference markers for Ag possible values	37
Figure 18 – XRD Analysis of Sample 15 with reference markers for Ag possible values	37
Figure 19 - SEM images of three different substrates coated with an AG-DLC film (4 at% Ag) with different magnifications (100x and 5000x): a,b) Cotton, c,d) Jersey Format and e,f) TNT	39
Figure 20 - SEM images of three different substrates coated with an AG-DLC film (10 at% Ag) with different magnifications (100x and 5000x): a,b) Cotton, c,d) Jersey Format and e,f) TNT	40
Figure 21 - TEM images and SEM images (10k magnification) of four different substrates uncoated and coated with an AG-DLC film (5 at% and 10 at% Ag): a) Virgin Cotton, b) 5 at% Ag Cotton, c) 10 at% Ag Cotton, d) Virgin Jersey Format, e) 5 at% Ag Jersey Format, f) 10 at% Ag Jersey Format, g) Virgin TNT, h) 5 at% Ag TNT, i) 10 at% Ag TNT, j) 5 at% Ag Silicon, k) 10 at% Ag Silicon, l) TEM image 5 at% Ag, m) TEM image 10 at% Ag.	41
Figure 22 - SEM images (10k and 20k magnification) of four different substrates coated with an AG-DLC film (10% Ag): a) Cotton 10k mag., b) Jersey Format 10k mag, c) Silicon 10k mag, d) TNT 10k mag, e) Jersey Format 20k mag, f) TNT 20k mag.	43
Figure 23 - Images of the Antibacterial tests carried out on silicon (deposition 16): a) Klebsiella pneumoniae bacteria was used; b) Staphylococcus aureus bacteria was used.	45
Figure 24 - SEM images (50k magnification) of three different substrates corresponding to deposition 24/25 (10 at% Ag) and 26/27 (12 at% Ag) a) Cotton – deposition 24/25., b) Cotton - deposition 26/27, c) Jersey Format - deposition 24/25, d) Jersey Format - deposition 26/27, e) TNT - deposition 24/25, f) TNT - deposition 26/27.	47

Figure 25 - SEM images (50k magnification) of three different substrates corresponding to deposition 28/29 (8 at% Ag) and 30/31 (13 at% Ag) a) Cotton – deposition 28/29., b) Cotton - deposition 30/31, c) Jersey Format - deposition 28/29, d) Jersey Format - deposition 30/31, e) TNT - deposition 28/29, f) TNT - deposition 30/31.	48
Figure 26 - SEM images (50k magnification) of three different substrates corresponding to deposition 32/33 (15 at% Ag) and 34/35 (23 at% Ag) a) Cotton – deposition 32/33., b) Cotton - deposition 34/35, c) Jersey Format - deposition 32/33, d) Jersey Format - deposition 34/35, e) TNT - deposition 32/33, f) TNT - deposition 34/35.	49
Figure 27 - SEM images (50k magnification) of two different substrates corresponding to deposition 36/37 (20 at% Ag) a) Cotton – deposition 36/37., b) TNT - deposition 36/37.	50
Figure 28 - SEM images (50k magnification) of three different substrates corresponding to deposition 26/27 (12 at% Ag) and 30/31 (13 at% Ag) a) Cotton – deposition 26/27., b) Cotton - deposition 30/31, c) Jersey Format - deposition 26/27, d) Jersey Format - deposition 30/31, e) TNT - deposition 26/27, f) TNT - deposition 30/31.	51
Figure 29 - SEM images (50k magnification) of two different substrates corresponding to deposition 34/35 (23 at% Ag) and to deposition 36/37 (20 at% Ag): a) Cotton – deposition 34/35, b) Cotton - deposition 36/37, c) TNT – deposition 34/35, d) TNT – deposition 36/37.	52
Figure 30 – Zones of inhibitions test images of virgin samples: a) klebsiella pneumoniae bacteria, b) staphylococcus aureus bacteria	53
Figure 31 – Zone of inhibition tests images of all samples for both bacteria, klebsiella pneumoniae on the left column and Staphylococcus aureus on the right column: a/b) Sample 24, c/d) Sample 26, e/f) Sample 28, g/h) Sample 30, i/j) Sample 32, k/l) Sample 34, m/n) Sample 36.....	54
Figure 32 – SEM images of virgin cotton and cotton from sample 26 after the zone of inhibition test: a) Virgin cotton - klebsiella pneumoniae, b) Virgin cotton - staphylococcus aureus, c) Cotton 26 - klebsiella pneumoniae, d) Cotton 26 - staphylococcus aureus.	55
Figure 33 - SEM images of virgin jersey format fabric and jersey format fabric from sample 26 after the zone of inhibition test: a) Virgin jersey format - klebsiella pneumoniae, b) Virgin jersey format - staphylococcus aureus, c) jersey format 26 - klebsiella pneumoniae, d) jersey format 26 - staphylococcus aureus.	56
Figure 34 - SEM images of virgin TNT and TNT from sample 26 after the zone of inhibition test: a) Virgin TNT - klebsiella pneumoniae, b) Virgin TNT - staphylococcus aureus, c) TNT 26 - klebsiella pneumoniae, d) TNT 26 - staphylococcus aureus.	57
Figure 35 – SEM images of the substrates of sample 26 after the antibacterial test: a) cotton, b) jersey format, c) TNT.	58

List of Tables

Table 1- Description of community masks fabric samples tested regarding air permeability, resistance to water absorption and filtration by particle size [31].	18
Table 2 - Chemical structure and action modes of the main antimicrobial agents, as well as the main fibers in which they are used [4].	20
Table 3 – Parameters varied during the deposition process.	30
Table 4 – Parameters used in the depositions: variation of the power given to the Ag target and respective Ag at%.	36
Table 5 - Parameters used in the depositions: variation of the power given to the C target and respective Ag at%.	36
Table 6 – Contact Angle results for Cotton, Jersey Format and TNT. These results are correspondent to a surface-water analysis.	44
Table 7 - Parameters used in the second series of depositions and respective Ag at%.	46
Table 8 - Contact Angle results for Cotton, Jersey Format and TNT. These results are correspondent to a surface-water analysis.	59
Table 9 – Summary of the results obtained in EDS, SEM and Antibacterial Tests	59

Abbreviations List

AgNPs - Silver nanoparticles

HAIs - Healthcare associated infections

HCW – Healthcare workers

PPE – personal protective equipment

TNT – Non-woven fabric

ASTM – American Society of Testing and Materials

PFE – Particulate Filtration Efficiency

BFE – Bacterial Filtration Efficiency

DP – Differential Pressure

DLC – Diamond-like Carbon

PVD – Physical Vapor Deposition

CAPVD - Cathodic Arc Physical Vapor Deposition

HiPIMS - High-power Impulse Magnetron Sputtering

DC – Direct Current

MS - Magnetron Sputtering

Ppm -Parts per million

NPs – Nanoparticles

W – Watts

Ag – Silver

DLC – Diamond-like carbon

C - Carbon

Cu – Copper

CuO – Copper Oxide

ZnO – Zinc Oxide

TiO₂ – Titanium Dioxide

AgDLC - Silver doped DLC

Pa – Pascal

s – Seconds

EDS - Energy-dispersive X-ray spectroscopy

SEM – Scanning Electron Microscopy

TEM - Transmission electron microscopy

XRD - X-ray powder diffraction

PP - Polypropylene

1.Introduction

Infections have been a major source of concern for human health in recent decades, and as the globe becomes increasingly connected, this threat is no longer speculative but very real. Pathogens that may spread from person to person are more likely to produce a global epidemic, and the Covid-19 Pandemic is a great illustration of this problem[1]. The best way to prevent an infectious disease spread via the respiratory way, when social distancing is not possible, is the use of personal protective equipment (PPE). PPEs, like masks, aprons, gowns, coveralls, goggles, and respirators, are considered critical components that can be used to protect not only healthcare workers but also the general population [1,2]. In addition, numerous pathogens, such as fungus, bacteria, and viruses, can be present in hospital facilities, pathogens that can be transported by any person that frequent this kind of facility [1–3]. It is expected that by 2030 the healthcare industry worldwide will employ around 80 million people, putting a huge amount of healthcare workers at constant exposure to fungi/bacteria/viruses and getting infections while treating infected people with highly infectious diseases [2]. PPEs like surgical masks and medical clothing are crucial to offering a barrier between the users and the environment surrounding them [2,3]. Moreover, the emergence of drug-resistant microorganisms is another issue that has been seen in hospital settings. Microorganisms, for instance bacteria, play an important role in the global cycling of elements, having a profound impact on the environment in which they live. However, they are also susceptible to the environment, which means that when they come into contact with antimicrobial elements, some microorganisms may develop resistance to them, resulting in the emergence of "multi-drug-resistant" bacteria [4].

When considering masks, several options are available, such as homemade face masks, surgical face masks, and respirators [4]. A few properties have to be taken in consideration when evaluating masks' performance: comfort, breathability, biocompatibility, fluid resistance, flammability, and filtration efficiency [1,2]. And it is with those properties in mind that masks are manufactured.

The PPEs available, particularly facial masks have shown a few problems. When studying patients infected with the influenza virus, surgical masks were showed to be highly effective in blocking virus-containing particles with bigger sizes ($\geq 5\mu\text{m}$) but less effective for smaller particles [1,2]. Some masks and respirators are made of materials like cotton and synthetic fabric, which have larger pore sizes and, therefore, will not be very effective in filtering tiny virus-laden droplets, pathogens, and nanosized contaminants [1,2]. Another concern is the negative impact that non-reusable PPEs brings to the environment. Recent research studies shown that healthcare workers worldwide used more than 44 million non-reusable PPEs every day during the COVID-19 pandemic. Most of these PPEs have their composition polypropylene, which is a cheap material and has good performance characteristics; however, these kinds of PPEs are of single-use and are normally incinerated or sent to a landfill aggravating the environmental impact [2,4].

To improve the efficiency of facial masks and other medical textiles, several studies have been performed, like employing modified filter layers, for instance, nanofibers, or by modifying the filter surfaces by adding materials with antimicrobial capabilities to improve their efficiency [3]. It is proven that adding antimicrobial agents to these products is a highly effective way to prevent infections caused by various pathogens through the inhibition of viruses, fungi, and bacteria [2]. There are different

chemical and physical methods to promote superficial changes in fabrics. Although the most used ones are solution-based processing, other methods have been attracted a lot of attention in the last years, like physical vapor deposition (PVD) methods [5–7]. The PVD technology has been implemented to modify various material surfaces, with particular attention to textiles. Several kinds of coatings can be obtained to modify the textile surface, but to introduce the hydrophobic character without toxicity, diamond-like carbon (DLC) is the most appropriate [8]. The antimicrobial feature is expected to be gained by doping the DLC with silver nanoparticles (AgNPs) in a non-toxic amount [9,10].

In this thesis, it will be analysed how DLC doped with AgNPs coatings can be an efficient approach to transform textiles commonly used in biomedical applications, a coating that will be deposited by using a Magnetron Sputtering process. The main focus will be to test if it is possible to give antibacterial and hydrophobic properties to the chosen textiles. Also, as a result of this thesis, a scientific article named “Carbon-based coatings in medical textiles surface functionalisation: the overview” was produced, an article focused on the current state of the art available on textile functionalisation techniques. The article is displayed in the annex section of this thesis.

2.State of the Art

2.1 Infectious Diseases

In the past few decades, infections have become a point of concern to human health (see *Figure 1*), and as the world is getting more interconnected by the day, this threat is no longer theoretical, but a very real one. Pathogens with the ability of human-to-human transmission can more easily cause a worldwide outbreak, and the Covid-19 Pandemic is the perfect example of this problem [1]. By October of 2021, more than 200 million confirmed cases and more than 4.5 million confirmed deaths have been caused by the Covid-19 pandemic, as reported by the World Health Organization.

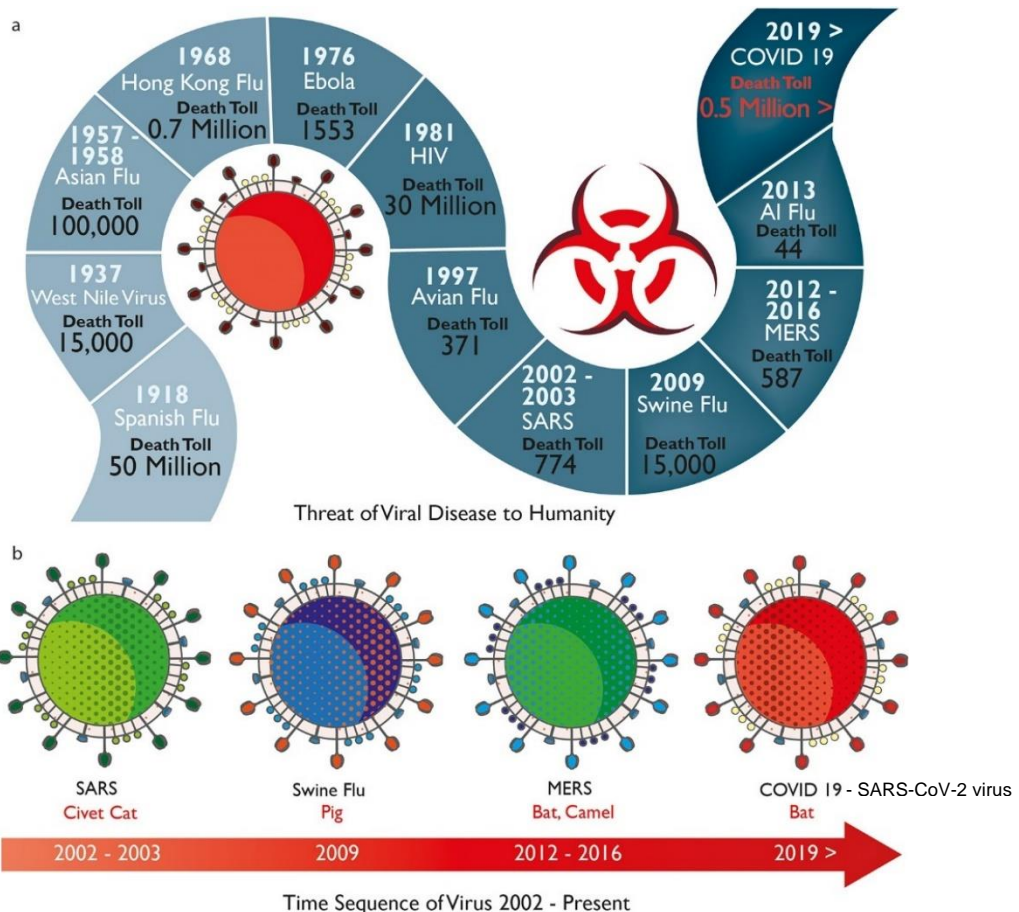


Figure 1 - History of viruses. (a) Threat of viral diseases to humanity at various years with number of human deaths. (b) Timeline of recent highly infectious viruses such as SARS, Swine Flu, MERS, and COVID-19 (Modified from source) [2].

But it is not only viral diseases that are a concern for human health. Healthcare associated infections (HAIs), which are infections acquired while receiving treatment in a hospital or other health care facility, also present a threat [11]. Infections like urinary tract infections, pneumonia, bloodstream infections and gastrointestinal infections are

the most common type of HAIs, and there are several sources for their occurrence: person-to-person transmission, medical equipment or devices, healthcare personnel, contaminated drugs and food. Medical textiles, which are very relevant for this project, are considered one of the possible vehicles of transmission [11,12].

2.1.1 Transmission Routes

A virus can spread via aerosols generated by coughing and sneezing in the air, by vectors such as insects, or by the transmission of body fluids such as saliva, blood, or semen [2]. In particular, for respiratory pathogens, they can be transmitted via droplets. When an infected person talks, sneezes, cough or exhales, viruses are released, and they can be found in particles of varied sizes that can contaminate mucosalivary droplets [2]. These droplets can spread the viruses through three different methods; airborne, contact and fomites, as shown in *Figure 2* [3].

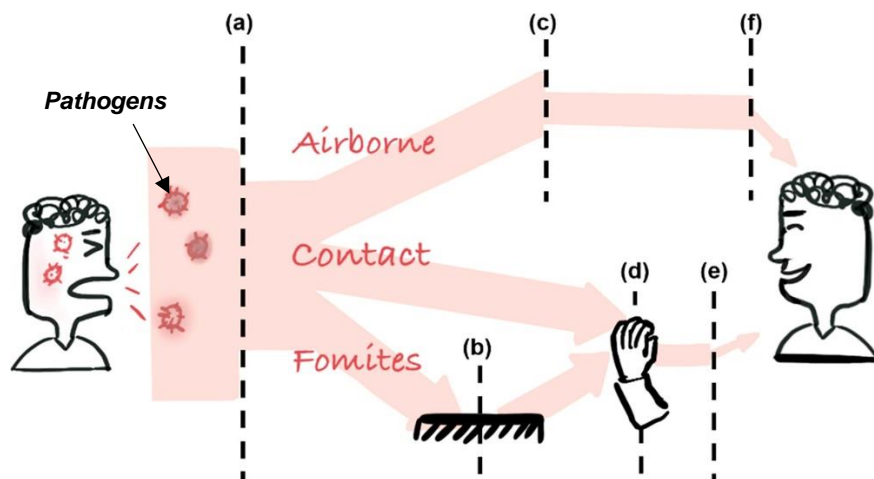


Figure 2 - Image illustrating common transmission pathways of respiratory diseases (Modified from source) [13].

Airborne transmission results in direct infection due to the inhalation of droplets in the air [3]. Contact transmission may be direct, as for example through a handshake, or may be indirect through fomites. Fomites are an indirect method whereby the droplets land on a surface and are then transmitted to an individual. For example a door handle or a escalator [2,3,13].

2.1.2 Viruses Mechanisms

Viruses are extremely small infectious agents (~20–400 nm), and are dependent on “host cells” of other living organisms to survive, thrive, and reproduce and cannot function or replicate on their own outside of a host cell [2]. Physical adsorption and electrostatic interactions are the two main mechanisms for viral adsorption on surfaces, and the more time a virus stays in a surface, higher is the amount of virus adsorbed. To reduce viral

infection the amount of time the virus interacts with a material should be decreased, or another way is to have materials with surface properties which are unfavourable for viruses, like having antibacterial agents present on the surface [2,14,15]. Figure 3 demonstrates how a virus is structured and how it interacts with a surface.

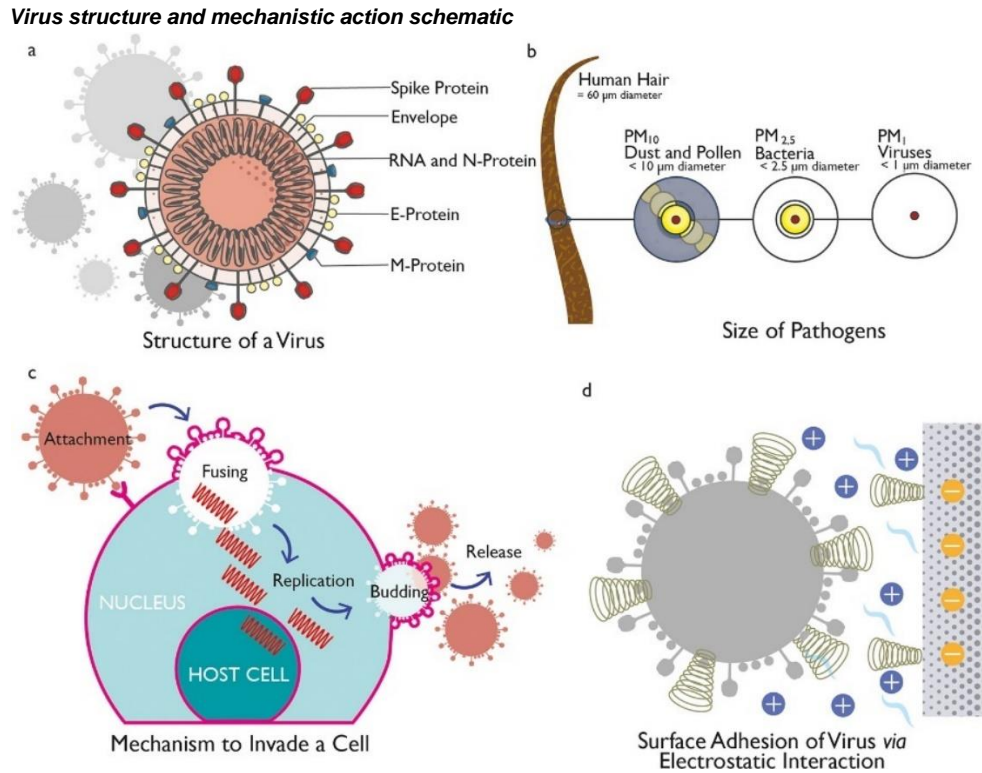


Figure 3 - Structure of virus and mechanistic action. (a) Structure of a coronavirus. (b) Relative size of various pathogens. (c) Mechanism to invade a cell via a virus. (d) Surface addition of viruses via electrostatic interaction (Modified from source) [2].

2.2 Medical Textiles

Medical textiles are considered as technical textiles, a textile material and product manufactured mainly for its technical and performance characteristics rather than its artistic or ornamental features [16]. Depending on the final product, there are many different types of fibers used in technical textiles. For example, natural fibers that are characterized by high modulus/strength, moisture intake, low elasticity and elongation, or synthetic fibers, like nylon, polyester, and PP, which possess high modulus/strength and elongation with an acceptable elasticity and comparatively low moisture intake [16]. By combining different kinds of fibers with functional finishing processes, it is possible to create tailor-made textiles with an improved performance when compared with conventional textiles. This is the case for many medical textiles [17].

Medical textiles are used in the manufacturing of PPEs and other medical applications, with the main purpose of mitigate the risks of exposure to hazardous and contagious substances. There are several different types of medical clothing products, including

coveralls, footwear covers, full body suits, gloves, independent sleeves, scrubs, surgical gowns, surgical masks, and scrub hats. Moreover, medical textiles can also be used in the manufacture of bedding textiles and drapes present in healthcare facilities [2].

Depending on their functionality and purpose, a huge variety of textiles can be used in the production of the examples mentioned above. In the case of disposable medical textiles like surgical masks or surgical gowns, they are usually made of synthetic fibers because of their better liquid barrier properties. In the case of scrubs, woven fabrics typically made from cotton or polyester/ cotton blends are commonly used [2,18].

In this project, the three textiles focused on were TNT, cotton, and jersey format. TNT is a type of textile created by connecting a mass of fibers using heat, chemical, or mechanical methods, rather than intertwining fibers like in traditional textiles. TNTs are very popular for medical clothing, in particular for disposable medical clothing, because of its comparatively low cost and speed of production, as well as its excellent levels of sterility and infection control, which are critical in such applications. Such nonwoven fabrics are typically made from PP [1,2,18].

Woven textiles made from pure cotton or polyester-cotton blends, such as jersey textiles, when compared with TNTs have worst barrier properties against liquids and bacteria, although they normally provide a better wearer comfort to the user and are able of sustaining several washing/cleaning processes, giving them a reusability property that TNTs usually fail to have. Moreover, nowadays sustainability and environmental factors must be considered, and more eco-friendly alternatives like natural fibers, are a good alternative to synthetic fabrics like TNT. Cotton is an excellent example of natural fibers that may be utilized to make medical clothing, not only because it is a sustainable material, but also because it is biodegradable, renewable, and lightweight [2,16,19].

2.2.1 Textiles problematic

Microbial contamination is of great concern, especially for textiles used in hospitals. Due to their large surface area and ability to retain moisture, textiles promote the growth of microorganisms such as bacteria and fungi, which can be found almost everywhere and are able to quickly multiply under certain circumstances. The growth of microorganisms on textiles causes several undesirable effects, not only on the textile, but also on the user. Effects such as generation of unpleasant odours, diminish mechanical strength, stains, discoloration and increased chance of user contamination [4].

Another problem usually associated with the use of textiles is the transmission of liquid through them. The transmission of liquid through textile materials could be described by two interchangeable but fundamentally different terminologies: penetration and permeation. Penetration involves the flow of gas, vapor, or liquid through a porous material, whereas permeation involves the diffusion of gas or vapor through a porous material. Penetration and permeation usually take place due to a pressure gradient and concentration gradient across the barrier, respectively. Pathogens are larger in size than gas and vapor molecules and are believed to penetrate and not permeate through materials. The coronavirus, which causes COVID-19, has been found to be transmitted via aerosols, being able to penetrate some textiles [2,20].

2.2.2 Textile Antimicrobial Enhancement

To provide antimicrobial ability to textiles, there are different approaches being studied and applied, such as: inclusion of antimicrobial compounds in the polymeric fibres that can leach from the polymeric matrix, grafting of certain moieties onto the polymer surface or the physical modification of fibres surface [4,21]. Some studies have reported that just by modifying the surface properties of a material, such as free energy, polarity or topography, it is possible to decrease the bacterial adhesion to the surface, during the initial stage of the biofilm formation process, without using chemical antimicrobial agents. Those modifications may create new functional groups and/or change the surface roughness [4].

Providing healthcare workers (HCWs) with protection from contaminated body fluids and other hazardous substances from infected patients is important, and there are specialised finishes that can be applied to medical textiles in order to provide protective effects. Finishes with the ability to repel fluids, for example, can be used to create barriers capable of preventing adsorbed fluids from penetrating fabrics [2].

Any antimicrobial treatment performed on a textile needs to satisfy certain requirements besides being efficient against microorganisms, being the main challenge being non-toxic to the consumer. It should not be cytotoxic or cause allergies, irritations and sensitization [4,21]. Besides the non-cytotoxic effect on users and efficiency against microorganisms requirement, antimicrobial treatments performed on textiles also need to be suitable for textile processing, present durability to laundering, dry cleaning and hot pressing, be environmentally friendly and should not damage the textile quality or appearance [4,22].

2.2.2.1 Antimicrobial Textile mode of action

Depending on the antimicrobial treatment applied on the textile, the textile may act by two different ways – contact and/or diffusion. In the case of contact mode, the antimicrobial agent is placed on the fiber and does not disperse, only acting when microorganism contact the textile surface. In the case of diffusion, the antimicrobial agent is on the fiber surface or in the polymeric matrix, needing to migrate from the textile to the external medium to attack the microorganisms [4].

Products containing silver are interesting materials for wound repair textile membranes, as metallic silver reacts with the moisture on the skin surface or with wound fluids, causing silver ions to be released and damage the bacterial DNA and RNA, inhibiting their replication. In addition, textile products with a sustained silver release may also manage wound exudates and odour [4,23].

2.2.3 Facial Masks

The best way to prevent an infectious disease spread via the respiratory route, when social distancing is not possible, is the use PPEs. PPEs like masks and respirators provide a physical barrier to respiratory droplets, both from the user, as well as from other people around.[1] There are several studies that verify the importance of PPEs in controlling the spread of viruses and bacteria. In a survey conducted in Hong Kong hospitals, it was found that wearing masks was the single most important protective measure in lowering the chance of getting infected when contacting infected people [1].

Also, a modelling study based on COVID-19 infection data gathered in New York and Washington suggested that a generalised mask use by the population can significantly reduce community transmission rate and death toll [1,24].

Masks filtering efficiency, and by consequence the level of protection against pathogens and pollutants, depends on the mask design and materials used in its manufacturing. Contaminants and pathogens in the air vary greatly in size, as shown in *Figure 4*. For example, the SARS-CoV-2 has a size ranging from 60 to 140 nm, which is smaller than many other contaminants like dust, pollen or bacteria [1].

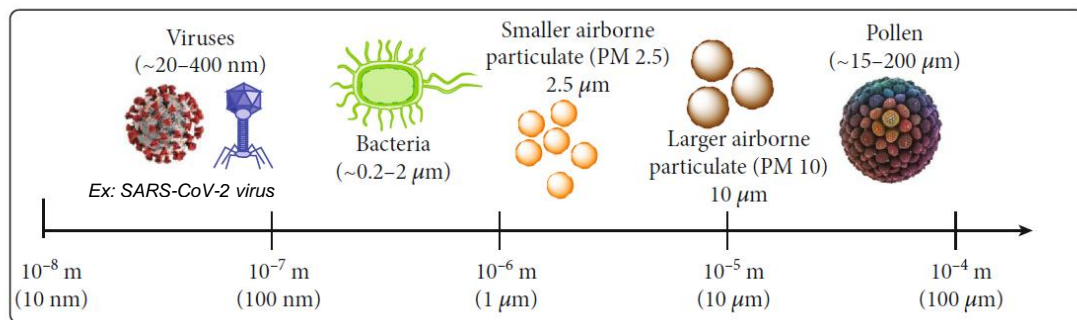


Figure 4 - Relative size chart of common airborne contaminants and pathogens (Modified from source) [1].

This size range brought up a few problems, as some masks and respirators are made of materials like cotton and synthetic fabric, which have larger pore sizes and therefore will not be very effective in filtering tiny virus-laden droplets, pathogens and contaminants of such a small size [1,25].

There are several mechanisms that affect masks filtering capacity: gravity sedimentation, inertial impaction, interception, diffusion and electrostatic attraction and thermal rebound [26,27]. Furthermore, masks may become viruses collectors during repeated breathing cycles particularly when its outer surface is exposed to contaminated droplets. As most masks do not have surfaces with antibacterial/antiviral properties, viruses and bacteria will stay on the surface and in the masks for a considerably long period of time. To make matters worse, during the respiration cycle it is created an environment of high humidity and temperature, causing the formation of steam that will accelerate the mechanism of penetration and faster spread of microorganisms to the inner parts of the mask [26,28,29]. So, achieving masks with higher filtration capacity, optimal comfort, as well as high efficiency in eliminating microorganism is extremely important [26].

In order to evaluate which materials are suitable to be used in face masks, the American Society of testing and Materials (ASTM) identified five performance characteristics required for materials used in medical face masks: particulate filtration efficiency (PFE), bacterial filtration efficiency (BFE), differential pressure (DP), fluid resistance and flammability [1].

PFE measures the filtration efficiency of face masks against monodisperse particles under a constant airflow rate. BFE quantifies the performance of the mask material in filtering out bacteria. DP measures the air flow restriction through the mask, providing information of the mask's breathability. Fluid resistance evaluates the mask's ability to prevent the transfer of fluids from its outer and inner layers due to splashing or spraying. Relatively to flammability, as hospitals contain various sources of ignition, such as heat,

oxygen and fuel sources, it is required that the flammable mask materials do not pose additional risks to the wearer due to speed and intensity of flame spreading [1].

2.2.3.1 Types of masks

There are several types of masks available on the market, but there are three types of masks that are of particular interest when considering textiles: homemade masks, surgical masks and N95 respirators. When comparing these three types of masks, homemade masks are affordable, have a high comfortability, are reusable and have reasonable breathability, however they have low efficiency and low sealing and fit. Surgical face masks are affordable, have a high comfortability and a reasonable breathability, however they only have moderate efficiency, are non-reusable and low sealing and fit. N95 respirators are the most efficient and have the better sealing and fit, but they are more expensive, more uncomfortable, have lower breathability and are non-reusable [1,26].

During the Covid-19 pandemic, homemade masks, like the one in *Figure 5* were firstly recommended for community use so that medical masks could be prioritized for healthcare professionals [30]. Their efficiency depends on the materials used, as well as on the number of layers. Tests were performed to assess the filtration capacity and breathability/ air permeability of some common household fabrics, with potential to be used as homemade masks materials *Table 1*. The filtration efficiency took into consideration the quantification, by size classes (0.5-5 μm), of the percentage of particles in the aspired air that passed through each fabric. When considering both filtration capacity and breathability, the two-layered TNT and jersey format knit were the ones with the best performance [31].



Figure 5 - Representation of the basic cloth homemade masks (Modified from source) [26].

Table 1- Description of community masks fabric samples tested regarding air permeability, resistance to water absorption and filtration by particle size, with two of the textiles of interest identified (Modified from source) [31].

Fabric sample	Air permeability (L/min)	Filtration by particle size (%)				
		0.5 μm	0.7 μm	1 μm	3 μm	5 μm
Nonwoven; 81 g—one layer	55	13	12	19	58	75
Nonwoven; 160 g—two layers	29	20	24	26	71	85
Plain weave woven (100% cotton); 120 g—two layers	3.9	28	39	42	66	79
Plain weave woven (70% polyester/30% cotton); 100 g—two layers	14.4	10	15	17	46	62
Oxford shirt woven (100% cotton); 130 g—two layers	5.2	21	29	32	64	69
Jersey T-shirt knit (100% cotton); 150 g—two layers	10.6	16	23	27	77	89
Flax shirt woven (100% flax); 145 g—two layers	60.0	10	15	17	53	70
Denim twill (100% cotton); 270 g—one layer	1.3	16	21	24	44	47
Plain weave denim (100% cotton); 310 g—one layer	7.5	11	13	13	25	31
Plain weave denim (lyocell); 160 g—one layer	34.7	9	12	13	29	37
Plain weave denim (lyocell); 320 g—two layers	16.7	7	16	20	49	58

The surgical masks, also called 3-ply surgical Mask, is the most commonly used mask during the present COVID-19 pandemic. This type of mask is made up of three different layers of TNT fabrics, with each layer having a specific function (see Figure 6).

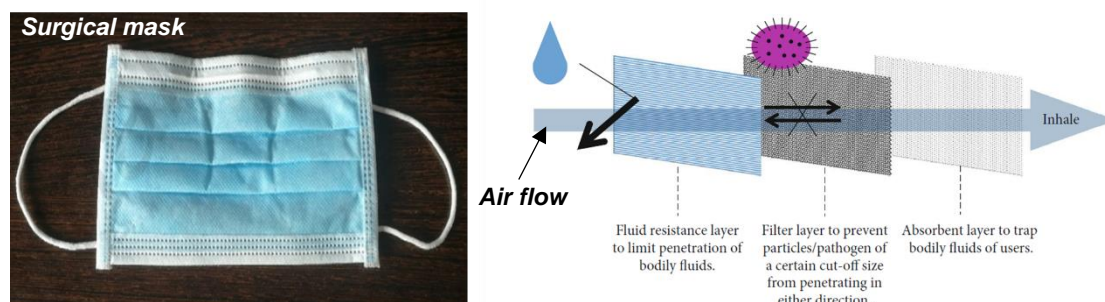


Figure 6 – Typical surgical mask and respective illustration showing the function of each individual layers (Modified from source) [1,26].

The outermost layer (typically blue) has hydrophobic characteristics, helping in repelling fluids such as mucosalivary droplets, the middle layer is a filter which its main purpose is preventing the penetration of particles or pathogens of a certain size in either direction and the innermost layer is made of absorbent materials so that it is capable of absorbing mucosalivary droplets of the user and moisture of the exhaled air [1].

The N95 respirator, as shown in Figure 7, typically consists of four different layers, three of TNT fabric like the surgical mask and an additional layer of modacrylic fabric. Both the external and internal layers (made of nonwoven Polypropylene (PP)) act as hydrophobic layers, helping to avoid the moisture absorbed by the respirator. The intermediate layers' function, on the one hand, as support to provide thickness and shape (made of modacrylic) to the equipment, and on the other hand, filtering (made of nonwoven PP) dangerous particles to the user [3]. In addition to that, they may also have a ventilator fan in order to increase the breathability and diminish the creation of steam inside it. The

word N95 is obtained from the fact that these types of masks can at least filter 95% of aerosols around 0.3 μm [26,32].

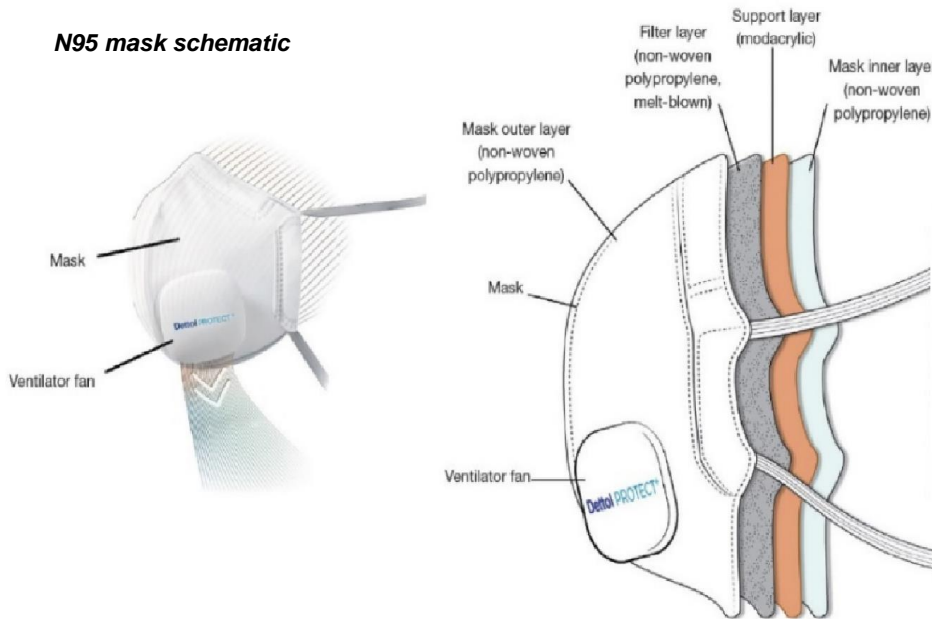
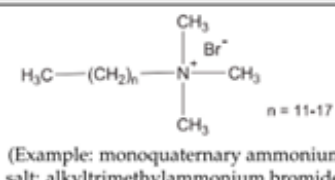
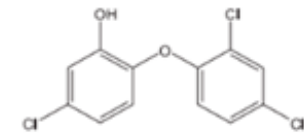
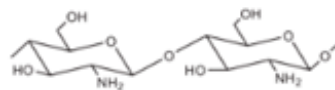
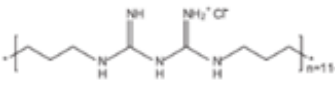
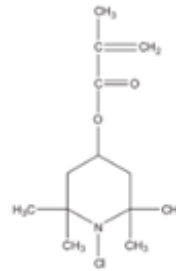


Figure 7 - Schematic representation of the N95 mask with various layers (Modified from source) [26].

2.3 Antimicrobial Agents

Most of the antimicrobial agents used in commercial textiles, like cotton, are biocides acting in different ways according to their chemical and structural nature and affinity level to certain target sites within microbial cells. Depending on the biocide, the action mode is different, and in this project, the biocide of greater interest is in the category of metals and metallic salts: Ag. Non-essential metals, like Ag, can be extremely toxic to most microbes, even in lower concentrations, and due to their biocidal activity, they have been widely used as antimicrobial agents in textiles [4,33,34].

Table 2 - Chemical structure and action modes of the main antimicrobial agents, as well as the main fibers in which they are used (Modified from source) [4].

Biocide	Chemical Structure	Action Modes	Fibers
QACs	 <p>(Example: monoquatery ammonium salt: alkyltrimethylammonium bromide)</p>	<ul style="list-style-type: none"> •Damage cell membranes; •Denature proteins; •Inhibit DNA production, avoiding multiplication 	Cotton Polyester Nylon Wool
Triclosan		Blocks lipid biosynthesis, affecting the integrity of cell membranes	Polyester Nylon Polypropylene Cellulose acetate Acrylic
Metals and metallic salts	Examples: TiO ₂ and ZnO	Generate reactive oxygen species, damaging cellular proteins, lipids and DNA	Cotton Wool Polyester Nylon
Chitosan		<ul style="list-style-type: none"> •Low Mw: inhibits synthesis of mRNA, preventing protein synthesis •High Mw: causes leakage of intracellular substances or blocks the transport of essential solutes into the cell 	Cotton Polyester Wool
PHMB		Interacts with membrane phospholipids, resulting in its disruption and the lethal leakage of cytoplasmic materials	Cotton Polyester Nylon
N-halamines	 <p>(Example: N-chloro-2,2,6,6-tetramethyl-4-piperidiny methacrylate)</p>	Precludes the cell enzymatic and metabolic processes, causing the consequent microorganism destruction	Cotton Polyester Nylon Wool

2.3.1 Antimicrobial mode of action

A living microbe, a bacterium or fungus, has an outermost cell wall composed of polysaccharides, which maintains the integrity of cellular components and protects the cell from the extracellular environment [4,35]. Beneath the cell wall is a semipermeable membrane, which encloses the intercellular organelles, enzymes, which are responsible for chemical reactions within the cell, and nucleic acids, which store all the genetic information. The survival and growth of microorganisms depend on the cell integrity, and, consequently, proper function. Therefore, an antimicrobial chemical agent or material may be classified according to the mode of action against cells' function or integrity. If their effect happens just due to the inhibition of cell growth, they have a biostatic effect, but if they can kill the microorganism, they have a biocidal effect [4,36].

There are several different antibacterial modes of action, as shown in *Table 2* [4]:

- Damage or inhibition of cell wall synthesis;
- Cell membrane function inhibition;
- Inhibition of protein synthesis;
- Inhibition of nucleic acid synthesis (both DNA and RNA);
- Other metabolic processes inhibition.

When considering metals, the metal reduction potential and the metal donor atom selectivity and/or speciation may provoke a biocidal effect. Redox-active metals can act as catalytic cofactors in a wide range of cell enzymes, and as consequence reactive oxygen species are generated, capable of inducing an oxidative stress, and ultimately damaging cellular proteins, lipids and DNA. External metal ions can substitute the metals present in biomolecules, causing cellular dysfunction [4].

Metal nanoparticles are an interesting and promising approach as a antimicrobial agent, due to their higher surface area and ability to dissolve faster in a given solution when compared to larger particles, leading to a higher amount of metal ions to be released and therefore presenting a stronger antimicrobial effect [4].

2.3.1.2 Drug resistant bacteria

When in the presence of some antimicrobial agents, some microorganisms may become resistant, and actually the appearance of multi-drug-resistant bacteria is increasing at a worrying rate. Microorganisms have an important role in the cycling elements at a global scale, deeply affecting the environment where they are present, but also are susceptible to environment themselves. These means that as antimicrobial agents are introduced into the environment, microorganism respond by becoming resistant to these agents [4,22,37].

The antimicrobial resistance mechanisms result from changes in the cellular physiology and structures of a microorganism due to changes in its usual genetic makeup by acquiring genes from resistant microorganisms in the same niche (acquired resistance) or by developing novel ways to prevent the entrance of those agents (intrinsic resistance) [4,37,38].

In the case of Ag compounds, some studies have reported bacterial resistance against them, suggesting that there is a need to better control the use of silver compounds and have an improved surveillance over their clinical use, so that their clinical utility can be preserved [4,39,40].

2.3.2 Silver and Silver Nanoparticles

The antimicrobial activity of silver was primarily identified as an oligodynamic effect, and in substances showing this oligodynamic effect, only very small portions of the active substance are needed for significant antimicrobial activity [41].

As shown in *Figure 8*, water molecules are able to penetrate the upper layers of almost every surface that is based in polymers, lacquers or resins, and if there are silver NPs

incorporated in those surfaces, those NPs will release silver ions (Ag^+) by specific corrosion processes. The silver ions are pulled to the upper layer of the surface by concentration gradients, where most of the moisture with less silver ions are present. This upper layer also contains the microbes, so the silver ions reach their target sites, where they will influence the microbial vitality through different mechanisms [41–43].

Silver ions present a broad antimicrobial profile against bacteria (both Gram-positive and Gram-negative bacteria), fungi and virus, even against bacteria strains known to be resistant against antibiotics. This makes silver and silver NPs an excellent biocidal substance for application in medical devices, as for example coated surgical instruments, polymer implants or textiles incorporated with Silver NPs [41,44]. The antimicrobial properties of silver particles have been exploited for a long time in general textiles, mainly in biomedical textiles, its broad-spectrum action being particularly significant in polymicrobial colonization associated with hospital-acquired infections [4].

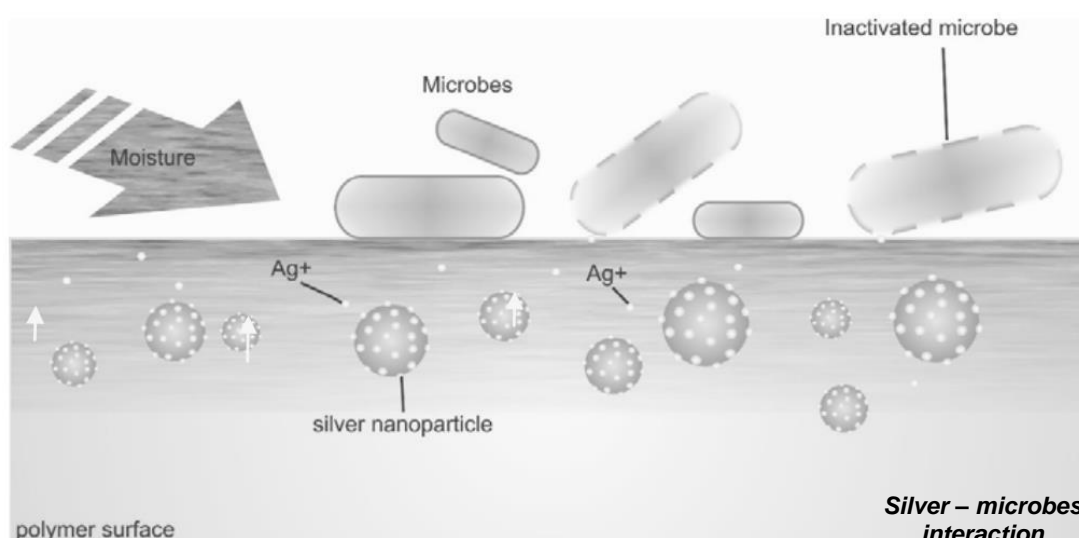


Figure 8 - Schematic overview of the nanosilver effect on surfaces (Modified from source)[41].

2.3.2.1 Cytotoxic Effect

There are some contradictory studies in relation to the content of silver in a film that can cause cytotoxic reaction. Some of those studies suggest that in DLC films, silver contents between 2.7 at% and 29 at% do not promote cytotoxicity. Others suggest that 7 at% or even 2 at% may cause negative effects [10,45].

When considering the presence of silver in parts per million (ppm), several studies referred that the maximum toxic concentration of silver tolerated by human cells is around 10 ppm. Films with silver percentage of 1.99, 9.46 and 16.53 at.% all released less than 60 parts per billion (ppb) after immersed in a NaCl solution for 24h and less than 120 ppb after one month, meaning that for this concentrations the release values were below the threshold [10,46].

In textiles containing antimicrobial agents, the type of action of the antimicrobial agent, its concentration in the textile, the exposures routes and the frequency of use will all influence the extent to which humans may be exposed to the textile. The parameters normally used to assess the risk profile of an antimicrobial agent associated with a textile

are the toxicity (acute and chronic), skin sensitization, skin irritation and disturbance of skin ecology [4]. For example, regarding Ag ions, which have a non-specific mode of action, they may interact with skin flora, and consequently cause the detachment of the cytoplasmic membrane from the cell wall of healthy bacteria. Furthermore, chronic contact with Ag may lead to the deposition of Ag and/or Ag sulphides particles on the skin, inducing skin discoloration (argyria) or ocular discoloration (argyrosis) [4,47,48].

2.3.2.2 Silver Ions and Nanoparticles release

Ag NPs dispersed over the surface may have different sizes, depending on the substrate and the thickness of the film. Usually, with a film thickness increase there is also an increase of silver segregation agglomeration at the surface. But it is also required the right morphology. The preferential pathways for Ag segregation are columns boundaries [10]. It is possible to observe a higher release of Ag ions in thicker coatings, since in these coatings exists a higher amount of silver available for being released, either on the surface or on the column boundaries where electrolytes can penetrate [10,49].

Ag ions are released from the NPs surface which is drastically reduced due to the decrease of the nanoparticle size. If no coalescence occurs, the size of the NPs decreases with Ag ions release, and consequently there is a reduction in the total surface in contact with the electrolyte. However, if coalescence occurs, the size of the NPs increases at the expense of a strong reduction of the NPs quantity, and consequently there is an overall decrease of the exposed area to the liquid medium [10,50].

The amount of released silver ions is directly linked to antimicrobial efficacy, meaning that AgNPs show a much higher biocidal activity while requiring less amounts when compared to micro silver or full silver coating [41].

Ion release is not the only way that silver can be released, as there is also the possibility of silver being released under the form of nanoparticles, since the segregation agglomeration process may promote the detachment of small nanoparticles present on the top of the surface [10].

The antibacterial activity is inversely proportional to the NPs' size [4]. As particles size decreases, the specific surface area increases, leaving a higher number of atoms available for redox, biochemical and photochemical reactions as well as to physiochemical interactions with cells [10,51–53].

2.3.3 Environmental Impact

When developing antimicrobial treatments for textiles, the advantages of the chosen antimicrobial agent should outweigh the potential environmental consequences and costs of its usage. The environmental impact of the antimicrobial textile is related to the textile substrate material, antimicrobial compound production, textile treatment processes and also to the subsequent use and disposal of the product. When antimicrobial agents are released from textiles, if they are not removed in the wastewater treatment, they may end up in an aquatic environment. Studies have shown that 85%-

99% of Ag particles and nanoparticles are effectively removed during waste treatment [4,22].

For example, products containing Ag are not considered biodegradable as they are considered mineral-derived materials, however, all silver forms are subjected to some transformation processes that may lead to their removal from the aquatic environment. Some studies have revealed that AgNPs may be immobilized by the formation of stable sulphide complexes, resulting in silver sulphide, which is very insoluble and less toxic and less bioavailable than dissolved Ag. So, the formation of these sulphides would decrease the risk of silver-based compounds in the aquatic environment [4,22,54].

2.4 Surface Modifications of textiles

In textile manufacturing, surface treatments, like printing, dyeing, and other chemical or physical treatments, are extremely important, as they have the ability to provide particular properties to textiles depending on the intended application. These surface treatments can improve the appearance or feel of textiles and add to textiles' unique functions, such as control of surface wetting or UV protection, among other factors functions. Most of these surface treatments rely on heavy use of heating sources during the process to dry the textiles, and consequently, are energy-intensive processes and expensive [55].

Due to these negative aspects associated with the surface treatments normally used in the textile sector, the sector is seeking new methods to improve existing product characteristics while minimizing environmental impact and energy use. Surface treatments like the Atomic Layer Deposition, Sol-gel techniques, Electrospinning and Plasma treatment techniques are all being studied and considered as possible tools to apply surface treatments on textiles [56–59].

Particularly, plasma treatment techniques in textiles can give characteristics to fabrics such as antibacterial activity, hydrophobicity, flame retardancy, and ultraviolet protection, depending on the materials employed in the procedure. Several studies have demonstrated that water-repellent characteristics may be bestowed on many fabrics, such as cotton, polyester and silk, utilizing plasma treatments. Also, with the introduction of metallic particles like Ag or Cu, it is possible to give antimicrobial properties to some textiles' surfaces [57,60].

2.4.1 Magnetron Sputtering in textile functionalization

Vapor deposition is a coating technique where a vapor phase material is condensed at the substrate in a vacuum environment to produce a thin coating. In some cases, the deposited substance interacts with the gaseous molecules, even more, resulting in a compound coating on the substrate. Physical vapor deposition (PVD) encompasses a wide range of vacuum deposition techniques and is typically split into two processes: evaporation and sputtering. These two processes can create vapor in the form of atoms, molecules, or ions supplied from a target, and these particles are subsequently transported and deposited on the substrate surface, resulting in the development of a film.

Since the evaporation technique requires high temperatures during the process, its use to coat textiles is not ideal, but on the other hand, the sputtering process is much more adequate. The sputtering process uses a substrate temperature that is far lower than the target material's melting point, making it a viable option for coating temperature-sensitive

materials like textiles. The most prominent sputtering processes are the cathodic arc physical vapor deposition (CAPVD) and the magnetron sputtering (MS), the process used in the project.

The MS process involves energetic ions colliding with a target surface, which usually results in the ejection of target atoms. The MS method confines the plasma to an area near the target using strong magnets, which dramatically enhances the deposition rate by maintaining a greater ion density, making the electron/gas molecule collision process much more efficient. Also, the MS method has a reduced electron bombardment of the substrate, making it greatly beneficial for temperature-sensitive substrates like textiles. Moreover, the technique is environmentally benign, therefore being an appealing alternative for adding new functions such as water repellency, mechanical and antibacterial characteristics and biocompatibility [61].

Because of all these advantages, the MS process is of great interest among the scientific community and among the medical textile industry, as it can be used in applications like face masks.

Not only the MS technique can be used for coating textiles, but it also provides an opportunity to improve high-quality coatings on textiles, as it offers new ways to functionalize textiles by combining oxide, metallic, and composite films to obtain various characteristics. Although the adherence of MS-deposited films on textiles is superior to that of other coating methods, it depends on the sputtering technique and textile used, as the adhesion between films and textiles was inconsistent. For example, by using High-power impulse magnetron sputtering (HiPIMS), the adhesion between films and textile substrates was enhanced when comparing with Direct current (DC) MS [62].

Aside from the fabric structure differences such as knitted textiles, woven textiles, and nonwoven textiles, a variety of other factors may influence the adhesion between the sputter film and textile substrates, such as surface morphology, different surface chemical properties, and porosity size of the fiber materials [63].

2.4.1 Diamond-like carbon coatings

The use of Diamond-like carbon (DLC) coatings is already a well-known technology, and this type of coating usually demonstrates properties like hydrophobicity, high hardness, transparency, excellent thermal conductivity, chemical stability and biocompatibility. There are several deposition techniques for DLC coatings, like ion beam deposition, pulsed laser deposition or MS deposition. The MS process in particular, is a very promising and versatile technique for performing DLC coatings because it allows carbon coating growth even at low substrate temperatures and delivers ion bombardment of the surface, which has the benefit of increasing coating adhesion to the substrate and thus improving coating quality.

For their role as outstanding protective coatings in bio-applications, DLC characteristics have been widely investigated. Some studies suggest that bacterial adherence to DLC films is linked to their sp² and sp³ hybridization and lowering the sp²/sp³ ratio improves antimicrobial efficacy significantly [64]. Because of this, DLC coatings having a large proportion (>80%) of sp³ bonds are often used for biomaterial films [65].

DLC coatings have a high hydrophobicity, a characteristic that can induce changes in bacterial cell membranes, leading to biological death [66]. Furthermore, the surface free energy is a key factor influencing DLC antibacterial efficacy. The initial attachment of microorganisms is significantly connected to the total surface energy of the coating,

because as the total surface energy of the coating decreases, the number of adherent cells also decreases and the bacterial removal increases [67].

Nanoparticles are commonly added to DLC coatings to activate or enhance their antibacterial characteristics. Incorporating a metal particle into the DLC structure can function as a catalyst for the formation of sp²-rich boundary sites [68,69]. In particular, some studies have shown that a low Ag concentration can reduce the number of C atoms bound in sp² configuration, which promotes sp³ bonding and better antimicrobial efficiency, but a greater Ag content raises the sp²/sp³ ratio and consequently decreases the antimicrobial efficiency [70].

2.4.2 DLC coating with Nanoparticles

Because of their small sizes, unique chemical and physical properties, and high specific surface, materials for instance metal nanoparticles, metal oxide nanoparticles, carbon nanomaterials, and their composites have been extensively used as new anti-microbial agents. This enables them to dissolve more quickly in a given solution than bigger particles, releasing more metal ions [4,71]. Furthermore, these compounds are readily incorporated into the polymeric matrix of fibers, making them excellent for use in textiles [4].

Consequently, the incorporation of Au, CuO, ZnO, TiO₂, or Ag Nanoparticles to DLCs, with Ag being the element most likely used to obtain antimicrobial properties, could allow fabrics, including those used in masks, to have the two properties that are crucial in this study: antimicrobial and hydrophobic properties [72]. Also, AgNPs are the most widely used antimicrobial nano agent because of their broad-spectrum antimicrobial properties and strong antimicrobial effectiveness against a large number of bacteria, viruses, and fungi, which is also higher when compared to particles made from other heavy metals such as Au and Zn [71].

In relation to the combination of DLC and Ag, there are several studies that show that silver doped DLC (AgDLC) coatings have an excellent antimicrobial effect [72]. The biocidal action of AgDLC thin films is longer than other substrates with metallic NPs, as the film surface is continuously renewed with Ag due to its segregation through the carbon matrix. Concentration gradients attract Ag ions to the top layer of the surface, where most of the moisture and less Ag ions are present. The bacteria are also contained in this higher layer, allowing the silver ions to reach their target locations and impact microbial viability [41]. As bacteria only interact with the surface' materials, AgDLC films exhibit improved and extended antimicrobial activity compared to films without silver segregation. This phenomenon shows the advantage of AgDLC films over AgNPs, as the Ag content can be reduced while maintaining a high antimicrobial activity, opening the possibility of controlling the antimicrobial action of this type of coating [72]. Therefore, a successful deposition of AgDLC coating in textiles may provide a wide range of possibilities in the biomedical sector, depending on the desired application.

3.Methods and Procedures

3.1 Materials

On this project, the main purpose was to study the interaction between textiles and Ag-DLC coatings deposited using a MS process. In order to do that it was required to first choose the textiles and also how the deposition process would occur. It was first decided

that it was required to choose three different fabrics that would be relevant for biomedical applications, especially for face masks. And then decide how the deposition parameters would be defined in order to have a set of different results, in which that Ag-DLC film thickness, Ag at% and film structure would be varied.

3.1.1 Fabrics

As mentioned on the previous Chapter 2, there is a wide range of textiles that have been used in biomedical applications, and for this study it was decided that the three different fabrics chosen should be commonly used in healthcare facilities, particularly in face masks [2].

The three fabrics that were picked were a 100% Cotton fabric, a Jersey format fabric (cotton + elastane) and TNT fabric (Polypropylene). All of these three fabrics were often used during the Covid-19 for homemade face masks [31]. In the case of cotton, it is also often used for bed sheets and drapes, and TNT has a wide range of biomedical applications: surgical masks, N95 respirators, scrubs, surgical gowns, footwear covers, etc.

3.1.2 Films

On this study the films deposited were carbon thin films, more precisely DLC films, that were doped with Ag. To deposit them the technique used was the MS process, in which it was used a C target and Ag target. The all process will be explained more in detail in a next chapter.

3.1.3 Samples preparation

To prepare the samples the first step was to cut a piece of each fabric as well as three pieces of silicon. The size of each fabric sample was around a 10x2 cm rectangle and the pieces of silicon were roughly a 1.5x1.5 cm square.

Then, it was necessary to ensure the samples had the minimum impurities on them, so in order to clean them they would go through an ultrasonic bath. In this process, firstly, the samples were put inside a container with acetone and placed in the ultrasonic bath machine for about 10 minutes. Then, the process would be repeated with ethanol (96%).

After the ultrasonic bath, the samples were dried using a dryer and then they were glued to the substrate holder. To glue the fabrics to the holder it was used glue tape and for the silicon samples it was used silver glue. Both the tape and the glue used were chosen taking into consideration the temperatures present on the magnetron sputtering chamber during the deposition process. After waiting for about 20 minutes, the glue would be dried up and the substrate holder was ready to be put inside the sputtering chamber. The final look of the substrate holder after the preparation process can be seen in *Figure 9*.

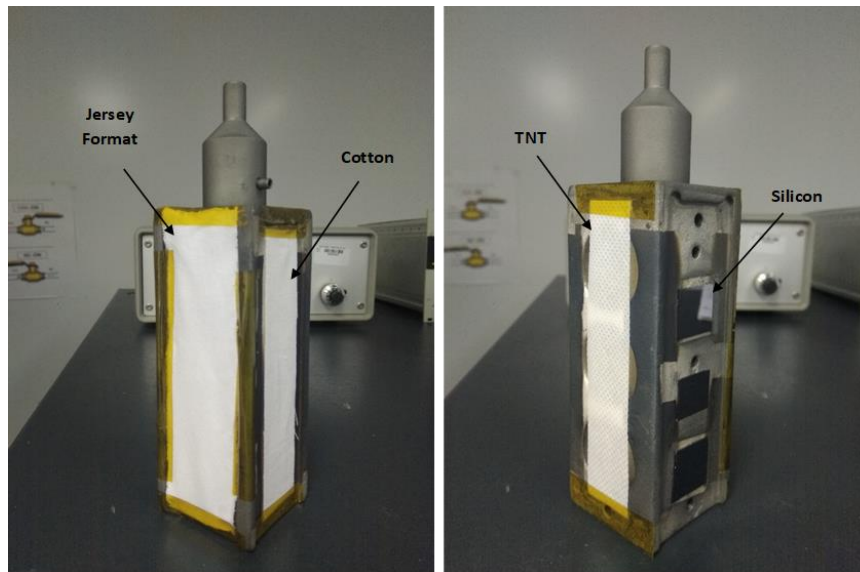


Figure 9 – Substrate holder prepared for the deposition process.

3.2 Magnetron Sputtering Process

As mentioned before, the technique used for the films depositions was a MS process. In this process, energetic ions collide with a target surface, in this case a C target and an Ag target, that will result in the ejection of target atoms. In order to confine the plasma to an area near the targets, it is used strong magnets, causing a higher ion density and consequently increase the chance of electron/gas collisions. Due to this area “restriction”, this sputtering process has a high deposition rate.

There are several different parameters to take into consideration during the sputtering process, as well as some procedures to ensure the process runs smoothly and the conditions inside the chamber are similar for all the depositions made.

Firstly, after introducing the substrate holder inside the deposition chamber, it was necessary to create high vacuum, around $10^{-6}/10^{-5}$ mbar, inside it. To do it, it was first necessary to use a vacuum pump that was used until the pressure inside the chamber was around $5,0 \times 10^{-1}$ mbar. After that, the connection to that pump would be compact and a connection to a second pump would be open to create the high vacuum needed. The scheme of the MS machine can be seen in *Figure 10*.

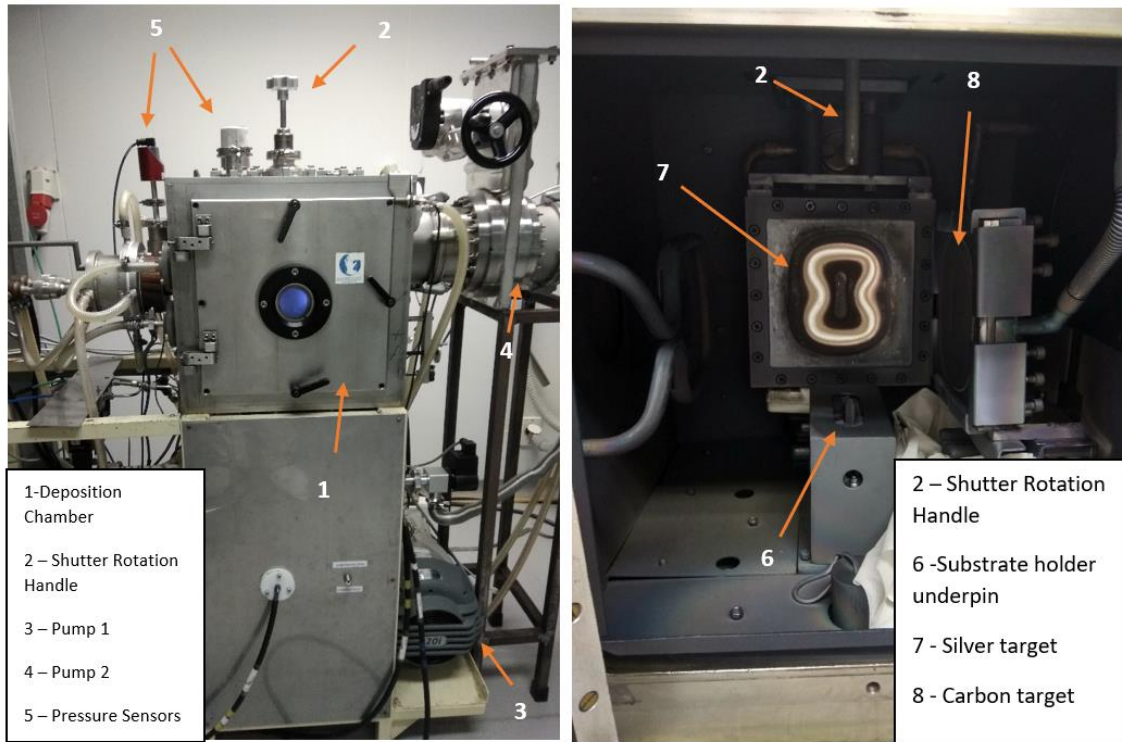


Figure 10 – Magnetron Sputtering machine scheme.

Before the start of the deposition process, it would be introduced in the chamber Argon gas (21.,9 sccm) and a rotation to the substrate holder was applied. It would also be necessary to perform a cleaning process. During this, first the shutter inside the chamber would be put between the Ag target and the substrates holder, and then a current would be applied to the Ag target for 3 minutes, in order to clean the target from residues of previous depositions. Next, the same procedure would be performed for the C target for 5 minutes.

After the cleaning process, the deposition process would start. The power provided to both targets would be adjusted to the parameters decided for the deposition being done and the shutter would be placed in zone where it could not interfere with the process.

Depending on the deposition, there were some parameters, besides the power given to targets, that would vary: the deposition time and the work pressure. This variation may be seen on *Table 3*. The variation of these parameters was done in order to give the coatings different characteristics like thickness, Ag at% and different film structure organisation. It should be mentioned that depositions 1-11, 22 and 23 are not in *Table 3* as they were only used for calibration of the deposition process.

Table 3 – Parameters varied during the deposition process

Deposition Number	Ag Power Variation (W)	C Power Variation (W)	Working Pressure (Pa)	Deposition Time (s)
Deposition 12	37	1500	0,8	180
Deposition 13	44	1500	0,8	180
Deposition 14	53	1500	0,8	180
Deposition 15	61	1500	0,8	180
Deposition 16	70	1500	0,8	180
Deposition 17	23	1500	0,8	180
Deposition 18	23	1400	0,8	180
Deposition 19	23	1300	0,8	180
Deposition 20	23	1200	0,8	180
Deposition 21	23	1100	0,8	180
Depositions 24/25	70	1500	0,8	160
Depositions 26/27	155	1500	0,8	150
Depositions 28/29	70	1500	1,0	160
Depositions 30/31	155	1500	1,0	150
Depositions 32/33	70	1500	1,0	300
Depositions 34/35	155	1500	1,0	290
Depositions 36/37	70	1500	1,0	600

3.3 Characterization Techniques

3.3.1 Transmission electron microscopy

Transmission electron microscopy (TEM) is a very powerful tool for qualitative and quantitative characterization of materials microstructures and nanostructures, and as well as their chemical composition. The examination of materials through this technique can give important information on topography, morphology, composition and crystallographic features [73].

The TEM technique consists of an electron gun that produces a stream of electrons which is going to be focused into a thin electron beam using condenser lenses. The beam will then hit the sample being analysed and part of that electron beam is transmitted. That transmission portion will be focused by objective lens, creating a image that can be magnified by passing down a column of adjustable intermediate and

projective lens. Through the use of specialised software, the TEM images can then be projected and better analysed in a viewing screen. In *Figure 11* there is a schematic representation of the TEM process [73].

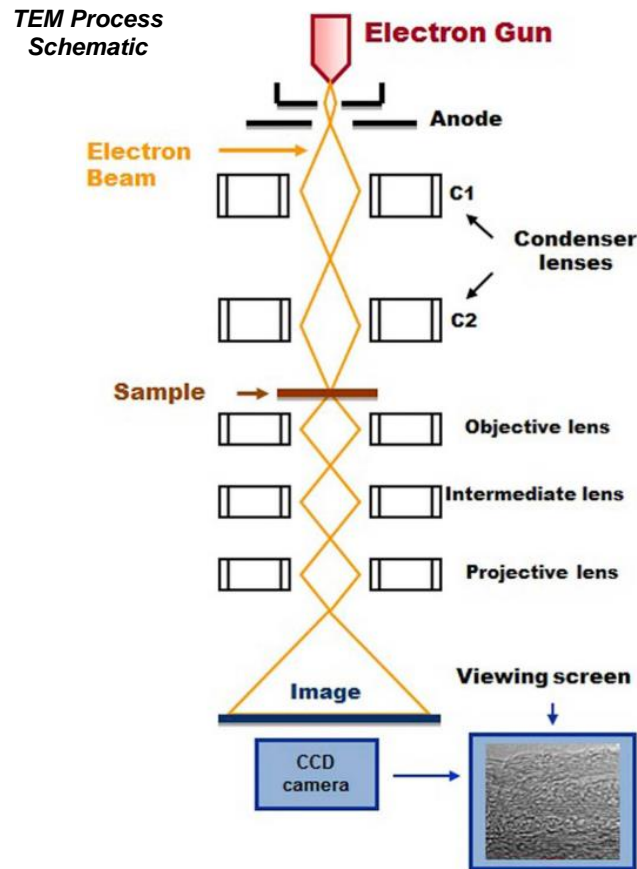


Figure 11 - Schematic drawing of a transmission electron microscope (Modified from source) [73].

3.3.2 X-Ray Diffraction

The X-Ray Diffraction technique (XRD) allows the evaluation of the atomic structure of materials, more precisely the evaluation of the crystalline structure and physical composition. In this technique, an electromagnetic radiation beam, in the X-Ray spectrum, will be focused on crystalline structure, that will cause those X-rays to scatter into many directions. The scattered X-rays will interfere with each other either constructively or destructively. When the interference is constructive, it means the directions the X-Rays scattered are well defined and obey to the Bragg equation $n\lambda = 2d_{hkl} \sin\theta$. $n\lambda$ represents a multiple ($n=1,2, 3,\dots$) of the used wavelength of the X-ray beam, d_{hkl} represents the distances between atoms defined by the Miller index (hkl) and θ the diffraction angle [74].

As the wavelength in XRD experiments is known and the angles at which constructive interference occurs are measured, with the Bragg equation use, it is possible to

determine the distance between the lattice planes of the material and the result of the measurement is a diffractogram [75].

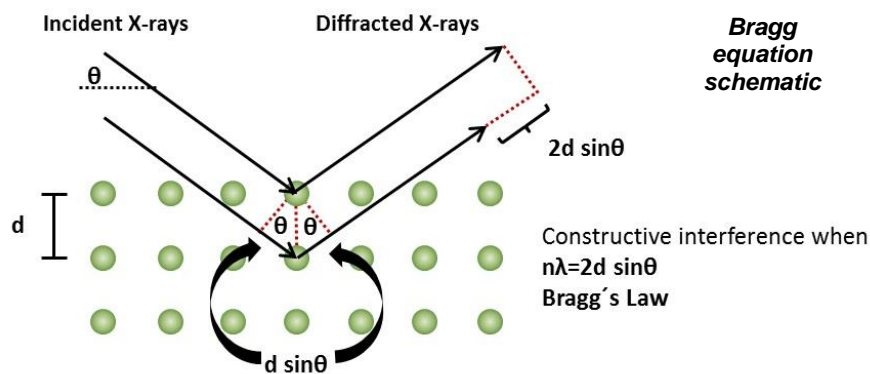


Figure 12 - Schematic representation of the Bragg equation (Modified from source) [75].

3.3.3 Scanning Electron Microscopy and Energy Dispersive Spectroscopy

The Scanning Electron Microscopy (SEM) is a technique that allows the acquisition of images with a high magnification, normally between 10x to 1000000x. [76] The fundamentals behind this technique are using a high energy electron beam that is emitted by thermal-ionic heating of a filament, accelerated by a potential difference and guided by electromagnetic lenses, the sample in analysis is bombarded by this beam that will go through the surface of the sample sequentially. This will cause the interaction between superficial zones of the sample with the beam and there will be the emission of several different types of radiation. The secondary electrons and the backscattered electrons will be detected, providing information that after software analysis allows the visualization of a topographic image. Figure 9.a shows a schematic of the SEM process [74].

By combining the SEM technique with a Energy Dispersive Spectroscopy (EDS), it is possible to detect X-rays that are unique to the atoms present in the sample being analysed, X-rays that are emitted as result of the ejection of electrons of the orbitals closer to core by collisions and the consequent filling of the space left by the ejected electrons by an electrons from an outer layer. The difference in energy between the higher-energy orbital and the lower energy orbital may be released in the form X-rays [74].

The SEM images acquired before the antibacterial tests were obtained using a ZEISS Merlin high resolution microscope combined with an EDS system of the Oxford Instruments.

For the second set of images, the ones acquired after the antibacterial test, it was required a different procedure to obtain the images. After the halo test, the samples were removed and carefully washed three times with distilled water. The samples were dehydrated by an immersion in increasing ethanol concentration solutions: 70, 95 and 100% (v/v) for 10, 10 and 20min, respectively, and placed in a sealed desiccator.

Afterwards, the samples were mounted on aluminum bases with carbon tape, sputter-coated with gold and observed with a scanning electron microscope (SEM) in a SEM, EDAX NovananoSEM 200 equipment.

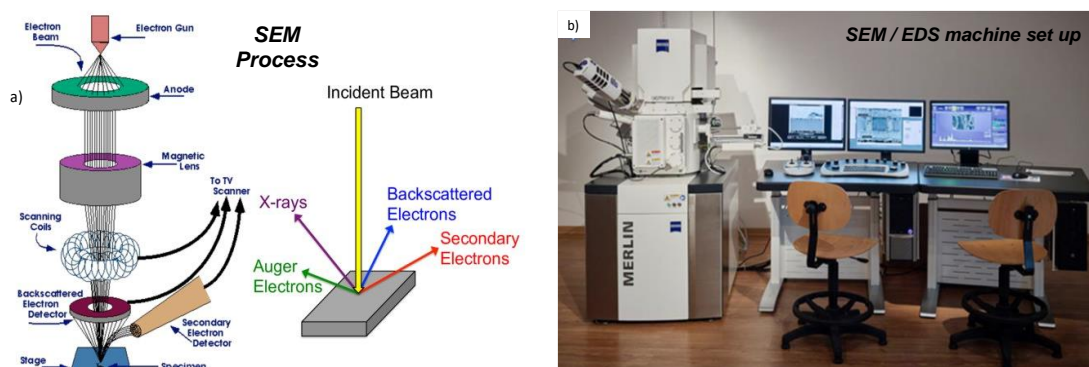


Figure 13 – a) Schematic of the SEM process (Modified from source) [77]; b) Photography of the SEM/EDS machine used to obtain the first set of images (Modified from source) [74].

3.3.4 Antibacterial Test – Zone of Inhibition Test

Zone of inhibition tests, *Figure 14*, adapted from Kirby-Bauer test [78], were carried out to determine the diffusion of silver from the coatings surface. The evaluation of the antibacterial activity was performed against two bacteria, one gram-positive, *staphylococcus aureus* (ATCC 6538 obtained from American Type Cell Collection) and one gram-negative *klebsiella pneumoniae* (ATCC 11296). The choice of these microorganisms is related with the applicability, the *staphylococcus aureus* is often found on the skin and the *klebsiella pneumoniae* causes different types of healthcare-associated infections, including respiratory infections such as pneumonia.

Initially, the inoculation of a single colony was carried out in 30 ml Tryptic soy broth (TSB, Merck) culture and incubated at 37 °C overnight at 120 rpm. The cell suspension obtained was adjusted to an optical density (OD) of 0.8 at 620 nm and properly diluted in culture media to 1×10^8 CFU/ml. An aliquot of cellular suspension (100 μ l) was spread in Tryptic Soy Agar (TSA, Merck) petri dishes. After medium solidification, the samples (previously sterilized by exposure of ± 1 h to UV light) were placed separately on the top of the agar plate, placing the side with treatment in contact with the agar and incubated for 24 h at 37 °C. After the incubation period, the halo (zone of transparent medium, which means that there is no bacteria growth) formed around the sample was photographed to record the results (images captured with Image Lab™ software).

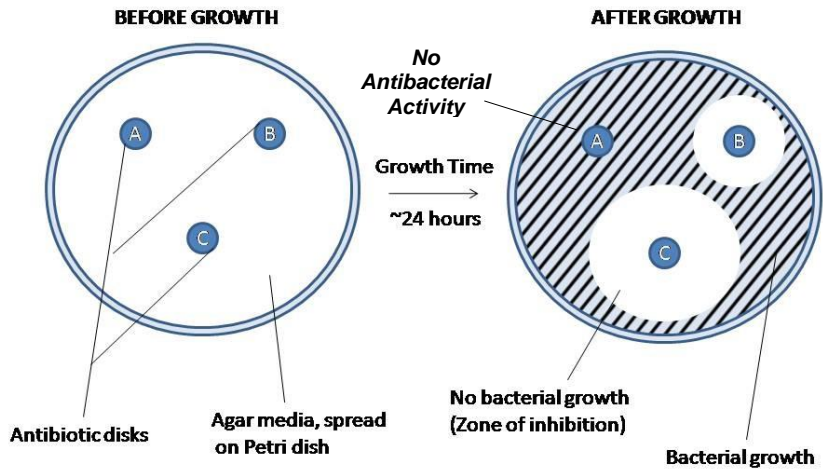


Figure 14 - Schematic of a typical zone of inhibition test (Modified from source) [79].

3.3.5 Contact Angles Analysis

The contact angle between a liquid and a solid surface is intertwined with the wetting ability, in other words, how a liquid is able to get that surface wet, consequence of the balance between the cohesion forces of the liquid molecules and the solid/liquid adhesion [74].

When a liquid drop is on a surface, there is a balance between the superficial tensions of the liquid/solid ($\sigma_{s/l}$), liquid/gas ($\sigma_{l/g}$) and solid/gas ($\sigma_{s/g}$) interfaces, maintaining its shape. The contact angle, θ , is the angle that the tangent to the liquid drop does with the point in which it touches the solid surface, and it can be calculated through the equation showed in Figure 15. The parameters displayed on the equation are defined by the chemical composition and rugosity of the solid surface as well as the characteristics of the liquid [74,80,81].

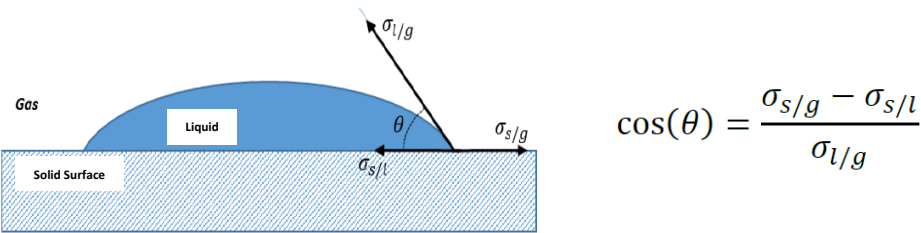


Figure 15- Representation of a liquid drop on solid surface and the respective equation that connects the surfaces tensions and angles between them (Modified from source) [74].

4. Results and Discussion

In this chapter, it will be presented the results obtained and their respective analysis and discussion. The main objective of this work project is to evaluate the interaction between the fabrics and the Ag-DLC coating, evaluate the hydrophobic and anti-microbial ability of the samples and evaluate the viability of the technology for future use.

Therefore, this chapter begins by analysing the effects of the deposition process on the three fabrics in study, Cotton, Jersey and TNT, as well as, their interaction, and after it is presented the results obtained relatively to their hydrophobic and anti-microbial performance.

4.1 Fabrics-Deposition Interaction

As it as mentioned earlier in chapter 3, after the selection of different types of fabrics, Cotton, Jersey Format and TNT, it was decided that it was needed to run two different set of depositions series. The first series of depositions to test and evaluate how to control the deposition process in order to get films with specified thickness, levels of Ag and deposited particles structure. The second series of depositions to get a set of samples with different variations of the parameters mentioned above that seemed to be the ones of most interest for the project.

4.1.1 First Series of Depositions

In the first series of depositions the main goal was to acquire enough information that would allow for a better control of the magnetron Sputtering Process, in particular, finding a correlation between the power given to the C and Ag targets, and the percentage of Ag in the film.

So, firstly it was required to go through a series of depositions, more specifically eleven depositions, in order to calibrate the sputtering machine and being able to create a stable plasma inside the sputtering chamber. After that calibration process, it was then possible to start the first series. This first series of depositions was divided into two phases: in the first phase a variation in the power given to the Ag target was applied and in the second phase the variation in power was in the C target.

Table 4 and *Table 5* show the variations on those parameters, and respective Ag at% obtained in the EDS analysis. ***Erro! A origem da referência não foi encontrada.*** shows the correlation between Ag target power and film Ag at% variation (each sample was analysed three times).

Table 4 – Parameters used in the depositions: variation of the power given to the Ag target and respective Ag at%.

Deposition Number	Ag Power Variation (W)	Working Pressure (Pa)	Deposition Time (s)	Ag at%
Deposition 12	37	0,8	180	4
Deposition 13	44	0,8	180	5
Deposition 14	53	0,8	180	7
Deposition 15	61	0,8	180	9
Deposition 16	70	0,8	180	10

Table 5 - Parameters used in the depositions: variation of the power given to the C target and respective Ag at%.

Deposition Number	C Power Variation (W)	Working Pressure (Pa)	Deposition Time (s)	Ag at%
Deposition 17	1500	0,8	180	5
Deposition 18	1400	0,8	180	6
Deposition 19	1300	0,8	180	5
Deposition 20	1200	0,8	180	7
Deposition 21	1100	0,8	180	8

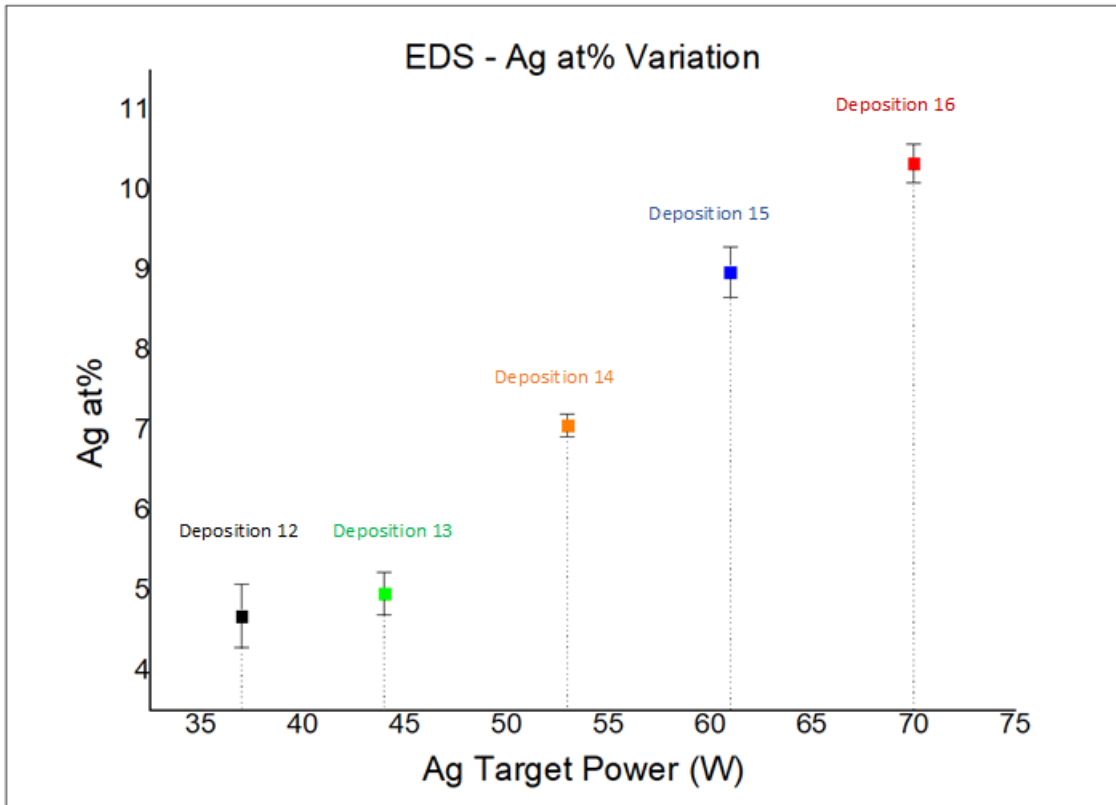


Figure 16 - EDS graphic correspondent to the series of depositions varying the power given to the Ag target

From this first set of results, it was possible to conclude that by varying the power given to the Ag target, the levels of Ag present on the film were better controlled than when the variation was applied on the C target. Moreover, in addition to the EDS analysis, a few other tests were performed in order to have a better understanding of how the deposition process went through and how the film and substrates interacted. Since it was the depositions 12-16 that were of most interest, those were the ones that were focused on during the remaining analysis of the first series of depositions.

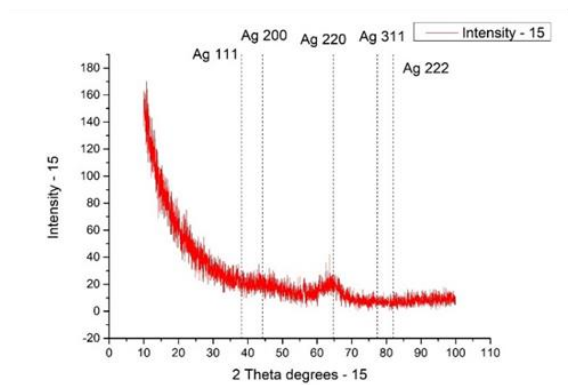


Figure 18 – XRD Analysis of Sample 15 with reference markers for Ag possible values

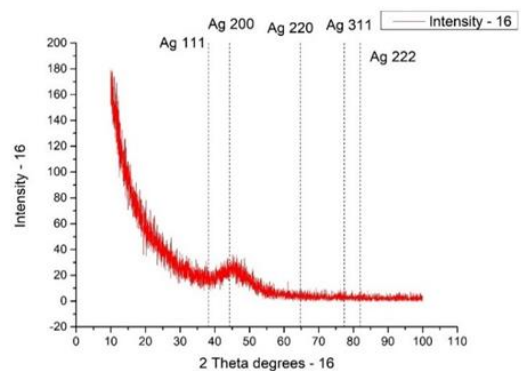


Figure 17 – XRD Analysis of Sample 16 with reference markers for Ag possible values

Besides the EDS analysis, a XRD analysis of depositions 15 and 16 (9 at% and 10 at% Ag respectively) was also performed to gather even more information about the presence of Ag in the films deposited in the substrates. As shown in *Figure 18* and *Figure 17*, it is possible to identify the presence of silver in the film. The crystallographic planes identified are different from one deposition to another. The reason why, could not be identified, and the fact that the data available was not extensive enough to produce better graphics, it was not possible to fully comprehend the XRD results. However, for both cases it is possible to identify at least one crystallographic plane associated with Ag [82].

The following depositions analysis were performed through the study of the images obtained in SEM and TEM. A comparison between the three fabrics in study and a comparison by Ag at% were the two criteria chosen to try to comprehend the similarities and differences in the film-substrates interactions.

4.1.1.1 Comparison between fabrics: SEM images

When comparing the samples by fabric, we can clearly distinguish the three different fabrics we are using as substrate for the Ag-DLC coating through the fibre's organisation and surface. In *Figure 19*, we have 6 images from one of the depositions, in which we have a coating with 4 at% Ag.

In these set of images, we can identify the presence of our substrate through the added layer present in the surface of the different fibres, but there is not a major difference in relation to the different film-substrates interaction that can be seen. The same cannot be said about the images in *Figure 20*.

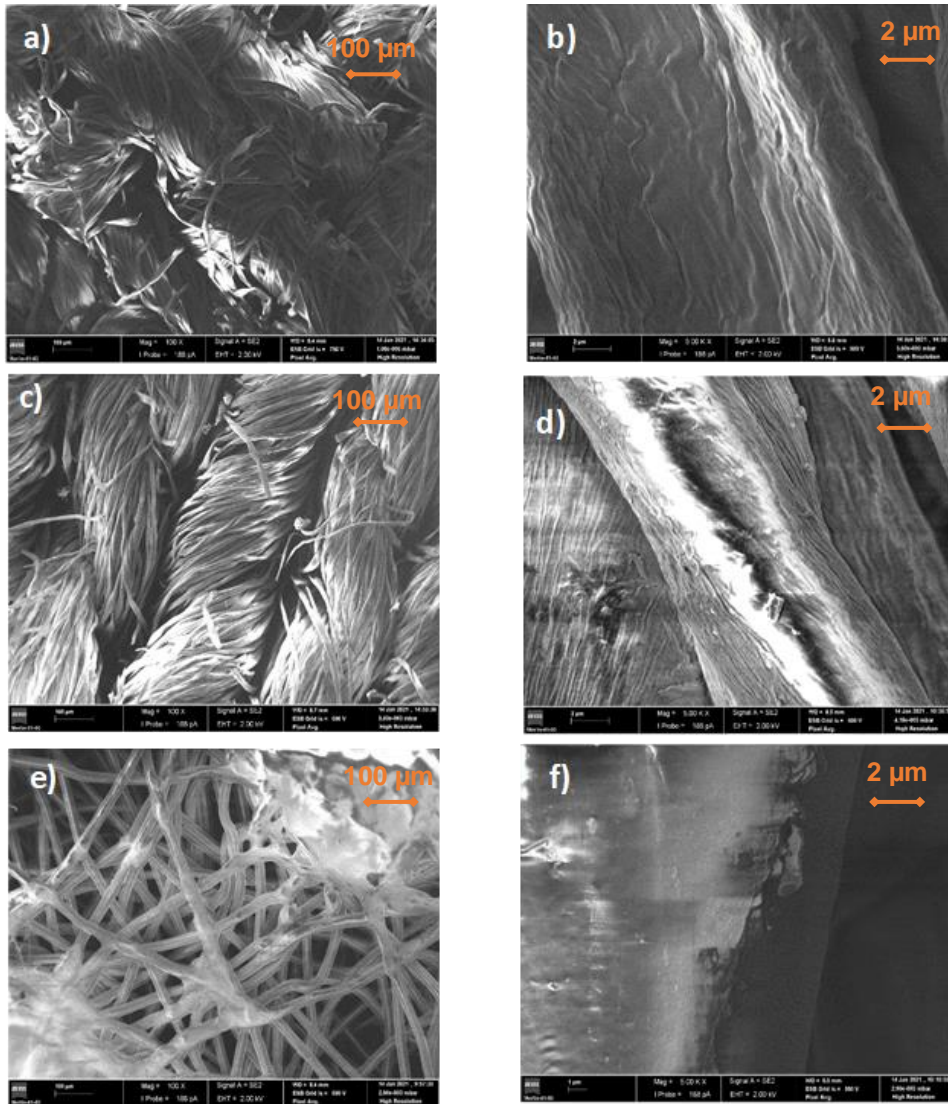


Figure 19 - SEM images of three different substrates coated with an AG-DLC film (4 at% Ag) with different magnifications (100x and 5000x): a,b) Cotton, c,d) Jersey Format and e,f) TNT

In Figure 20, we have 6 images from another deposition, in which we have a coating with 10 at% Ag. In this case, the film-substrates interaction is clearly distinguishable when comparing different substrates. With a magnification of 100x those differences are not observable, but when the magnification is increased to 5000x it is possible to observe that the coating is reacting differently.

With the increase of Ag percentage, we started to see a different organization of the coating in the surface, mostly in the cotton, where it seems there are different layers overlapping each other, and in the TNT, where there are multiple cracks in the coating. These findings might imply that not only the different substrates influence the coating-surface interaction, but also the Ag percentage might have an important role in it. It also important to mention that sputtering process does not seem to cause damage on the fabrics' fibres.

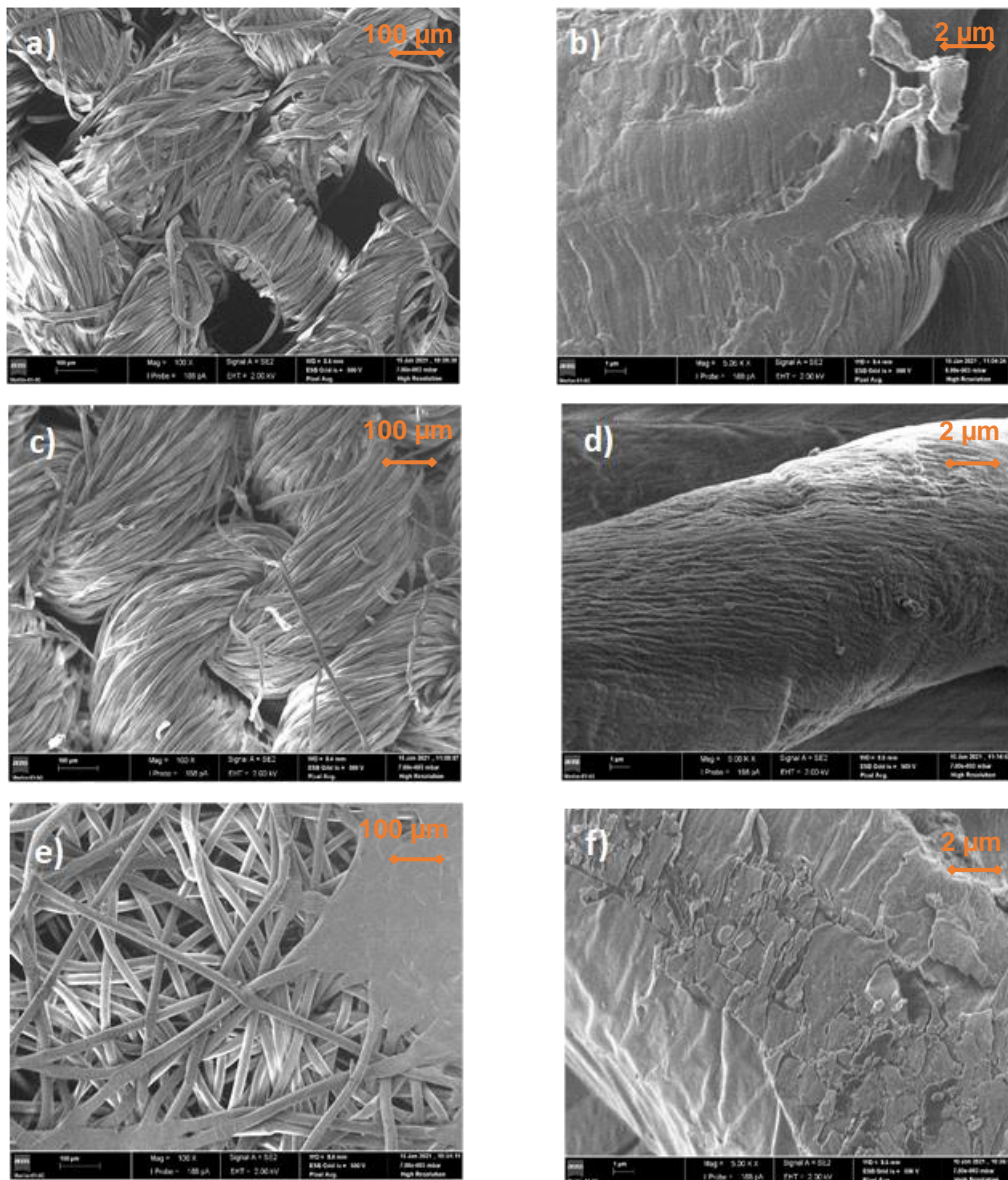


Figure 20 - SEM images of three different substrates coated with an AG-DLC film (10 at% Ag) with different magnifications (100x and 5000x): a,b) Cotton, c,d) Jersey Format and e,f) TNT

4.1.1.2 Comparison by Ag at%: SEM and TEM images

To compare the samples by Ag percentage, in *Figure 21*, we have 13 images (11 SEM images and 2 TEM images) from 2 different depositions and from Virgin substrates (without the coating). When comparing the Virgin substrates images with the rest of the SEM images, the substrate surface seems to have more rugosity and a presence of one or more layers, which indicates that the coating is indeed present. These features are more prominent as the percentage of Ag increases. In fact, the images corresponding to Deposition 16 (Ag at% =10), in the Cotton and TNT cases there are present several cracks in the coating, especially in TNT case. This finding might indicate that the Ag percentage is a contributing factor in the surface-coating interaction, and it can possible worsen the adherence of the coating to the fibers. When it comes to the Silicon SEM images, there are no differences observed. This and the fact that we cannot observe the presence of Ag particles in any of the SEM images of the substrates, might be the consequence of the coating being too dense, and therefore, the Ag particles need more

time to segregate to the surface. However, the presence of Ag is confirmed not only by the EDS Data but also by the TEM images. In the TEM images of *Figure 21*, it is possible to observe Ag NPs in both cases, being more easily identified in image m), where Ag clusters have already started to form.

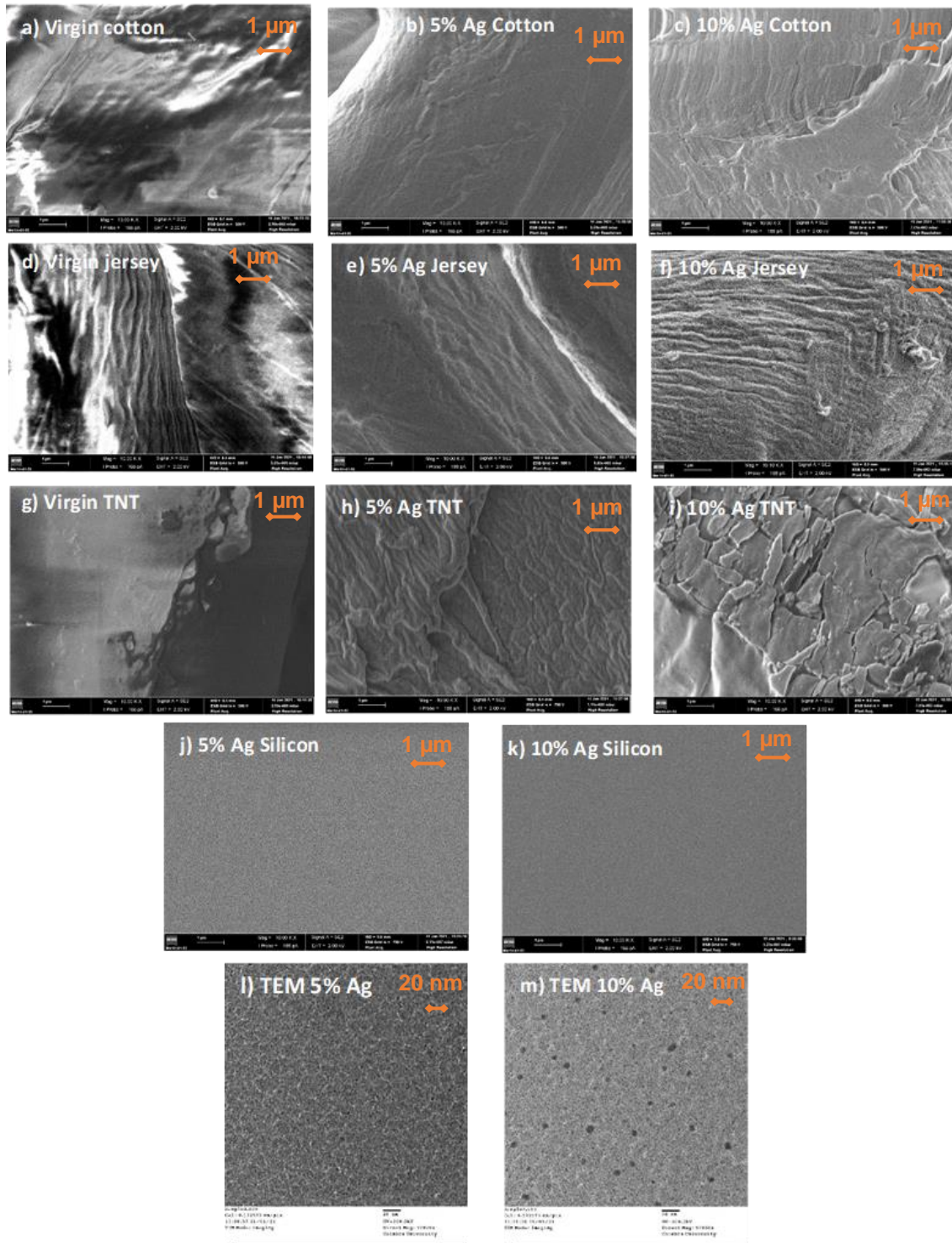


Figure 21 - TEM images and SEM images (10k magnification) of four different substrates uncoated and coated with an AG-DLC film (5 at% and 10 at% Ag): a) Virgin Cotton, b) 5 at% Ag Cotton, c) 10 at% Ag Cotton, d) Virgin Jersey Format, e) 5 at% Ag Jersey Format, f) 10 at% Ag Jersey Format, g) Virgin TNT, h) 5 at% Ag TNT, i) 10 at% Ag TNT, j) 5 at% Ag Silicon, k) 10 at% Ag Silicon, l) TEM image 5 at% Ag, m) TEM image 10 at% Ag.

As mentioned above, it was not possible to observe the presence of silver in the surface of the film, even in SEM images with a 20k magnification, and one the reasons could be that the film was so dense that the silver particles could not reach the surface or might take longer to do it. Due to this possibility, two months after the first SEM images were taken, the sample corresponding to the deposition 16, in which the Ag at% was the highest (10 at% Ag), was once again analysed by SEM.

As demonstrated in *Figure 22*, it is now possible to observe the presence of Ag particles on the surface of the three substrates, only the cotton remained without visible Ag particles on the surface, meaning that indeed the Ag particles were capable of segregate to the surface as it was expected, however the amount visible is still lower than expected when considering the Ag at% present on the film.

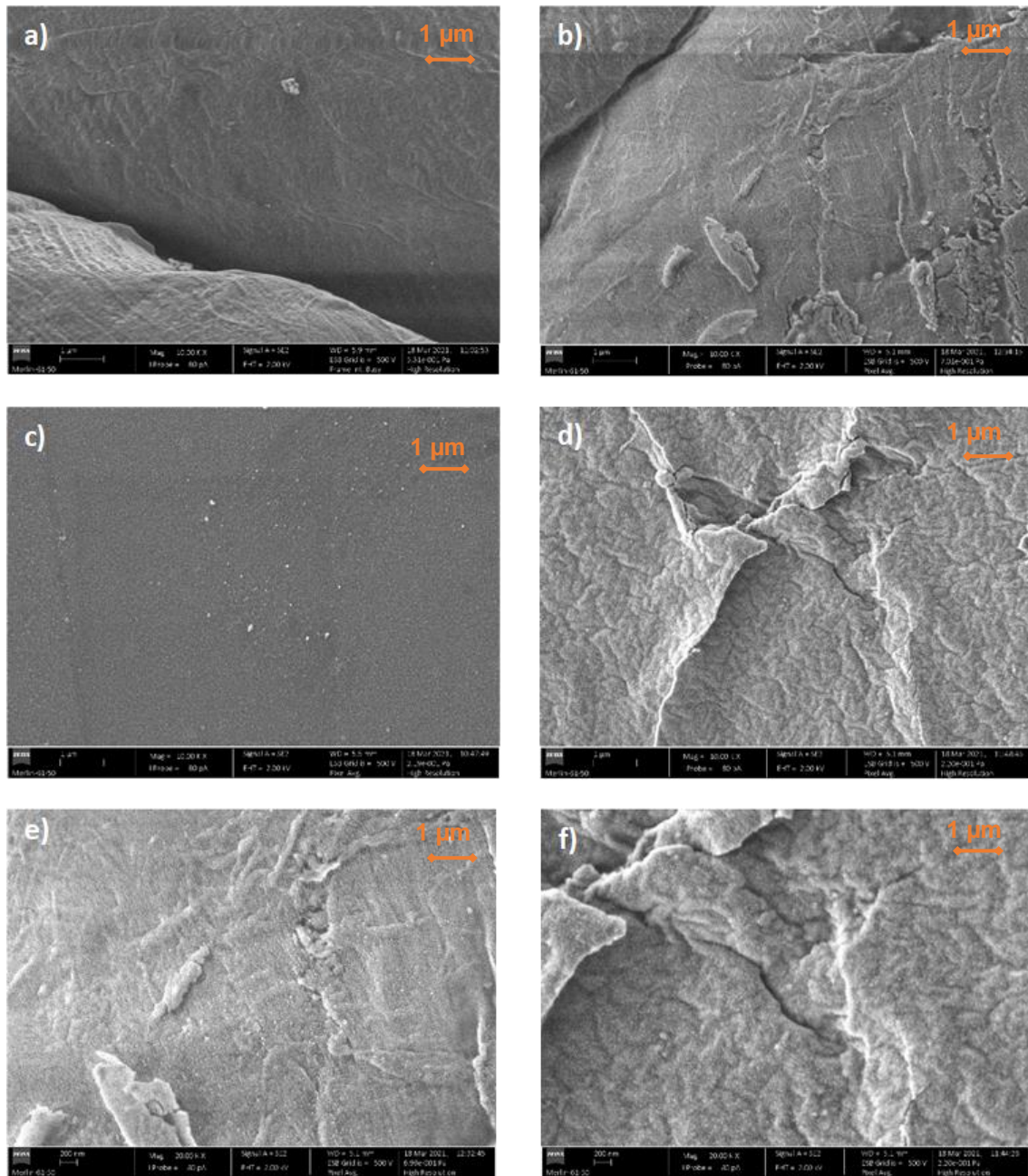


Figure 22 - SEM images (10k and 20k magnification) of four different substrates coated with an AG-DLC film (10% Ag): a) Cotton 10k mag., b) Jersey Format 10k mag, c) Silicon 10k mag, d) TNT 10k mag, e) Jersey Format 20k mag, f) TNT 20k mag.

4.1.1.3 Contact Angle and Antibacterial Results

The two main properties wanted for the samples in study are antibacterial and hydrophobic properties. So, to analyse if the samples have these capabilities, it was performed Contact Angle tests to study the hydrophobic ability and a zone of inhibition test to study the antibacterial ability.

The Contact Angles test results are shown on *Table 6*. As mentioned in chapter 3, for a surface to be considered hydrophobic it is necessary that the contact angle between the surface and the liquid, in this case water, be higher than 90° . If the contact angle is lower

than 90 °, then the surface is considered hydrophilic and if the contact angle is higher than 150 ° the surface is considered super hydrophobic.

From *Table 6* it is possible to observe that the addition of the film did not generate the same results for the three fabrics. These three fabrics all are composed by different fibres, and therefore, the film-fabric interaction will be different as well as their interaction with water particles. For instance, the cotton has been highly influenced by the presence of the film, as the virgin cotton is hydrophilic (contact angle of 60.73 ° ± 4.82 °) but as the film increases in Ag at% it is possible to also observe an increase in the contact angles, to the point that the cotton gains hydrophobic properties. However, for the cases of the jersey format and TNT fabrics, the addition of the film did not seem to increase their hydrophobic ability except when the Ag at% is of 10 at%. The influence of the increase on Ag at% of the film in the hydrophobic ability is discussed during the analysis of the results of the second series of depositions.

Table 6 – Contact Angle results for Cotton, Jersey Format and TNT. These results are correspondent to a surface-water analysis.

Deposition Number	Cotton	Jersey Format	TNT
Virgin Samples	60.73 ° ± 4.82	108.18 ° ± 1.73	114.87 ° ± 3.41
Deposition 12 (4 at% Ag)	58.13 ° ± 20.99	100.33 ° ± 11.68	97.06 ° ± 3.97
Deposition 14 (7 at% Ag)	83.49 ° ± 18.93	99.67 ° ± 7.85	98.86 ° ± 9.30
Deposition 16 (10 at% Ag)	110.26 ° ± 22.22	121.27 ° ± 5.78	115.11 ° ± 10.15

Regarding the Antibacterial tests, since the first series of depositions main objective was to better understand and control the sputtering process and its interaction with the fabrics, it was decided that only the silicon sample with highest Ag at% (deposition 16) would be tested. The results acquired were not the expected, as the sample showed no antibacterial properties, *Figure 23*, and according to some literature [50] and previous projects in the department, the Ag present on the sample should have been enough to trigger a good antibacterial response.

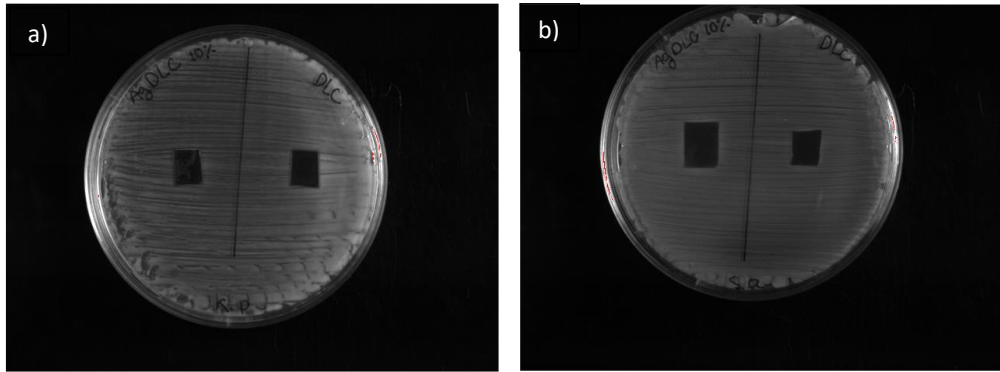


Figure 23 - Images of the Antibacterial tests carried out on silicon (deposition 16): a) *Klebsiella pneumoniae* bacteria was used; b) *Staphylococcus aureus* bacteria was used

By studying *Figure 23*, it possible to observe that the zones of inhibitions are extremely small or inexistent, which means that the presence of the film in the surface of the silicon did not cause an reasonable antibacterial response when interacting with the two types of bacteria, the *klebsiella pneumoniae* bacteria and the *staphylococcus aureus* bacteria .

With all the results in mind, especially the SEM images analysis and the antibacterial results, it was possible to conclude that the film being deposited on the substrates was in some way not allowing the silver particles to segregate to the surface, and to try to solve this issue, a few changes were implemented in the sputtering process. These changes will be explained in chapter 4.1. 2..

4.1.2 Second Series of Depositions

In the second series of depositions, having already a lot of information on how to better control the Ag levels in the deposited films, the main goals were to find a way to give antibacterial properties to the samples and to have a series of samples in which it was possible to compare and correlate the results obtained on XRD, EDS, SEM, Contact Angle and Antibacterial tests.

The first step was to decide on how the magnetron sputtering process specifications needed to be altered so that the Ag segregation problem could be solved. The solution was to have a film with a more open structure, so that the silver could more easily reach the surface of the film. In an open structure, the C and Ag particles tend to agglomerate more easily around each other, almost like having an “anchoring point”, creating a kind of shadow effect that will not allow the deposition of many particles around each agglomerate and creating space between them. Consequently, there will be more space to Ag particles to emerge.

With that in mind, it was decided to have depositions 22 and 23 to test if the sputtering process was still being performed without problems and then start a series of depositions in which the same parameters would be applied in groups of two, in order to have enough samples to run all of the test intended. Throughout this deposition series, there were a few different parameters varied: Ag target power variation, film structure and film

thickness, as it is showed in *Table 7*. The respective Ag at% obtained in the EDS analysis is also included.

Table 7 - Parameters used in the second series of depositions and respective Ag at%.

Deposition Number	Ag Power Variation (W)	Ag at%	Working Pressure (Pa)	Type of film structure	Deposition Time (s)	Theoretical Film Thickness (nm)
Depositions 24/25	70	10	0,8	Compact	160	50
Depositions 26/27	155	12	0,8	Compact	150	50
Depositions 28/29	70	8	1,0	Open	160	50
Depositions 30/31	155	13	1,0	Open	150	50
Depositions 32/33	70	15	1,0	Open	300	100
Depositions 34/35	155	23	1,0	Open	290	100
Depositions 36/37	70	20	1,0	Open	600	200

The first observation that is possible to make by analysing the *Table 7* is the fact that the Ag at% of the films were not as controllable as the ones in the first series, but nonetheless, the results obtained still give important information to try to establish a comparison between the different samples.

As was the case in the first series, the samples were further analysed using 3 different techniques: SEM, Contact Angles and Antibacterial tests. During this second series more parameters were altered on the sputtering process, so firstly an analysis between parameters will be made and later on an overall comparison.

4.1.2.1 SEM images

To have a better perspective on how altering the sputtering process conditions affects the deposited films as well as their interaction with the three substrates, cotton, jersey format and TNT, the samples are analysed and compared taking into consideration that only one of the parameters during the sputtering process differed from sample to sample. So, the comparison is made by only having different Ag at%, then by only having different film structure and finally by only having different film thickness.

At first, the samples were divided into 4 groups: 24/25 - 26/27, 28/29 – 30/31, 32/33 – 34/35 and 36/37. For each group, the films of the samples have the same thickness, the same structure but differ on Ag at%.

The *Figure 24*, shows the SEM images with a 50k magnification of three different substrates corresponding to deposition 24/25 (10 at% Ag, 50nm thickness) and 26/27

(12 at% Ag, 50nm thickness). By analysing the images, it is possible to observe that with the increase in Ag at%, the Ag-DLC film has more well organised and defined agglomerates on the surface, and it is possible to identify Ag particles independently of the type of substrate. On the jersey format case, several cracks can be seen, more abundantly for sample 24/25. The appearance of these cracks may be caused by the fact that the jersey format fabric fibres have a lot of elasticity, and due to the need of handling the fabric to perform the different tests, it might have caused the film to crack.

Regarding the TNT, this kind of image is now more similar to others found in similar studies, in which on TNT fabrics were deposited coatings containing Ag [83]. However, on those cases the Ag at% were much lower to the Ag at% used in these coatings

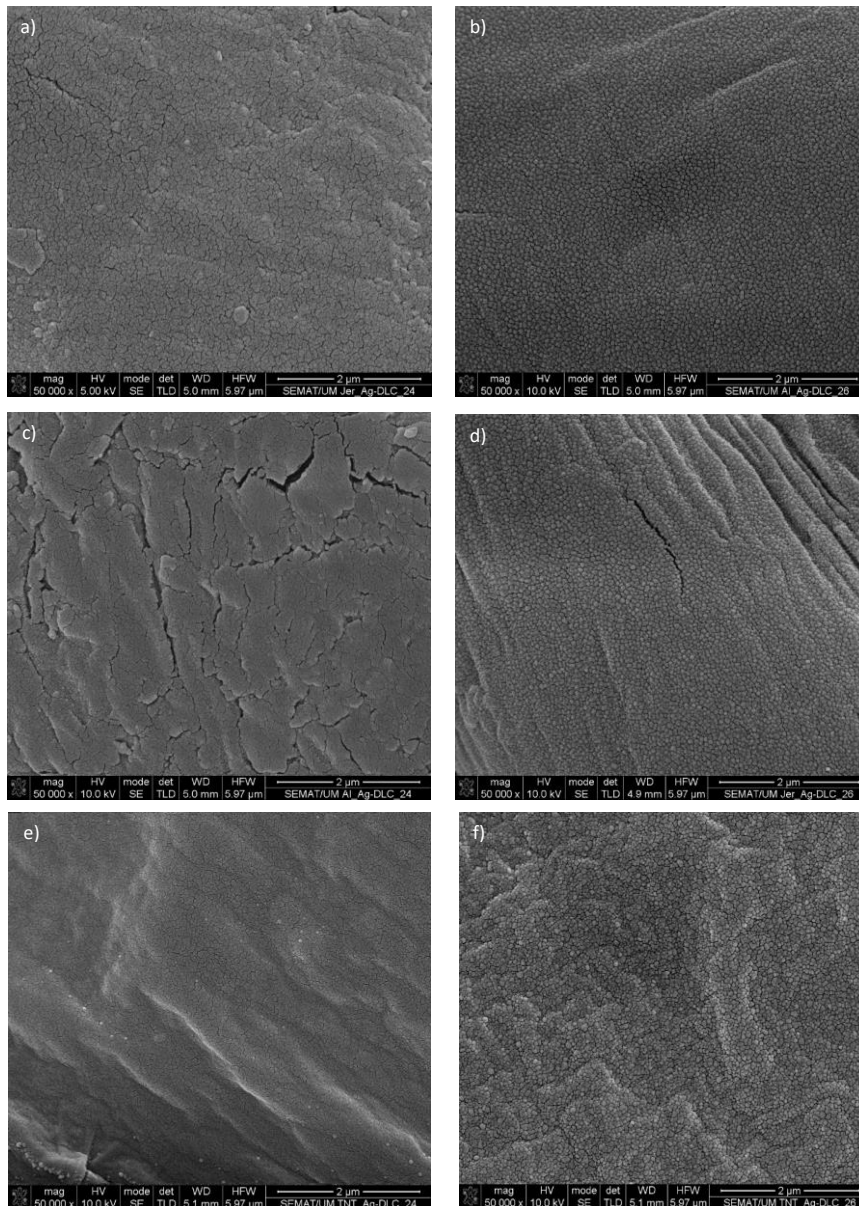


Figure 24 - SEM images (50k magnification) of three different substrates corresponding to deposition 24/25 (10 at% Ag) and 26/27 (12 at% Ag) a) Cotton – deposition 24/25., b) Cotton - deposition 26/27, c) Jersey Format - deposition 24/25, d) Jersey Format - deposition 26/27, e) TNT - deposition 24/25, f) TNT - deposition 26/27.

The same analysis can be made for the case of depositions 28/29 (8 at% Ag, 50nm thickness) and 30/31 (13 at% Ag, 50nm thickness), as shown in *Figure 25*, except that in this case it is not possible to observe the cracks on the jersey format images. In these depositions the film structure is also different from the previous ones. In depositions 28/29 and 30/31 the film structure is open, meaning the structure is less compact and less susceptible to crack, therefore this fact may also be a reason why there are not visible cracks on the jersey format images.

Moreover, the agglomerates seem to be even more easily identified, which might be caused by the fact the film surface structure is more open than in the previous case.

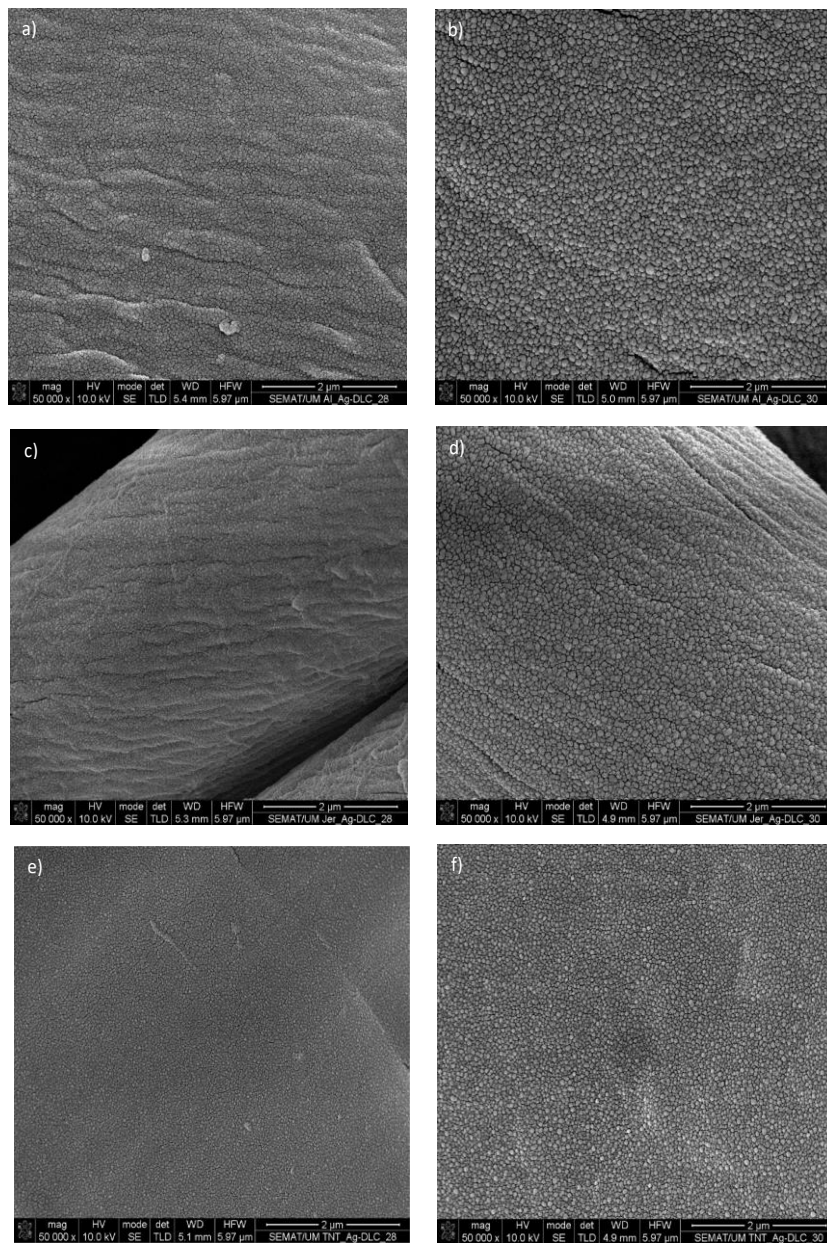


Figure 25 - SEM images (50k magnification) of three different substrates corresponding to deposition 28/29 (8 at% Ag) and 30/31 (13 at% Ag) a) Cotton – deposition 28/29., b) Cotton - deposition 30/31, c) Jersey Format - deposition 28/29, d) Jersey Format - deposition 30/31, e) TNT - deposition 28/29, f) TNT - deposition 30/31.

On *Figure 26*, SEM images of depositions 32/33 (15 at% Ag, 100nm thickness) and 34/35 (23 at% Ag, 100nm thickness) are displayed. In this case, the increase in Ag at% seems to cause an increase in size of each agglomerate, independently of the substrate. Also, when comparing samples 32/33 with the samples with thinner films (50 nm) and similar Ag at%, samples 30/31, it is possible to observe an increase in the agglomerates' sizes, supporting the idea that the film thickness influences this aspect of the film.

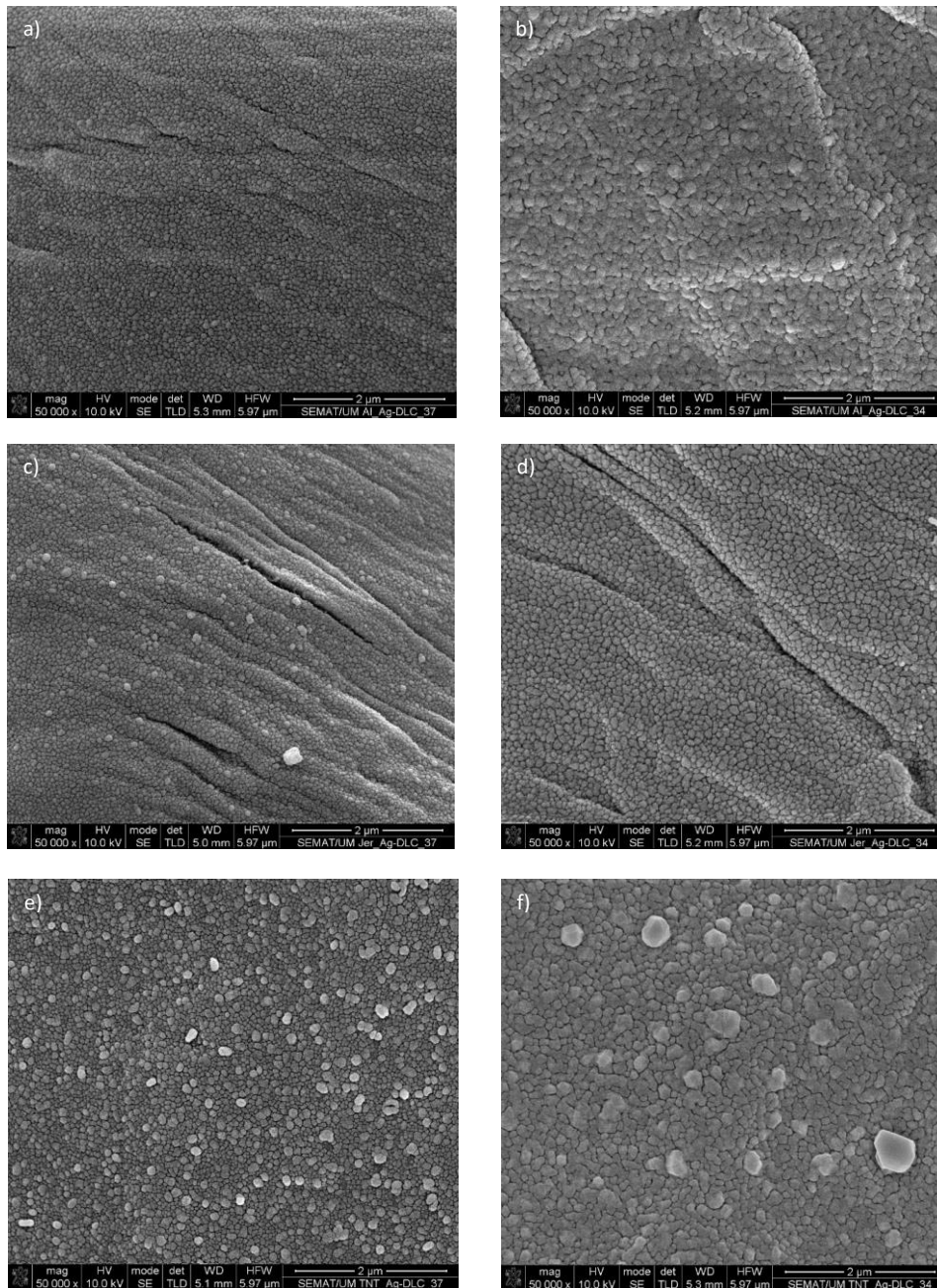


Figure 26 - SEM images (50k magnification) of three different substrates corresponding to deposition 32/33 (15 at% Ag) and 34/35 (23 at% Ag) a) Cotton – deposition 32/33., b) Cotton - deposition 34/35, c) Jersey Format - deposition 32/33, d) Jersey Format - deposition 34/35, e) TNT - deposition 32/33, f) TNT - deposition 34/35.

On *Figure 27* it is displayed the SEM images of deposition 36/37 (20 at% Ag, 200nm thickness). This is the sample with the thickest film, and due to this fact, the agglomerates are much bigger and the fissures/space between them are more easily identified when compared to previous samples. Before the SEM analysis process, the film deposited on the jersey format fabric of this deposition unstuck, and therefore it was not analysed. This problem of fabric/film adhesion may be linked with the thickness of the film, as this issue only occurred for the thickest film. Also, this only happened for the jersey format fabric, probably due to the elasticity of the fabric.

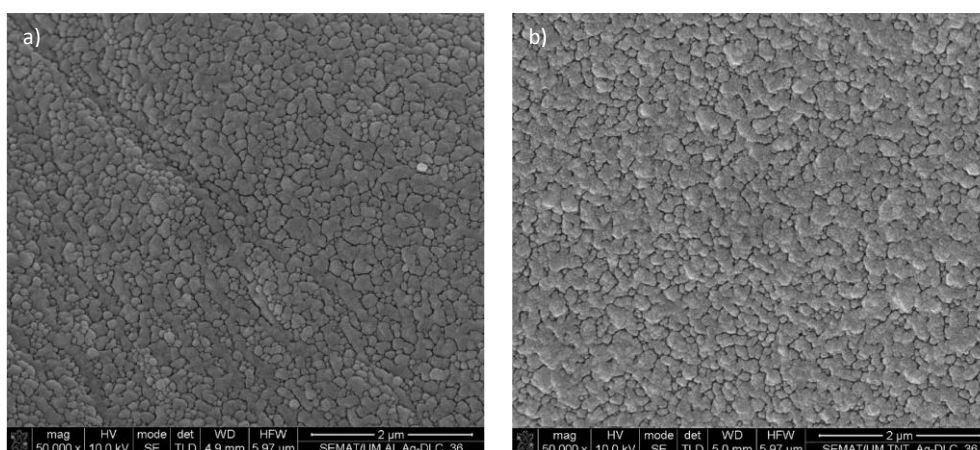


Figure 27 - SEM images (50k magnification) of two different substrates corresponding to deposition 36/37 (20 at% Ag) a) Cotton – deposition 36/37., b) TNT - deposition 36/37.

Figure 28, shows the SEM images with a 50k magnification of three different substrates corresponding to deposition 26/27 (12 at% Ag, 50nm thickness) and 30/31 (13 at% Ag, 50nm thickness). On this analysis, it is the difference in film structure that is being focused on, as the thickness and Ag at% are very similar, but for deposition 26/27 the film structure is compact but for deposition 30/31 the film structure is open.

In order to obtain these two structures, during the deposition process it was applied a variation in pressure inside the chamber, With the increase in pressure it was possible to obtain a more open and less compact structure. This comparison of samples with different film structures aims to check if Ag can more easily segregate to the surface when the film is less compact.

For cotton and jersey format samples, the agglomerates are indeed bigger and more easily identified for the open structure case. However, the same cannot be said for the TNT sample, as the film seems to be almost identical for both structures.

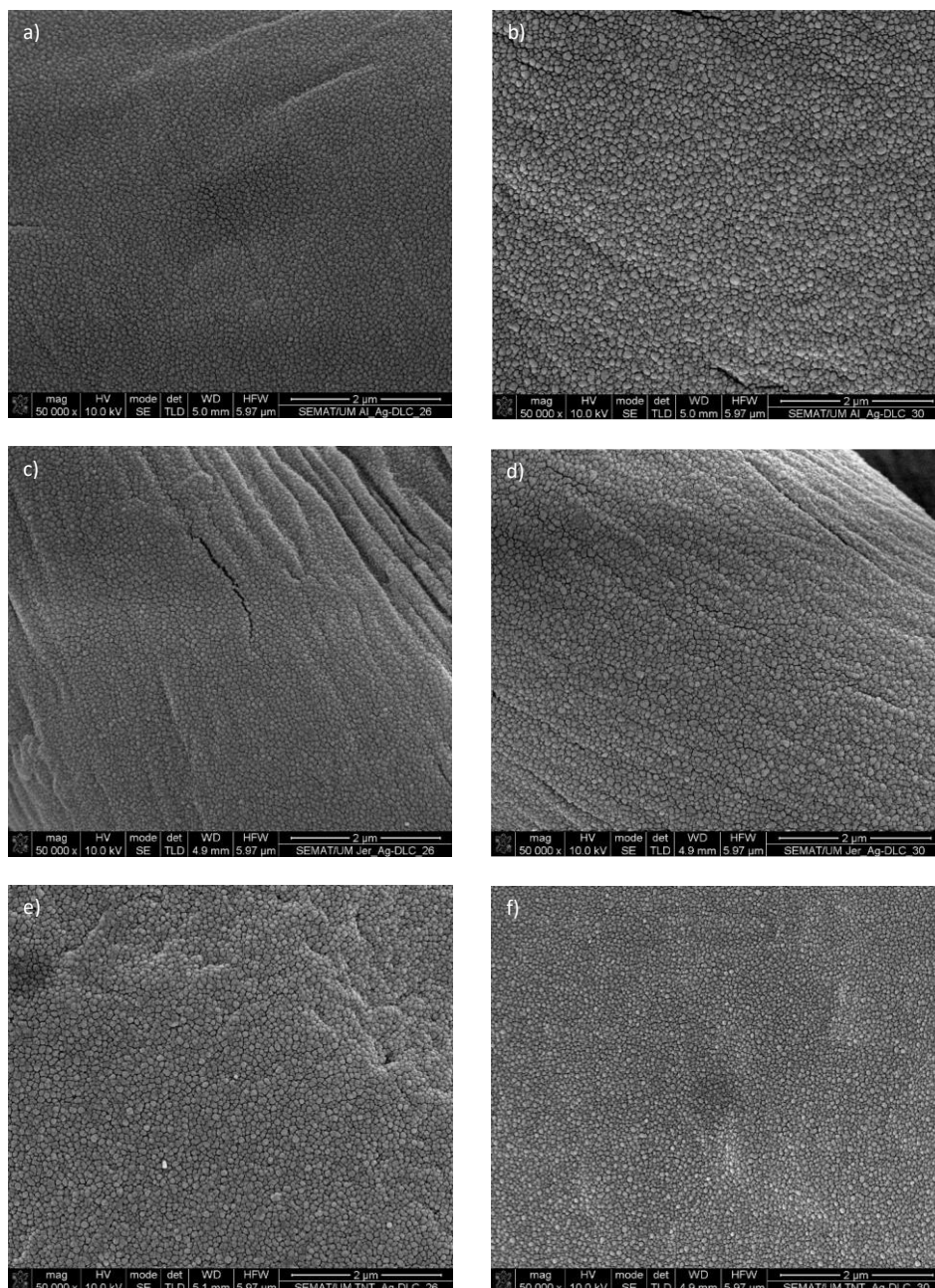


Figure 28 - SEM images (50k magnification) of three different substrates corresponding to deposition 26/27 (12 at% Ag) and 30/31 (13 at% Ag) a) Cotton – deposition 26/27., b) Cotton - deposition 30/31, c) Jersey Format - deposition 26/27, d) Jersey Format - deposition 30/31, e) TNT - deposition 26/27, f) TNT - deposition 30/31.

In Figure 29, there are displayed two samples with different film thickness, but similar Ag at% and same film structure, corresponding to depositions 34/35 (23 at% Ag, 100nm thickness) and 36/37 (20at % Ag, 200nm thickness). As expected, it is sample 36/37 that shows a film with bigger agglomerates, although they both have a similar surface organization. The jersey format images were not analysed for the same reason as mentioned before.

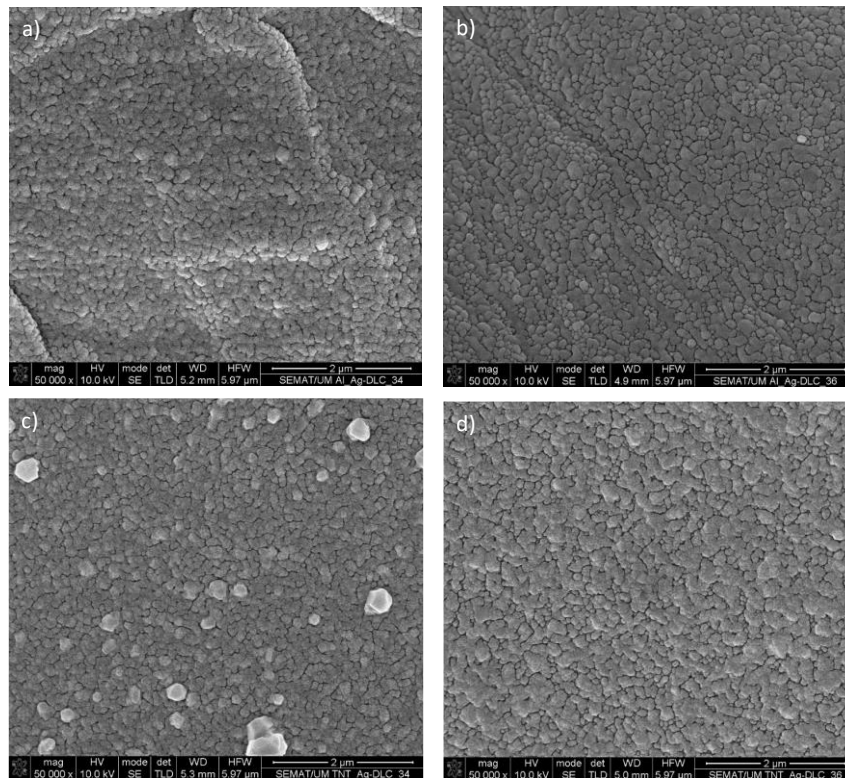


Figure 29 - SEM images (50k magnification) of two different substrates corresponding to deposition 34/35 (23 at% Ag) and to deposition 36/37 (20 at% Ag): a) Cotton – deposition 34/35, b) Cotton - deposition 36/37, c) TNT – deposition 34/35, d) TNT – deposition 36/37.

4.1.2.2 Antibacterial tests analysis

To evaluate the antibacterial activity of the samples, a Zone of Inhibition Test was performed to all samples. As explained in chapter 3, two types of bacteria were used for this evaluation, and in most cases is easy to identify a zone of inhibition, independently of the type of bacteria and the type of fabric, when comparing them with their virgin counterpart. However, there are cases in which the zone of inhibition is more easily identified, and it seems that several factors are affecting their inhibition efficiency: % of Ag, thickness of the film, type of bacteria and the type of fabric. In *Figure 30* it is shown the zone of inhibitions test images of the virgin samples, in which it is possible to observe that there no inhibition zones, and therefore no antibacterial properties can be associated with the virgin samples, as with was expected [84].

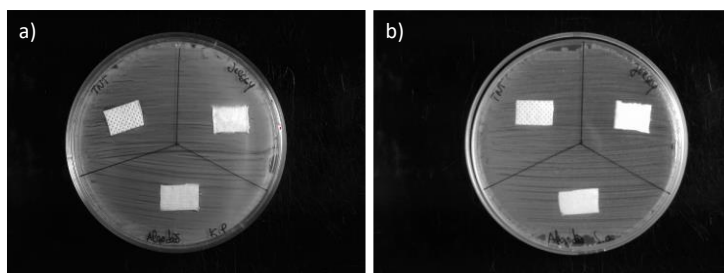


Figure 30 – Zones of inhibitions test images of virgin samples: a) *klebsiella pneumoniae* bacteria, b) *staphylococcus aureus* bacteria

As shown on *Figure 31*, on the tests using the bacteria *klebsiella pneumoniae*, only the samples 32 and 36 do not show a zone of inhibition and sample 30 displays small and irregular halos. In the case of the bacteria *staphylococcus aureus*, all the samples showed zones of inhibition, however, samples 34 and 36 display more irregular halos.

The samples with the highest thickness seem to show the worst results for antibacterial inhibition, especially for TNT and Jersey format samples. The samples with lowest thickness and with at% of Ag between 7 at% and 13 at% (samples 24, 26, 28 and 30) show a good antibacterial response, and all have similar zones of inhibition for both bacteria. These results may indicate that film thickness affects the way Ag interacts with bacteria. When considering the type of fabric, TNT seems to have the lowest antibacterial response, as in some samples its zone of inhibition is minimal and lower than the zones of the other two fabrics.

Regarding the *staphylococcus aureus* bacteria tests, the results obtained for the cotton and jersey format samples with the thinnest coating are similar to the results obtained in other study in which a DLC/Ag coating was deposited on silk, which is a woven fabric like cotton and jersey format [50].

One thing to take into consideration, is the fact that in this type of antibacterial test it is impossible to quantify the amount of the antimicrobial agent diffused into the medium surrounding the samples [85]. So it is not possible to know which samples are releasing more Ag or if the samples with the thickest film are releasing much less than the others.

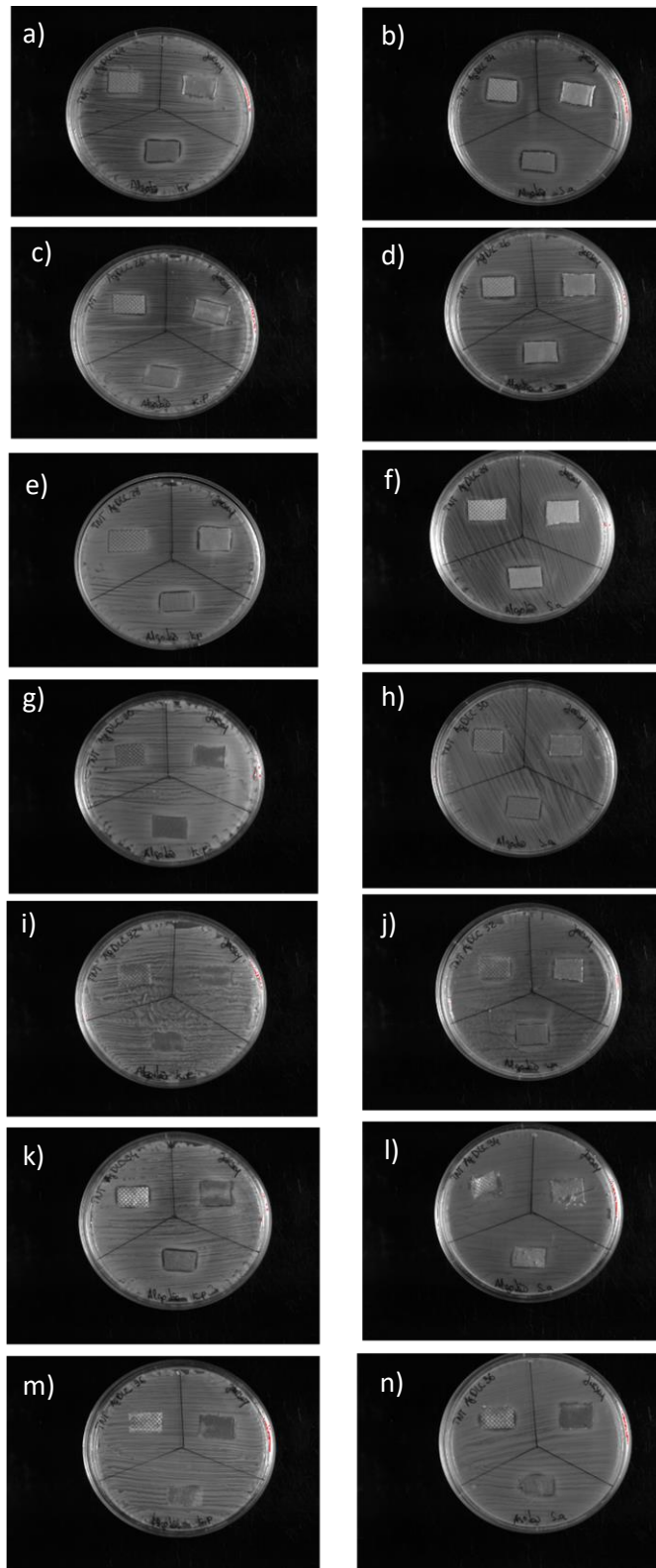


Figure 31 – Zone of inhibition tests images of all samples for both bacteria, klebsiella pneumoniae on the left column and Staphylococcus aureus on the right column: a/b) Sample 24, c/d) Sample 26, e/f) Sample 28, g/h) Sample 30, i/j) Sample 32, k/l) Sample 34, m/n) Sample 36

In addition to the Zone of inhibition tests, SEM images of the samples that went through the zone of inhibition test were also taken, to verify if it was possible to identify the

presence of bacteria on the samples. Due to lack of time, only images of samples 24, 26 and of the virgin fabrics were obtained. On *Figure 32*, *Figure 33* and *Figure 34* are displayed, by fabric, the images obtained from sample 26 (12 at% Ag) and their respective virgin samples.

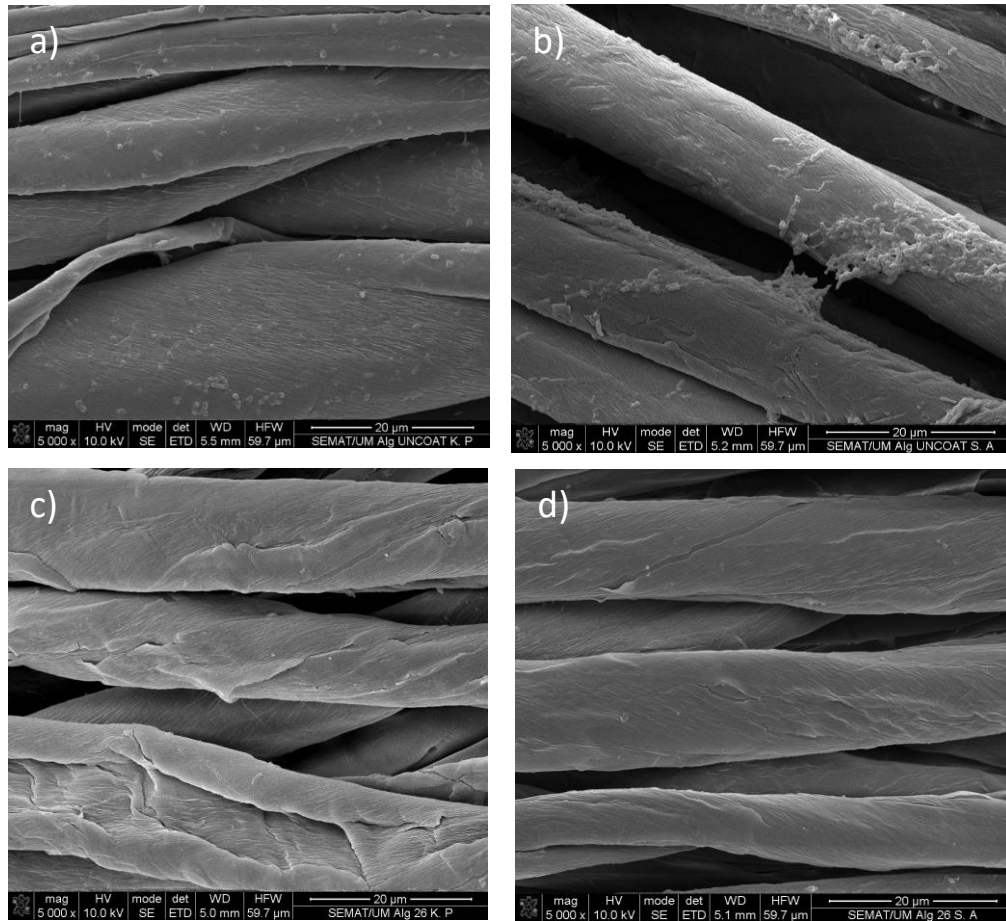


Figure 32 – SEM images of virgin cotton and cotton from sample 26 after the zone of inhibition test: a) Virgin cotton - *klebsiella pneumoniae*, b) Virgin cotton - *staphylococcus aureus*, c) Cotton 26 - *klebsiella pneumoniae*, d) Cotton 26 - *staphylococcus aureus*.

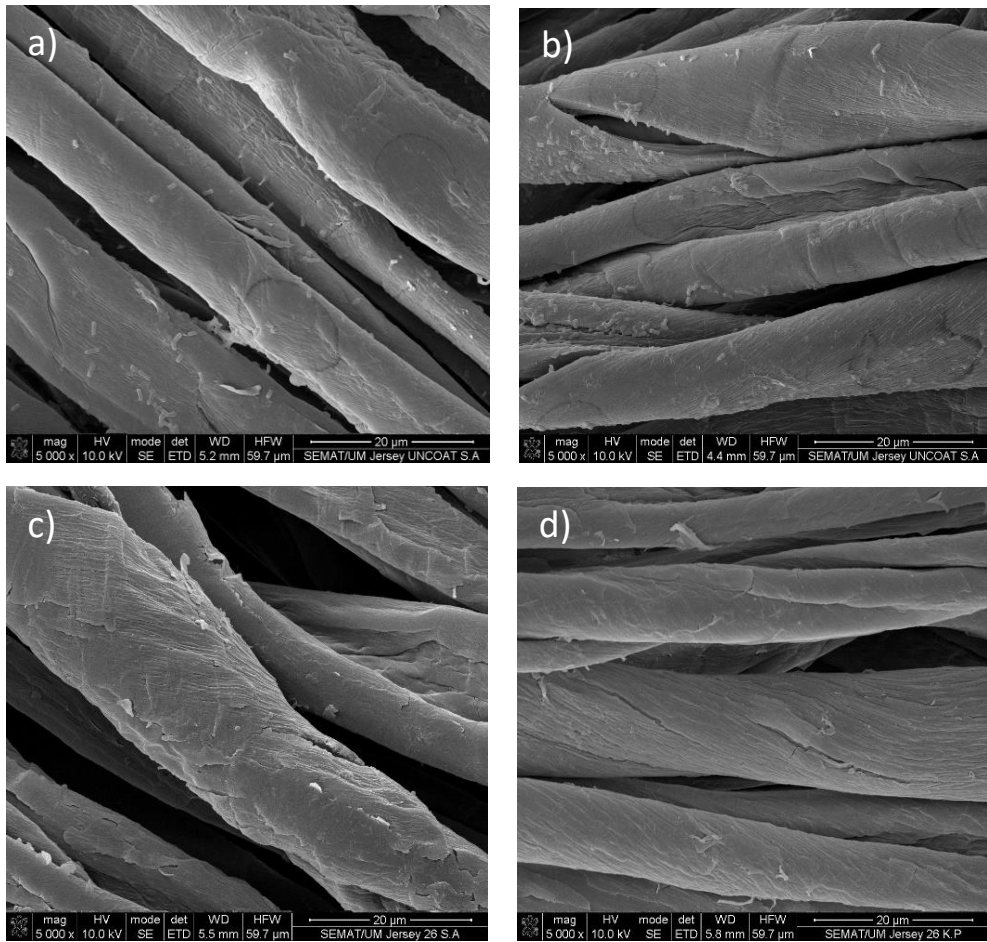


Figure 33 - SEM images of virgin jersey format fabric and jersey format fabric from sample 26 after the zone of inhibition test: a) Virgin jersey format - *klebsiella pneumoniae*, b) Virgin jersey format - *staphylococcus aureus*, c) jersey format 26 - *klebsiella pneumoniae*, d) jersey format 26 - *staphylococcus aureus*.

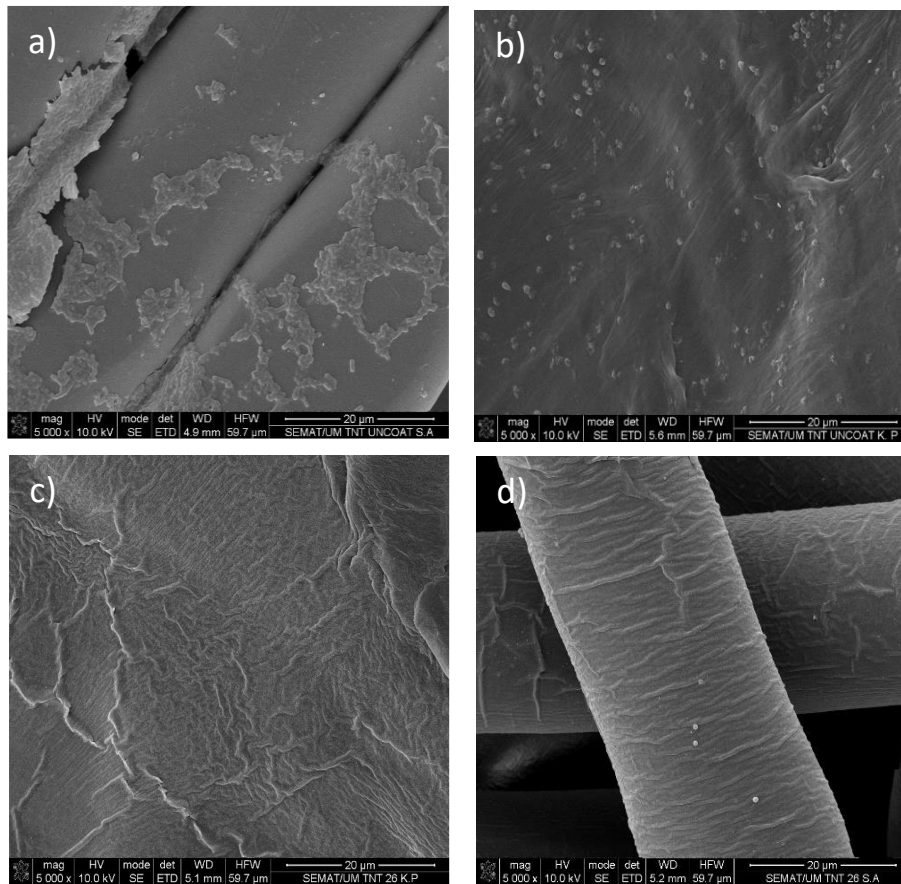


Figure 34 - SEM images of virgin TNT and TNT from sample 26 after the zone of inhibition test: a) Virgin TNT - klebsiella pneumoniae, b) Virgin TNT - staphylococcus aureus, c) TNT 26 - klebsiella pneumoniae, d) TNT 26 - staphylococcus aureus.

By analysing the figures above, it is possible to observe that for all three coated substrates, there is not any bacteria present on the surface, independently of the type of bacteria, demonstrating they indeed have antibacterial activity, as was expected due to the results obtained in the zone of inhibition test.

On the case of the virgin samples, they did not show any antibacterial activity in the zone of inhibition test and the same can be said by studying the images above. It is possible to see the presence of bacteria colonies on all the fabrics.

It is also important to refer that after the zone of inhibition tests, it was possible to observe the presence of Ag particles on the surface of all three substrates, *Figure 35*, meaning that the film still retained the ability to segregate Ag to the surface after having antibacterial activity.

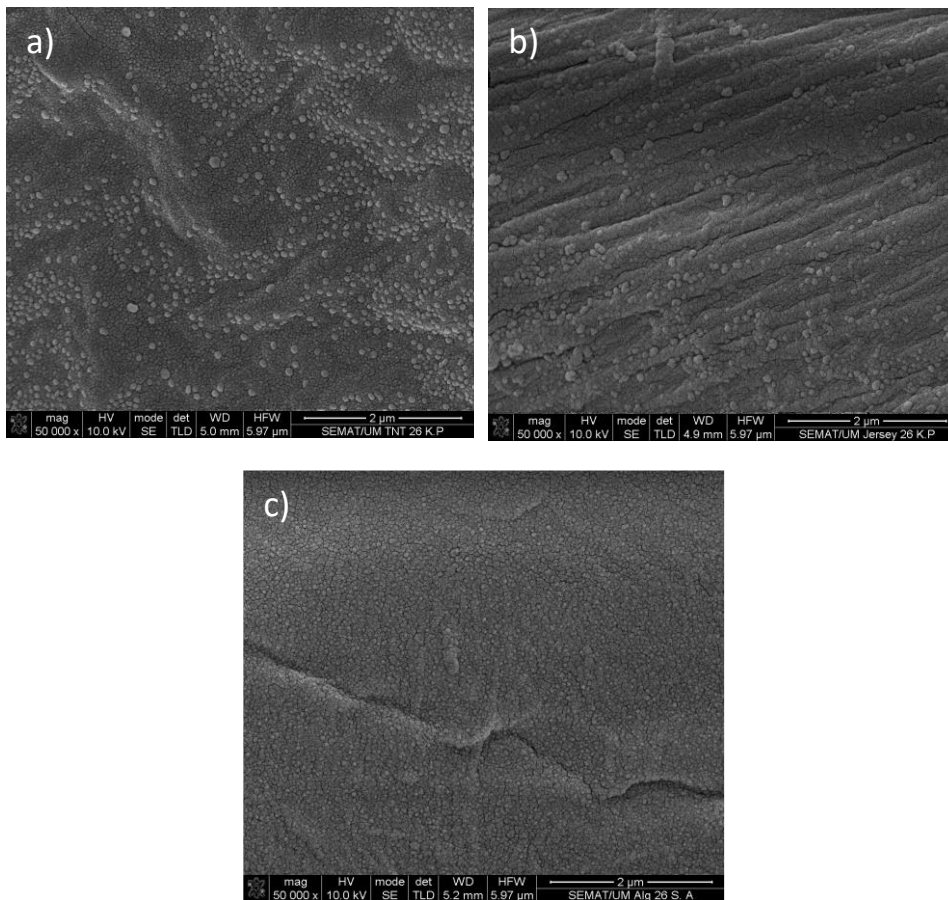


Figure 35 – SEM images of the substrates of sample 26 after the antibacterial test: a) cotton, b) jersey format, c) TNT.

4.1.2.3 Contact angles analysis

The Contact Angles test results are shown on *Table 8*. One conclusion that can be taken from this table is that all samples seem to have hydrophobic characteristics, independently of the Ag at%, film structure or film thickness. Also, it appears it is the cotton fabric that gains more in terms of hydrophobic properties, as the virgin cotton is hydrophilic but with the addition of the film its contact angle values almost double in every sample.

Furthermore, between samples with the same film structure and film thickness, samples 24/25 – 26/27, 28/29 – 30/31, it is possible to identify an increase in the contact angle when there is also an increase in Ag at%, except when comparing samples 32/33 and 34/35. In that particular case, the contrary happens, which might suggest that film thickness may have an influence on the hydrophobic properties of the samples. Other than that, is hard to identify any particularity between samples.

Table 8 - Contact Angle results for Cotton, Jersey Format and TNT. These results are correspondent to a surface-water analysis.

Deposition Number	Cotton	Jersey Format	TNT
Virgin Samples	60.73 ° ± 4.82	108.18 ° ± 1.73	114.87 ° ± 3.41
Deposition 24/25 (10 at% Ag)	121.90° ± 1.55	94.63 ° ± 1.66	109.49° ± 1.84
Deposition 26/27 (12 at% Ag)	126.30° ± 2.60	119.50 ° ± 9.81	121.20 ° ± 3.24
Deposition 28/29 (8 at% Ag)	107.60° ± 4.56	108.20° ± 14.00	99.40° ± 4.37
Deposition 30/31 (13 at% Ag)	115.26 ° ± 7.11	131.27 ° ± 7.31	115.70 ° ± 3.62
Deposition 32/33 (15 at% Ag)	137.70 ° ± 9.70	125.90 ° ± 12.55	116.00 ° ± 2.55
Deposition 34/35 (23 at% Ag)	117.20 ° ± 1.9	106.10 ° ± 1.62	112.70 ° ± 0.85
Deposition 36/37 (20 at% Ag)	117.8 ° ± 3.90	149.03 ° ± 5.02	116.90 ° ± 1.79

4.2 Overall Discussion

After analysing all the results obtained from the second series of depositions, it is important to check if it is possible to make a correlation between the different properties of the films. On *Table 9* it is presented a summary of all the results discussed before.

Table 9 – Summary of the results obtained in EDS, SEM and Antibacterial Tests

Deposition Number	Ag at%	Hydrophobic Properties	Antibacterial Properties (<i>klebsiella pneumoniae</i>)	Antibacterial Properties (<i>staphylococcus aureus</i>)	Type of film Structure	Film Thickness (nm)
Deposition 24/25	10	Hydrophobic	Yes	Yes	Compact	50
Deposition 26/27	12	Hydrophobic	Yes	Yes	Compact	50
Deposition 28/29	8	Hydrophobic	Yes	Yes	Open	50
Deposition 30/31	13	Hydrophobic	Irregular	Yes	Open	50
Deposition 32/33	15	Hydrophobic	No	Yes	Open	100
Deposition 34/35	23	Hydrophobic	Yes	Irregular	Open	100
Deposition 36/37	20	Hydrophobic	No	Irregular	Open	200

The first point to be made is regarding the hydrophobic properties of the samples. One of the main objectives of this project was to have coated fabrics with hydrophobic characteristics, and overall, the film seemed to improve or maintain that across the three fabrics.

Secondly, after the antibacterial activity results obtained from the first series of depositions, it was not expected that depositions 24/25 and 26/27, which have a compact film structure, had these antibacterial activity results. The fact the structure was compact does not seem to influence the antibacterial properties of the substrates, at least for Ag at% equal or above 10.

When considering the samples with an open film structure, it seems that with an increase in the film thickness, the antibacterial activity becomes more irregular, especially for gram-negative bacteria (*klebsiella pneumoniae*). And even if the films have a higher Ag at%, that seems not to improve the antibacterial activity.

Finally, one of the correlations that can be made is the fact that the Ag-DLC film had a better performance with a 50nm thickness, for both compact and open film structures.

5. Conclusion and Future Research

In the beginning of this project, one of the main concerns was if the MS process could be used to apply coatings to the textiles chosen. After analysing the results obtained throughout the project, it is possible to conclude that the technology can indeed be used, and with some good results. The textile fibers did not seem to be damaged in the sputtering process and the coating seemed to have a good adhesion to them, except for the case in which the thickest coating (200nm) was deposited on the jersey format fabric. This may be an indication that the coating has a lower adhesion to the jersey format fabric.

Moreover, one of the main goals was to give hydrophobic properties to the textiles, and that was accomplished for all three textiles. However, the antibacterial results were not as satisfactory as the hydrophobic ones. Most of the samples seemed to have antibacterial properties, for both gram-positive and gram-negative bacteria, but a few of the samples displayed irregular results. What might have caused these irregularities is unknown and should be studied further in order to realise if it might be caused by the type of the film structure, by a higher Ag at%, by the thickness of the film or by a combination of any of these. Also, the increase of the film thickness seems to have a negative impact in the samples' antibacterial properties. Regarding the type of film structure, there is only information for thin compact structures (50nm) and not for thicker ones, so it is not possible to know how thick (100nm and 200nm) compact films would perform.

Through the study of all the data gathered during the project, it seems that there are two depositions that stand out from the rest: depositions 24/25 and 26/27. Both these depositions have compact thin films (50nm) and similar Ag at% (10% and 12 at% respectively), and both display hydrophobic and good antibacterial properties for all three substrates.

When considering the type of fabric, cotton is the one that seems to have a better overall performance and the one that benefits the most by the presence of the film, as it was able to provide cotton hydrophobic properties that it did not have prior to the deposition, as well as displaying good antibacterial properties. The TNT fabric was the one that displayed the most irregular antibacterial results, and the jersey format fabric had an ok overall performance, however, the fact that it might exist an adhesion issue is a point of concern.

There are also more characterization analysis that can be performed in the future that are of interest. Due to the possible applications of the technology studied in this project, it would also be interesting to evaluate how the coated textiles would perform in air filtration and breathability tests, evaluate for how long the coating retains hydrophobic and antibacterial properties or evaluate if any of the coated textiles could be washed and reused.

Also, only three different textiles were tested. There are a lot more textiles of interest for biomedical applications that could also benefit from the application of coating like the one done in this project. Furthermore, only antibacterial capability was tested, and it would be interesting to know, especially because of the pandemic period the world has been on, if the coated textiles have also antiviral properties.

Finally, regarding the deposition process, there could also be some further parameters modifications applied for future research, so that different densities, Ag at% and different

thicknesses can all be studied, as well as check if a DC MS could also be used with success.

6. References

1. Chua, M.H.; Cheng, W.; Goh, S.S.; Kong, J.; Li, B.; Lim, J.Y.C.; Mao, L.; Wang, S.; Xue, K.; Yang, L.; et al. Face Masks in the New COVID-19 Normal: Materials, Testing, and Perspectives. *Research* **2020**, *2020*, 1–40, doi:10.34133/2020/7286735.
2. Karim, N.; Afroj, S.; Lloyd, K.; Oaten, L.C.; Andreeva, D. V.; Carr, C.; Farmery, A.D.; Kim, I.D.; Novoselov, K.S. Sustainable personal protective clothing for healthcare applications: A review. *ACS Nano* **2020**, *14*, 12313–12340, doi:10.1021/acsnano.0c05537.
3. O'Dowd, K.; Nair, K.M.; Forouzandeh, P.; Mathew, S.; Grant, J.; Moran, R.; Bartlett, J.; Bird, J.; Pillai, S.C. Face masks and respirators in the fight against the COVID-19 pandemic: A review of current materials, advances and future perspectives. *Materials (Basel)*. **2020**, *13*, doi:10.3390/ma13153363.
4. Morais, D.S.; Guedes, R.M.; Lopes, M.A. Antimicrobial approaches for textiles: From research to market. *Materials (Basel)*. **2016**, *9*, 1–21, doi:10.3390/ma9060498.
5. Li, G.; Liu, H.; Li, T.; Wang, J. Surface modification and functionalization of silk fibroin fibers/fabric toward high performance applications. *Mater. Sci. Eng. C* **2012**, *32*, 627–636, doi:10.1016/j.msec.2011.12.013.
6. Wang, H.; Wei, Q.; Gao, W. Sputter deposition of antibacterial nano-silver on PLA nonwoven medical dressings. *AATCC Rev.* **2009**, *9*, 34–37.
7. Jelil, R.A. *A review of low-temperature plasma treatment of textile materials*; Springer US, 2015; Vol. 50; ISBN 1085301591524.
8. Peralta-Videa, J.R.; Zhao, L.; Lopez-Moreno, M.L.; de la Rosa, G.; Hong, J.; Gardea-Torresdey, J.L. Nanomaterials and the environment: A review for the biennium 2008–2010. *J. Hazard. Mater.* **2011**, *186*, 1–15, doi:10.1016/j.jhazmat.2010.11.020.
9. Kitahara, N.; Sato, T.; Isogawa, H.; Ohgoe, Y.; Masuko, S.; Shizuku, F.; Hirakuri, K.K. Antibacterial property of DLC film coated on textile material. *Diam. Relat. Mater.* **2010**, *19*, 690–694, doi:10.1016/j.diamond.2010.03.013.
10. Carvalho, I.; Curado, M.; Palacio, C.; Carvalho, S.; Cavaleiro, A. Ag release from sputtered Ag/a:C nanocomposite films after immersion in pure water and NaCl solution. *Thin Solid Films* **2019**, *671*, 85–94, doi:10.1016/j.tsf.2018.12.010.
11. Murphy, F.; Tchetchik, A.; Furxhi, I. Reduction of Health Care-Associated Infections (HAIs) with Antimicrobial Inorganic Nanoparticles Incorporated in Medical Textiles: An Economic Assessment. *Nanomaterials* **2020**, *10*, 999, doi:10.3390/nano10050999.
12. Fijan, S.; Turk, S.Š. Hospital Textiles, Are They a Possible Vehicle for Healthcare-Associated Infections? *Int. J. Environ. Res. Public Health* **2012**, *9*, 3330–3343, doi:10.3390/ijerph9093330.
13. Huang, H.; Fan, C.; Li, M.; Nie, H.L.; Wang, F.B.; Wang, H.; Wang, R.; Xia, J.; Zheng, X.; Zuo, X.; et al. COVID-19: A Call for Physical Scientists and Engineers. *ACS Nano* **2020**, *14*, 3747–3754, doi:10.1021/acsnano.0c02618.
14. Kilinc, F.S. A Review of Isolation Gowns in Healthcare: Fabric and Gown Properties. *J. Eng. Fiber. Fabr.* **2015**, *10*, 180–190, doi:10.1177/155892501501000313.
15. Leonas, K.K.; Jenkins, R.S. The relationship of selected fabric characteristics and the barrier effectiveness of surgical gown fabrics. *Am. J. Infect. Control* **1997**, *25*, 16–23, doi:10.1016/S0196-6553(97)90048-1.
16. Aldalbahi, A.; El-Naggar, M.E.; El-Newehy, M.H.; Rahaman, M.; Hatshan, M.R.; Khattab, T.A. Effects of technical textiles and synthetic nanofibers on environmental pollution. *Polymers (Basel)*. **2021**, *13*, 1–26, doi:10.3390/polym13010155.

17. Gorberg, B.L.; Ivanov, A.A.; Mamontov, O. V.; Stegnin, V.A.; Titov, V.A. Modification of textile materials by the deposition of nanocoatings by magnetron ion-plasma sputtering. *Russ. J. Gen. Chem.* **2013**, *83*, 157–163, doi:10.1134/S1070363213010350.
18. Virk, R.K.; Ramaswamy, G.N.; Bourham, M.; Bures, B.L. Plasma and Antimicrobial Treatment of Nonwoven Fabrics for Surgical Gowns. *Text. Res. J.* **2004**, *74*, 1073–1079, doi:10.1177/004051750407401208.
19. Thyavihalli Girijappa, Y.G.; Mavinkere Rangappa, S.; Parameswaranpillai, J.; Siengchin, S. Natural Fibers as Sustainable and Renewable Resource for Development of Eco-Friendly Composites: A Comprehensive Review. *Front. Mater.* **2019**, *6*, 1–14, doi:10.3389/fmats.2019.00226.
20. Guo, Z.-D.; Wang, Z.-Y.; Zhang, S.-F.; Li, X.; Li, L.; Li, C.; Cui, Y.; Fu, R.-B.; Dong, Y.-Z.; Chi, X.-Y.; et al. Aerosol and Surface Distribution of Severe Acute Respiratory Syndrome Coronavirus 2 in Hospital Wards, Wuhan, China, 2020. *Emerg. Infect. Dis.* **2020**, *26*, 1583–1591, doi:10.3201/eid2607.200885.
21. Bshena, O.; Heunis, T.D.; Dicks, L.M.; Klumperman, B. Antimicrobial fibers: therapeutic possibilities and recent advances. *Future Med. Chem.* **2011**, *3*, 1821–1847, doi:10.4155/fmc.11.131.
22. Windler, L.; Height, M.; Nowack, B. Comparative evaluation of antimicrobials for textile applications. *Environ. Int.* **2013**, *53*, 62–73, doi:10.1016/j.envint.2012.12.010.
23. Shahidi, S.; Wiener, J. Antibacterial Agents in Textile Industry. In *Antimicrobial Agents*; InTech, 2012.
24. Eikenberry, S.E.; Mancuso, M.; Iboi, E.; Phan, T.; Eikenberry, K.; Kuang, Y.; Kostelich, E.; Gumel, A.B. To mask or not to mask: Modeling the potential for face mask use by the general public to curtail the COVID-19 pandemic. *Infect. Dis. Model.* **2020**, *5*, 293–308, doi:10.1016/j.idm.2020.04.001.
25. Zhu, N.; Zhang, D.; Wang, W.; Li, X.; Yang, B.; Song, J.; Zhao, X.; Huang, B.; Shi, W.; Lu, R.; et al. A Novel Coronavirus from Patients with Pneumonia in China, 2019. *N. Engl. J. Med.* **2020**, *382*, 727–733, doi:10.1056/NEJMoa2001017.
26. Tcharkhtchi, A.; Abbasnezhad, N.; Zarbini Seydani, M.; Zirak, N.; Farzaneh, S.; Shirinbayan, M. An overview of filtration efficiency through the masks: Mechanisms of the aerosols penetration. *Bioact. Mater.* **2021**, *6*, 106–122, doi:10.1016/j.bioactmat.2020.08.002.
27. Yi, L.; Fengzhi, L.; Qingyong, Z. Numerical simulation of virus diffusion in facemask during breathing cycles. *Int. J. Heat Mass Transf.* **2005**, *48*, 4229–4242, doi:10.1016/j.ijheatmasstransfer.2005.03.030.
28. Li, Y.; Leung, P.; Yao, L.; Song, Q.W.; Newton, E. Antimicrobial effect of surgical masks coated with nanoparticles. *J. Hosp. Infect.* **2006**, *62*, 58–63, doi:10.1016/j.jhin.2005.04.015.
29. Hashmi, M.; Ullah, S.; Kim, I.S. Copper oxide (CuO) loaded polyacrylonitrile (PAN) nanofiber membranes for antimicrobial breath mask applications. *Curr. Res. Biotechnol.* **2019**, *1*, 1–10, doi:10.1016/j.crbiot.2019.07.001.
30. Sunjaya, A.P.; Jenkins, C. Rationale for universal face masks in public against <sc>COVID</sc> -19. *Respirology* **2020**, *25*, 678–679, doi:10.1111/resp.13834.
31. Sousa-Pinto, B.; Fonte, A.P.; Lopes, A.A.; Oliveira, B.; Fonseca, J.A.; Costa-Pereira, A.; Correia, O. Face masks for community use: An awareness call to the differences in materials. *Respirology* **2020**, *25*, 894–895, doi:10.1111/resp.13891.
32. Rodriguez-Martinez, C.E.; Sossa-Briceño, M.P.; Cortés, J.A. Decontamination and reuse of N95 filtering facemask respirators: A systematic review of the literature. *Am. J. Infect. Control* **2020**, *48*, 1520–1532, doi:10.1016/j.ajic.2020.07.004.

33. Palza, H. Antimicrobial Polymers with Metal Nanoparticles. *Int. J. Mol. Sci.* **2015**, *16*, 2099–2116, doi:10.3390/ijms16012099.
34. Xu, F.F.; Imlay, J.A. Silver(I), Mercury(II), Cadmium(II), and Zinc(II) Target Exposed Enzymic Iron-Sulfur Clusters when They Toxicify Escherichia coli. *Appl. Environ. Microbiol.* **2012**, *78*, 3614–3621, doi:10.1128/AEM.07368-11.
35. Yuan Gao; Cranston, R. Recent Advances in Antimicrobial Treatments of Textiles. *Text. Res. J.* **2008**, *78*, 60–72, doi:10.1177/0040517507082332.
36. Rahman, M.A.; Ahsan, T.; Islam, S. Antibacterial and antifungal properties of the methanol extract from the stem of *Argyrea argentea*. *Bangladesh J. Pharmacol.* **2010**, *5*, doi:10.3329/bjp.v5i1.4700.
37. Radhouani, H.; Silva, N.; Poeta, P.; Torres, C.; Correia, S.; Igrejas, G. Potential impact of antimicrobial resistance in wildlife, environment and human health. *Front. Microbiol.* **2014**, *5*, doi:10.3389/fmicb.2014.00023.
38. Nwosu, V.C. Antibiotic resistance with particular reference to soil microorganisms. *Res. Microbiol.* **2001**, *152*, 421–430, doi:10.1016/S0923-2508(01)01215-3.
39. Reidy, B.; Haase, A.; Luch, A.; Dawson, K.; Lynch, I. Mechanisms of Silver Nanoparticle Release, Transformation and Toxicity: A Critical Review of Current Knowledge and Recommendations for Future Studies and Applications. *Materials (Basel)*. **2013**, *6*, 2295–2350, doi:10.3390/ma6062295.
40. Randall, C.P.; Gupta, A.; Jackson, N.; Busse, D.; O'Neill, A.J. Silver resistance in Gram-negative bacteria: a dissection of endogenous and exogenous mechanisms. *J. Antimicrob. Chemother.* **2015**, doi:10.1093/jac/dku523.
41. Schneider, G. Antimicrobial silver nanoparticles - Regulatory situation in the European Union. *Mater. Today Proc.* **2017**, *4*, S200–S207, doi:10.1016/j.matpr.2017.09.187.
42. Percival, S.L.; Bowler, P.G.; Russell, D. Bacterial resistance to silver in wound care. *J. Hosp. Infect.* **2005**, *60*, 1–7, doi:10.1016/j.jhin.2004.11.014.
43. Hahn, A.; Brandes, G.; Wagener, P.; Barcikowski, S. Metal ion release kinetics from nanoparticle silicone composites. *J. Control. Release* **2011**, *154*, 164–170, doi:10.1016/j.jconrel.2011.05.023.
44. Bechert, T.; Böswald, M.; Lugauer, S.; Regenfus, A.; Greil, J.; Guggenbichler, J.-P. The erlanger silver catheter: In vitro results for antimicrobial activity. *Infection* **1999**, *27*, S24–S29, doi:10.1007/BF02561613.
45. Mihailescu, I.N.; Bociaga, D.; Socol, G.; Stan, G.E.; Chifiriuc, M.-C.; Bleotu, C.; Husanu, M.A.; Popescu-Pelin, G.; Duta, L.; Luculescu, C.R.; et al. Fabrication of antimicrobial silver-doped carbon structures by combinatorial pulsed laser deposition. *Int. J. Pharm.* **2016**, *515*, 592–606, doi:10.1016/j.ijpharm.2016.10.041.
46. Jamuna-Thevi, K.; Bakar, S.A.; Ibrahim, S.; Shahab, N.; Toff, M.R.M. Quantification of silver ion release, in vitro cytotoxicity and antibacterial properties of nanostructured Ag doped TiO₂ coatings on stainless steel deposited by RF magnetron sputtering. *Vacuum* **2011**, *86*, 235–241, doi:10.1016/j.vacuum.2011.06.011.
47. Wollina, U.; Abdel-Naser, M.B.; Verma, S. Skin Physiology and Textiles – Consideration of Basic Interactions. In *Biofunctional Textiles and the Skin*; KARGER: Basel, 2006; pp. 1–16.
48. Lansdown, A.B.G. Silver in Health Care: Antimicrobial Effects and Safety in Use. In *Biofunctional Textiles and the Skin*; KARGER: Basel, 2006; pp. 17–34.
49. Manninen, N.K.; Calderon, S.; Carvalho, I.; Henriques, M.; Cavaleiro, A.; Carvalho, S. Antibacterial Ag/a-C nanocomposite coatings: The influence of nano-galvanic a-C and Ag couples on Ag ionization rates. *Appl. Surf. Sci.* **2016**, *377*, 283–291, doi:10.1016/j.apsusc.2016.03.113.
50. Juknius, T.; Ružauskas, M.; Tamulevičius, T.; Šiugždinienė, R.; Jukniene, I.; Vasiliauskas, A.; Jurkevičiute, A.; Tamulevičius, S. Antimicrobial properties of

- diamond-like carbon/silver nanocomposite thin films deposited on textiles: Towards smart bandages. *Materials (Basel)*. **2016**, *9*, doi:10.3390/ma9050371.
51. Choi, O.; Hu, Z. Size Dependent and Reactive Oxygen Species Related Nanosilver Toxicity to Nitrifying Bacteria. *Environ. Sci. Technol.* **2008**, *42*, 4583–4588, doi:10.1021/es703238h.
 52. Carlson, C.; Hussain, S.M.; Schrand, A.M.; K. Braydich-Stolle, L.; Hess, K.L.; Jones, R.L.; Schlager, J.J. Unique Cellular Interaction of Silver Nanoparticles: Size-Dependent Generation of Reactive Oxygen Species. *J. Phys. Chem. B* **2008**, *112*, 13608–13619, doi:10.1021/jp712087m.
 53. Martínez-Castañón, G.A.; Niño-Martínez, N.; Martínez-Gutierrez, F.; Martínez-Mendoza, J.R.; Ruiz, F. Synthesis and antibacterial activity of silver nanoparticles with different sizes. *J. Nanoparticle Res.* **2008**, *10*, 1343–1348, doi:10.1007/s11051-008-9428-6.
 54. Eckelman, M.J.; Graedel, T.E. Silver Emissions and their Environmental Impacts: A Multilevel Assessment. *Environ. Sci. Technol.* **2007**, *41*, 6283–6289, doi:10.1021/es062970d.
 55. Gowri, S.; Almeida, L.; Amorim, T.; Carneiro, N.; Pedro Souto, A.; Fátima Esteves, M. Polymer Nanocomposites for Multifunctional Finishing of Textiles - a Review. *Text. Res. J.* **2010**, *80*, 1290–1306, doi:10.1177/0040517509357652.
 56. Brozena, A.H.; Oldham, C.J.; Parsons, G.N. Atomic layer deposition on polymer fibers and fabrics for multifunctional and electronic textiles. *J. Vac. Sci. Technol. A Vacuum, Surfaces, Film.* **2016**, *34*, 010801, doi:10.1116/1.4938104.
 57. Nadi, A.; Boukhriss, A.; Bentis, A.; Jabrane, E.; Gmouh, S. Evolution in the surface modification of textiles: a review. *Text. Prog.* **2018**, *50*, 67–108, doi:10.1080/00405167.2018.1533659.
 58. Camlibel, N.O.; Arik, B. Sol-Gel Applications in Textile Finishing Processes. *Recent Appl. Sol-Gel Synth.* **2017**, 2011–2013, doi:10.5772/67686.
 59. Poshina, D.; Otsuka, I. Electrospun Polysaccharidic Textiles for Biomedical Applications. *Textiles* **2021**, *1*, 152–169, doi:10.3390/textiles1020007.
 60. Susan, A.I.; Widodo, M.; Nur, M. Corona Glow Discharge Plasma Treatment for Hydrophobicity Improvement of Polyester and Cotton Fabrics. *IOP Conf. Ser. Mater. Sci. Eng.* **2017**, *214*, doi:10.1088/1757-899X/214/1/012031.
 61. Hegemann, D.; Hossain, M.M.; Balazs, D.J. Nanostructured plasma coatings to obtain multifunctional textile surfaces. *Prog. Org. Coatings* **2007**, *58*, 237–240, doi:10.1016/j.porgcoat.2006.08.027.
 62. Ehasarian, A.; Pulgarin, C.; Kiwi, J. Inactivation of bacteria under visible light and in the dark by Cu films. Advantages of Cu-HIPIMS-sputtered films. *Environ. Sci. Pollut. Res.* **2012**, *19*, 3791–3797, doi:10.1007/s11356-011-0734-7.
 63. Chodun, R.; Wicher, B.; Skowrński, Ł.; Nowakowska-Langier, K.; Okrasa, S.; Grabowski, A.; Minikayev, R.; Zdunek, K. Multi-sided metallization of textile fibres by using magnetron system with grounded cathode. *Mater. Sci.* **2017**, *35*, 639–646, doi:10.1515/msp-2017-0078.
 64. Wang, J.; Huang, N.; Pan, C.; Kwok, S.C.; Yang, P.; Leng, Y.; Chen, J.; Sun, H.; Wan, G.; Liu, Z.; et al. Bacterial repellence from polyethylene terephthalate surface modified by acetylene plasma immersion ion implantation–deposition. *Surf. Coatings Technol.* **2004**, *186*, 299–304, doi:10.1016/j.surfcoat.2004.02.046.
 65. Kinnari, T.J.; Soininen, A.; Esteban, J.; Zamora, N.; Alakoski, E.; Kouri, V.; Lappalainen, R.; Konttinen, Y.T.; Gomez-Barrena, E.; Tiainen, V. Adhesion of staphylococcal and Caco-2 cells on diamond-like carbon polymer hybrid coating. *J. Biomed. Mater. Res. Part A* **2008**, *86A*, 760–768, doi:10.1002/jbm.a.31643.
 66. Maas, M. Carbon Nanomaterials as Antibacterial Colloids. *Materials (Basel)*. **2016**, *9*, 617, doi:10.3390/ma9080617.
 67. Su, X.J.; Zhao, Q.; Wang, S.; Bendavid, A. Modification of diamond-like carbon coatings with fluorine to reduce biofouling adhesion. *Surf. Coatings Technol.*

- 2010**, 204, 2454–2458, doi:10.1016/j.surfcoat.2010.01.022.
68. Chan, Y.-H.; Huang, C.-F.; Ou, K.-L.; Peng, P.-W. Mechanical properties and antibacterial activity of copper doped diamond-like carbon films. *Surf. Coatings Technol.* **2011**, 206, 1037–1040, doi:10.1016/j.surfcoat.2011.07.034.
 69. Ji, L.; Li, H.; Zhao, F.; Chen, J.; Zhou, H. Microstructure and mechanical properties of Mo/DLC nanocomposite films. *Diam. Relat. Mater.* **2008**, 17, 1949–1954, doi:10.1016/j.diamond.2008.04.018.
 70. Bociąga, D.; Jakubowski, W.; Komorowski, P.; Sobczyk-Guzenda, A.; Jędrzejczak, A.; Batory, D.; Olejnik, A. Surface characterization and biological evaluation of silver-incorporated DLC coatings fabricated by hybrid RF PACVD/MS method. *Mater. Sci. Eng. C* **2016**, 63, 462–474, doi:10.1016/j.msec.2016.03.013.
 71. Crisan, C.M.; Mocan, T.; Manolea, M.; Lasca, L.I.; Tăbăran, F.A.; Mocan, L. Review on silver nanoparticles as a novel class of antibacterial solutions. *Appl. Sci.* **2021**, 11, 1–18, doi:10.3390/app11031120.
 72. Sohbatzadeh, F.; Farhadi, M.; Shakerinasab, E. A new DBD apparatus for super-hydrophobic coating deposition on cotton fabric. *Surf. Coatings Technol.* **2019**, 374, 944–956, doi:10.1016/j.surfcoat.2019.06.086.
 73. Kwiecińska, B.; Pusz, S.; Valentine, B.J. Application of electron microscopy TEM and SEM for analysis of coals, organic-rich shales and carbonaceous matter. *Int. J. Coal Geol.* **2019**, 211, 103203, doi:10.1016/j.coal.2019.05.010.
 74. Fróis, A. Funcionalização de Ligas Ortodônticas com Revestimentos DLC. *Funcionalização Ligas Ortodônticas com Revestimentos DLC* **2018**.
 75. X-Ray diffraction Available online: <https://wiki.anton-paar.com/cz-cs/rentgenovadifrakce-xrd/> (accessed on Oct 23, 2021).
 76. Zhou, W.; Apkarian, R.; Wang, Z.L.; Joy, D. Fundamentals of Scanning Electron Microscopy (SEM). In *Scanning Microscopy for Nanotechnology*, Springer New York: New York, NY, 2006; pp. 1–40.
 77. Walock, M. Schematic-drawing-of-a-the-typical-Scanning-Electron-Microscope-SEM-column-170_W640 Available online: https://www.researchgate.net/publication/281184428_Nanocomposite_coatings_based_on_quaternary_metal-nitrogen_and_nanocarbon_systems/figures?lo=1 (accessed on Oct 23, 2021).
 78. Bauer, A.W.; Kirby, W.M.; Sherris, J.C.; Turck, M. Antibiotic susceptibility testing by a standardized single disk method. *Am. J. Clin. Pathol.* **1966**, 45, 493–6.
 79. Sommer36 Agar Diffusion Method 1 Available online: https://en.wikipedia.org/wiki/Disk_diffusion_test#/media/File:Agar_Diffusion_Method_1.jpg (accessed on Oct 23, 2021).
 80. Kwok, D.Y.; Neumann, A.W. Contact angle measurement and contact angle interpretation. *Adv. Colloid Interface Sci.* **1999**, 81, 167–249, doi:10.1016/S0001-8686(98)00087-6.
 81. Yuan, Y.; Lee, T.R. Contact Angle and Wetting Properties. In; 2013; pp. 3–34.
 82. Manninen, N.K.A. de S. Silver segregation in Ag/a-C nanocomposite coatings for potential application as antibacterial surfaces.
 83. Balagna, C.; Perero, S.; Percivalle, E.; Nepita, E.V.; Ferraris, M. Virucidal effect against coronavirus SARS-CoV-2 of a silver nanocluster/silica composite sputtered coating. *Open Ceram.* **2020**, 1, 100006, doi:10.1016/j.oceram.2020.100006.
 84. Scholz, J.; Nocke, G.; Hollstein, F.; Weissbach, A. Investigations on fabrics coated with precious metals using the magnetron sputter technique with regard to their anti-microbial properties. *Surf. Coatings Technol.* **2005**, 192, 252–256, doi:10.1016/j.surfcoat.2004.05.036.
 85. Balouiri, M.; Sadiki, M.; Ibnsouda, S.K. Methods for in vitro evaluating antimicrobial activity: A review. *J. Pharm. Anal.* **2016**, 6, 71–79, doi:10.1016/j.jpha.2015.11.005.

Annex I

In this Annex, the article produced as the result of this master thesis is provided.

Carbon-based coatings in medical textiles surface functionalisation: the overview

José Antunes¹, Karim Matos¹, Sandra Carvalho¹, Albano Cavaleiro^{1,2}, Sandra Cruz^{1,2}, and Fábio Ferreira¹

1 Department of Mechanical Engineering, CEMMPRE, University of Coimbra, Rua Luis Reis Santos, 3030-788 Coimbra, Portugal

2 Laboratory for Wear, Testing & Materials, Instituto Pedro Nunes, Rua Pedro Nunes, 3030-199 Coimbra, Portugal

Abstract: The COVID-19 pandemic has, even more, highlighted the need for antimicrobial surfaces, especially those used in a healthcare environment. Textiles are the most difficult surfaces to modify since their typical use is in direct human body contact, and, consequently, some aspects need to be improved, such as wear time and filtration efficiency, antibacterial and anti-viral capacity, or hydrophobicity. To this end, several techniques can be used for the surface modification of tissues, being Magnetron Sputtering (MS) one of those that have been growing in the last years to meet the antimicrobial objective. The current state of the art available on textile functionalisation techniques, the improvements obtained by using MS, and the potential of Diamond-Like-Carbon (DLC) coatings on fabrics for medical applications, will be discussed in this review in order to contribute to a higher knowledge of functionalised textiles thematic.

Keywords: Magnetron Sputtering, Medical textiles, DLC, Antimicrobial

1. Introduction

Infections have been a major source of concern for human health in recent decades, and as the globe becomes increasingly linked, this threat is no longer speculative but very real. Pathogens that may spread from person to person are more likely to produce a global epidemic, and the Covid-19 Pandemic is a great illustration of this problem [1]. The best way to prevent an infectious disease spread via the respiratory way, when social distancing is not possible, is the use of personal protective equipment (PPE). PPEs, like masks, aprons, gowns, coveralls, goggles, and respirators, are considered critical components that can be used to protect not only healthcare workers but also the general population from infected droplets with virus/bacteria originated from infected people when sneezing and coughing, besides contaminated surfaces [1,2]. In addition, numerous pathogens, such as fungus, bacteria, and viruses, can be present in hospital facilities. These pathogens can be transported by any person that frequent this kind of facility, being transmitted through three ways: respiratory droplet transmission via the infected person when talking, sneezing, or coughing; indirect or direct contact with an infected person; and airborne transmission [1-3]. It is expected that by 2030 the healthcare industry worldwide will employ around 80 million people, putting a huge amount of healthcare workers at constant exposure to fungi/bacteria/viruses and getting infections while treating infected people with highly infectious diseases [2]. PPEs like surgical masks and medical clothing are crucial to offering a barrier among the users and the environment surrounding them [2,3]. The emergence of drug-resistant microorganisms is another issue that has been seen in hospital settings. Microorganisms, for instance bacteria, play an important role in the

global cycling of elements, having a profound impact on the environment in which they live. However, they are also susceptible to the environment, which means that when they come into contact with antimicrobial elements, some microorganisms may develop resistance to them, resulting in the emergence of "multi-drug-resistant" bacteria [4].

When considering masks, several options are available, such as basic cloth face masks (possible to be homemade), surgical face masks, and respirators [4]. A few properties have to be taken in consideration when evaluating masks' performance: comfort, breathability, biocompatibility, fluid resistance, flammability, and filtration efficiency [1,2]. And it is with those properties in mind that the masks recommended to use are manufactured. Basic cloth face masks/ homemade face masks are the simplest types of masks, with an efficiency highly dependent on the materials used [4-6]. Surgical masks are disposable, and their structure is composed of 3 layers of nonwoven textile, having one specific function [1]. The external layer has hydrophobic characteristics, helping in repelling fluids (for instance, mucosalivary fluid). The intermediate layer acts as a filter with the main purpose of avoiding the penetration of unwanted elements (for instance, dangerous particles or pathogens). The internal layer is produced with an absorbent material to absorb the mucosalivary fluid expelled by the user and moisture of the exhaled air [1]. There are also respirators, which are built by a structure of 4 layers of filters. Both the external and internal layers (made of nonwoven Polypropylene (PP)) act as hydrophobic layers, helping to avoid the moisture absorbed by the respirator. The intermediate layers' function, on the one hand, as support to provide thickness and shape (made of modacrylic) to the equipment, and on the other hand, filtering (made of nonwoven PP) dangerous particles to the user [3]. When comparing the different kinds of masks mentioned before, some studies indicate that rudimentary cloth face masks/ homemade face masks have a low filtration efficiency; however, they are reusable, comfortable, and have a satisfactory breathability. Surgical masks are comfortable, present a satisfactory breathability, and show a higher filtration efficiency than the homemade masks. Although, their filtration efficiency for micro and nanoparticles is not great. Moreover, surgical masks are not reusable. Respirators are the ones with the better filtration efficiency performance for particles from all sizes, however they are also not reusable and present a low breathability. All in all, respirators have an overall better performance [4,6,7].

The PPEs available, particularly facial masks, have shown a few problems: face masks are more efficient with higher filtration, with the possibility of being reusable, and with antimicrobial capabilities [1,3]. When studying patients infected with the influenza virus, surgical masks were showed to be highly effective in blocking virus-containing particles with bigger sizes ($\geq 5\mu\text{m}$) but less effective for smaller particles [1,2]. Some masks and respirators are made of materials like cotton and synthetic fabric, which have larger pore sizes and, therefore, will not be very effective in filtering tiny virus-laden droplets, pathogens, and nanosized contaminants [1,2]. Another concern is the negative impact that this non-reusable PPE brings to the environment. Recent research studies shown that healthcare workers worldwide used more than 44 million non-reusable PPEs every day during the COVID-19 pandemic. The majority of these PPEs have their composition polypropylene, which is a cheap material and has good performance characteristics; however, these kinds of masks are of single-use and are normally incinerated or sent to a landfill aggravating the environmental impact [2,4].

To improve the efficiency of facial masks and other medical textiles, several studies have been performed, like employing modified filter layers, for instance, nanofibers, or by modifying the filter surfaces by adding materials with antimicrobial capabilities to improve their efficiency [3]. It's proven that adding antimicrobial agents to these products is a highly effective way to prevent infections caused by various pathogens through the inhibition of viruses, fungi, and bacteria [2].

There are different chemical and physical methods to promote superficial changes in fabrics. Although the most used ones are solution-based processing, other methods have been attracted a lot of attention in the last years for fabric surface modification, such as

spray coating, sol-gel processing, direct chemical grafting, dip-coating, or physical vapor deposition (PVD) methods [8-11]. The sputtering process (PVD technique) is a coating method performed in a vacuum atmosphere. The coating material (target) is sputtered with a noble gas (typically Ar). Then, in a vapor phase, it is transported until it reaches and condenses at the substrate, forming a coating. It is even possible to introduce a reactive gas that will interact with the growing film forming a compound coating [11]. This technology has been implemented to modify various material surfaces, with particular attention to textiles. Several kinds of coatings can be obtained to modify the textile surface, but to introduce the hydrophobic character without toxicity, diamond-like carbon (DLC) is the most appropriate [12]. The antimicrobial feature is gained with this coating, but if the DLC is doped with silver nanoparticles (AgNPs) in a non-toxic amount, the fabric becomes efficient against microbial colonization [13,14].

In this review, it is intended to show the most relevant improvements in the surface treatment of textiles, especially by using the sputtering technique. It will also be shown how DLC doped with AgNPs can be an efficient approach to transform simple textiles, giving them the properties that the population needs to be able to live a healthier life, especially during a pandemic period.

2. Technical Textiles

A technical textile can be defined as a textile material and product manufactured mainly for its technical and performance characteristics rather than its artistic or ornamental features [15]. There is a huge variety of fibers used for technical textiles, depending on the end-product: natural fibers that are characterized by high modulus/strength, moisture intake, low elasticity and elongation; regenerated cellulosic fibers that possess low modulus/strength and elasticity as well as high elongation and moisture intake; and synthetic fibers, for instance, nylon, polyester, and PP, which possess high modulus/strength and elongation with an acceptable elasticity and comparatively low moisture intake [15]. The combination of all these different fibers with functional finishing processes allows the creation of tailor-made textiles that have an improved performance when compared to conventional textiles. When referred to the textile industry, medical textiles have attracted the most attention in the last years and are the one with the fastest progress in the textile field [16].

2.1 Medical Textiles

The variety of textiles available for use in biomedical applications is vast, and various textiles are chosen based on the purpose. Natural wool, for example, may provide great thermal insulation and physical protection to the user in many situations (dry and wet conditions) due to its outstanding characteristics (hydrophobicity, etc). [17].

However, there are a few concerns regarding the application of textiles in medical products. Because of their capacity to retain humidity and large surface area, numerous textiles are prone to facilitate the growth of microorganisms, for instance fungi and bacteria, and their quick multiplication under ideal circumstances [1,4]. This causes several negative effects such as diminished mechanical strength, production of unpleasant odors and discoloration of the textiles, and, more importantly, increased chance of user contamination [4]. With the intention of find solutions to these problems and improve or give certain properties to some textiles, several superficial modifications are being studied. For example, with plasma treatments is possible to confer to the surface of the textiles very low surface energy, giving to these textiles hydrophobic capabilities, which make them water-repellent with a bonus of not affecting the original characteristics of the textiles, for instance, the hand feels as well as the breathability [10]. Moreover, depending on the used finishing agent, plasma treatments can also provide other functional properties to textiles: UV protection, flame-retardant, antimicrobial, and cosmetic properties[18].

For medical textiles, there are many textiles materials used depending on their functionality. They can be used as implantable materials (sutures, vascular grafts), as non-implantable materials (pressure garments, secondary dressings), in healthcare/hygiene (clothing, masks, wipes), or intelligent medical and healthcare textiles (chromic materials, phase changing materials) [19]. In the example of the PPE's, nonwoven fabrics (TNTs), cloth, and jersey format fabrics are the most commonly used.

TNT is created by connecting a mass of fibers using heat, chemical, or mechanical methods, rather than intertwining fibers like in traditional textiles. TNTs are the most commonly utilized material for medical clothing, despite being mechanically weaker than its counterpart. This is owing to its comparatively low cost and speed of production, as well as its excellent levels of sterility and infection control, which are critical in applications such as medical clothing. For these reasons, TNTs are frequently used in the production of disposable medical clothing, such as surgical masks, surgical caps, and surgical gowns [1,2]. Regarding surgical masks, they are typically produced with nonwoven fibrous, for instance, glass papers, PP, and woolen felt [3].

Alternatively, homemade masks are typically produced by woven textiles made from pure cotton or polyester-cotton blends, such as jersey textiles [2]. The downside of using woven fabrics in protective clothing when compared with TNTs are their worst barrier properties against liquids and bacteria; however, they normally provide a better wearer comfort to the user and are able of sustaining several washing/cleaning processes, giving them a reusability property that TNTs usually fail to have [2]. Furthermore, while selecting materials for medical textiles, sustainability and environmental factors must be considered [15]. As a result of the rising limits on the use of synthetic fabrics (such as TNTs), eco-friendly alternatives, such as natural fibers, are being used to manufacture these items. Cotton is an excellent example of natural fibers that may be utilized to make medical clothing, not only because it is a sustainable material, but also because it is inexpensive, biodegradable, renewable, and lightweight [15,20].

3. Surface modification of textiles

3.1 Current research in the textile surface modification

Nowadays, in textile manufacturing, surface treatments are of the most importance to give the desirable properties for its application. Surface treatments, including printing, dyeing, and other chemical or physical treatments, can improve the appearance or feel of textiles and add to textiles' unique functions, such as control of surface wetting or UV protection, among other factors functions. Most of these surface treatments rely on heavy use of heating sources during the process to dry the textiles, and consequently, are energy-intensive processes and expensive. Thus, the textile sector is seeking new methods to improve existing product characteristics while minimizing environmental impact and energy use. Some surface modification methods are following described.

The Atomic layer deposition (ALD) is a surface modification method that can coat substrates with excellent uniformity across large areas with complex topographies. Due to these characteristics, ALD has been studied as a possibility to coat textiles give them new capabilities [17].

It is known that when textiles are exposed to ultraviolet rays, the fiber mechanical performance degrades and also leads to visible color changes. The ALD technique by coating textiles and fibers increases physical stability and ultraviolet protection [17]. The desire for high-performance and self-cleaning fabrics has prompted researchers to investigate how ALD might manipulate fiber surface wetting characteristics. Increased surface energy, which may be obtained by the deposition of polar metal oxide nanocoatings using ALD, is one approach to improve fiber wetting capacities. Inorganic ALD layers on polymer films have been shown in certain experiments to considerably decrease the passage of water and other vapors into and through the polymer. ALD has also been investigated by various research groups for biocompatible and bio-adhesive surface treatments, and to

alter and regulate nanomaterial toxicity. All of these characteristics might be useful in biomedical applications such as face masks and medical gowns [17].

The high temperatures involved with the process, which some fabrics may not tolerate without damage, and the fact that traditional batch processing is too slow and expensive for most applications, are the most difficult hurdles for ALD use in textiles. This final point might indicate that ALD will be used first in high-value items such as specialty medicinal materials [17].

The sol-gel technique is a low-temperature approach for synthesizing materials that are either completely inorganic or partially inorganic and organic and is based on the hydrolysis and condensation reaction of organometallic compounds [21]. Sol-gel chemistry has been used to treat textiles with modified inorganic sols in recent years, bringing up a slew of new options for fiber surface functionalization [21, 22]. The use of sol-gel technology in textiles offers several advantages, including reduced chemical use, less water use, low-temperature treatment, ease of application, and the ability to provide textile materials several functional characteristics in one step by combining suitable inorganic precursors (multifunctional finishing). Sol-gel technique, on the other hand, has drawbacks such as high precursor material prices, the potential to limit the elasticity of textile materials, and limited washing durability [21, 22].

Water or oil repellency, dyeing, antimicrobial properties, self-cleaning properties, bioactivity, thermal and tensile properties, UV protection, and reduced flammability are just a few of the functional properties that can be given to textile materials using sol-gel technology, many of which are of interest for biomedical applications [21, 22]. A hydrophobic effect can be achieved by lowering the surface tension of textile materials against liquids. A sol-gel technique and a mixture of nano-sol containing silica nanoparticles, triethoxysilane, and hexadecyltrimethoxysilane, certain experiments in cotton, cotton/polyester, and polyester textiles were able to give those materials superhydrophobic characteristics [22]. Furthermore, functions such as ultraviolet protection may be achieved via the sol-gel technique, for example, by incorporating TiO₂ and ZnO nanoparticles into textile materials. Through a photocatalytic reaction, TiO₂ nanoparticles provide ultraviolet protection as well as self-cleaning, a process that can also lead to the breakdown of organic and inorganic contaminants. This indicates that the photocatalytic reaction provides antibacterial characteristics in addition to ultraviolet protection and self-cleaning [22]. When considering giving antimicrobial properties to textiles using sol-gel technology, there are plenty of antimicrobial substances that can be applied through this technique. For example, silver chloride (AgCl) is usually used in cotton fabrics against fungi, ZnO is applied in cellulosic fibers, and chitosan is applied in wool to give it antimicrobial activity [22].

With the introduction of polymer nanocomposites, a new class of nano finishing materials for textiles may be developed, each with its own set of structure-property relationships that are only tangentially connected to their components and their micron and macro-scale composite counterparts. Although polymer nanocomposites with inorganic fillers of various dimensionality and chemistry are feasible, research into the immense potential of these novel materials has only just begun [23]. Significant research activities have been directed towards developing antimicrobial coatings to protect high-touch surfaces in healthcare institutions to minimize the financial burden and avoidable fatalities caused by healthcare-associated infections (HAIs). Surface hydrophilisation has been widely used as a new paradigm to minimize microorganism colonization in recent years. Surface hydration layers induced by hydrophilic polymers could give anti-biofouling properties to surfaces because a layer of tightly bound water acts as an energetic and physical barrier to biofouling processes such as protein attachment, initial bacterial attachment, and subsequent biofilm formation [24].

Electrospinning is a simple but powerful technique for producing a continuous stream of nano- and microfibers from natural and manmade polymers, as well as inor-

ganic oxide materials. The following are the fundamental ideas of a typical electrospinning process: To produce the fiber, a high voltage is utilized to create an electrically-charged jet of polymer solution or melt, which dries or hardens on extrusion [25].

Conventional fiber spinning processes typically generate polymer fibers with diameters in the micrometer range, but when the fiber diameter is lowered to nanometers, the surface area to volume ratio increases dramatically. High specific surface area, nanoscale interstitial space, heat insulating capabilities, electromagnetic shielding, biocompatibility, adjustable porosity, and mechanical resistance are all structural characteristics of electrospun nanofibers and nonwoven textiles. Electrospun fibers have a large specific surface area, which allows them to have a high capacity and a large amount of adsorption sites for the effective absorption or release of molecules, particles, and functional groups [25-28]. Because the porosity may be adjusted in the electrospinning process, it is feasible to produce a high porosity, which allows for the development of extra channels for air to move through the fabric while preventing the passage of undesirable particles. Consequently, by providing selective permeability for water droplets or vapor, the high porosity and well-designed pores provide the feasibility of waterproof and moisture permeable fabrics [27,28].

Different functions can also be produced depending on the materials utilized in the electrospinning method. Electrospun textiles made of natural polymers, for example, nucleic acids, proteins, and polysaccharides, have inherent biocompatibility. Additionally, introducing different antibiotics and antimicrobials such as ZnO and AgNPs has shown an increase in the antimicrobial effectiveness of electrospun textiles[25]. To give this antimicrobial ability, there are two different methods. The first technique involves electrospinning precursor liquids or suspensions containing polymers and antimicrobial chemicals in one step to produce antimicrobial nanofibers. The second technique consists of two steps: electrospun polymeric nanofiber production and antimicrobial nanofiber post-functionalization [26]. These characteristics make electrospun textiles promising scaffolds for various applications.

Electrospun materials have piqued attention in recent years, not only in traditional textile sectors, but also in cutting-edge research disciplines such as fundamental and applied biomedical research. The COVID-19 pandemic, for example, has generated a surge in demand for PPE, underlining the relevance of electrospun fabrics, such as those used in mask filters, in effectively preventing nanoscale contaminants like viruses [25].

Nanotechnology applied to textile materials might result in the addition of a variety of functional characteristics to the underlying substrate. These functional qualities are crucial since they provide substantial benefits in wear comfort and maintenance. The implementation of nanotechnology in textiles might result in introducing or improving various functional properties, such as antimicrobial ability, flame-retardant, UV protection, and easy-care finishes, in particular with the application of metal oxide and metal nanoparticles. Novel uses of textile materials utilizing nanotechnology in biological detection, hazardous gas breakdown, and self-decontamination are also being researched and investigated [29].

Plasma is an ensemble of charged, excited, and neutral species that includes any or all of the following: electrons, positive and negative ions, atoms, molecules, radicals, and photons. It is frequently referred to as the fourth state of matter.[21,30]. These particles, which are formed by the electrical dissociation of inert gases, receive their own energy from the applied electric field and lose it when they collide with the material surface. Chemical bonds in the material surface are disrupted during surface collisions, resulting in the formation of free radical groups on the surface. These particles are chemically active and can add new functional groups to the material's surface, which can then be employed as polymerization precursors [30]. Because plasma surface modification does not need the use of wet-chemical compounds, it is considered a low-cost and ecologically friendly method [21,31]. One of the primary benefits of plasma treatment is that it only affects the surface characteristics of substrates, not the bulk qualities [32].

Plasma treatment technique in textiles can bring characteristics to fabrics such as antibacterial activity, hydrophobicity, flame retardancy, and ultraviolet protection, depending on the materials employed in the procedure. Many research has demonstrated that water-repellent characteristics may be bestowed on many fabrics, such as cotton, polyester, and silk, utilizing plasma treatments. Also, with the introduction of metallic particles like Ag or Cu, it is possible to give antimicrobial properties to some textiles' surfaces[21,31].

3.2 Magnetron Sputtering (MS) in medical textile functionalization

Vapor deposition is a coating technique where a vapor phase material is condensed at the substrate in a vacuum environment to produce a thin coating. In some cases, the deposited substance interacts with the gaseous molecules, even more, resulting in a compound coating on the substrate. Metals and non-metals can both be deposited in general [33]. To satisfy this requirement, a variety of deposition methods are used. These approaches use a vacuum to reduce undesired interactions with the environment and make it easier to shape the coating composition.

PVD stands for physical vapor deposition and encompasses a wide range of vacuum deposition techniques. PVD is typically split into two processes: evaporation and sputtering. To create vapor in the form of atoms, molecules, or ions supplied from a target, physical techniques such as sputtering and evaporation are utilized. The particles are subsequently transported and deposited on the substrate surface, resulting in the development of a film.

The evaporation technique requires high temperatures during the process, which limits the use of this technique to coat textiles.

Sputtering, on the other hand, uses a substrate temperature that is far lower than the target material's melting point, making it a viable option for coating temperature-sensitive materials like textiles. This leads to the sputtering technique becoming more relevant among physical vapor deposition techniques to meet the constant increase in market demands.

The most prominent sputtering processes are the cathodic arc physical vapor deposition (CAPVD) and the magnetron sputtering (MS).

The CAPVD is a technique that includes passing a low-voltage high-density electric current across two electrodes. Due to the simultaneous vaporization and ionization of the cathodic substance, this action is carried out under a vacuum, culminating in the creation of plasma. Unlike other PVD processes, the coatings produced are intermixed layers with improved adherence, which is owing to the high kinetic energy [34].

The MS process involves energetic ions colliding with a target surface, which usually results in the ejection of target atoms. The MS method confines the plasma to an area near the target using strong magnets, which dramatically enhances the deposition rate by maintaining a greater ion density, making the electron/gas molecule collision process much more efficient. Alloys, elements, and compounds may all be sputtered and deposited using the MS method. The sputtering target also provides a steady and long-lasting material supply. Reactive deposition may be accomplished in a variety of conditions by utilizing reactive gaseous species activated in plasma. The cathode and substrates can be positioned close together in this technique, resulting in a compact system chamber. Another benefit of magnetron sputtering is the reduced electron bombardment of the substrate, which is beneficial for temperature-sensitive substrates like textiles. As a result of these advantages, the MS technique is of great interest among the scientific community since the obtained coatings allow a much larger surface area with improved durability and functionality without any adverse effect on the textile feel. Furthermore, because of the nano-scaled alteration on textiles, it is an environmentally benign technique that provides an appealing alternative for adding new functions such as water repellency, mechanical and antibacterial characteristics, and biocompatibility [35]. Consequently, it can

be applied in a large number of industrial applications, with a particular focus on surgical/medical applications such as face masks.

There are opportunities for improvements using the versatile MS technique for high-quality coatings on temperature-sensitive substrates like textiles. Sputter films offer new ways to functionalize textiles by combining oxide, metallic, and composite films to obtain various characteristics. The most significant benefit of sputtering deposition is that even the highest melting point materials may be sputtered on textile substrates at low temperatures. Nanocomposite films can also be made by co-sputtering different materials. The sputtering approach for functionalizing textiles is usually applied only on the side facing the target due to the technology's directed deposition [36].

The adherence of MS-deposited films to textiles is superior to that of other coating methods. Despite this, due to sputtering techniques and varied textile substrates, adhesion between films and textiles was inconsistent. HiPIMS, for example, enhanced adhesion between films and textile substrates by operating at higher energies and with a greater density of electron/metal ion pairs than DCMS [37]. Aside from the fabric structure differences such as knitted textiles, woven textiles, and nonwoven textiles, a variety of other factors may influence the adhesion between the sputter film and textile substrates, such as surface morphology different surface chemical properties, and porosity size of the fiber materials. When adhesion was lacking, it was feasible to significantly improve adhesion by correctly correcting inadequate fiber surface activation, thermal expansion coefficient discrepancies, and internal stress [38]. The adherence of coatings and fabrics can be improved by plasma pretreatment of the fabric substrates. The effect on adhesion was universally positive. Chen et al., for example, utilized oxygen plasma to pretreat polyester cloth for one minute before applying a brass coating by HIPIMS [39]. The brass coating's adherence to the cloth was significantly enhanced. Because it produces activation and the required material surface functionalization, the coating adherence is improved by pretreatment with oxygen plasma. In addition to physically cleaning the textile surface, the chemical significance conferred by the oxygen plasma pretreatment is critical. Before applying a TiO₂ coating to a polylactic acid textile, Saffari et al. employed low temperature plasma to pretreat it [40]. The TiO₂ particles on the polylactic acid fibers' surface grew more compact as the plasma treatment time and sputtering time were increased. The initial TiO₂ coating and the chemical change caused by the oxygen plasma pretreatment significantly improved film adherence and resistance to washing. Al₂O₃ coatings on the surface of polyester woven and nonwoven fabrics were applied by Depla et al. Plasma pretreatment significantly improved the adhesion, continuity, and compactness of the films in all samples [41]. Hegemann et al. have demonstrated an alternate approach for depositing Ag on textiles, plasma sputtering, which combines cleaning and deposition in a single step. With smooth films, they were able to obtain excellent adherence to polyester fibers [36].

The application of MS for the deposition of metallic and oxide films on textiles has grown in popularity in recent years for functional purposes in a variety of medical applications. UV resistance and antibacterial characteristics were found in textiles coated with Cu films [43]. MS-coated Cu film textiles exhibited good antibacterial activities against *E. coli*. The bacteriostatic rates against *Escherichia coli* of the Cu film produced by HiPIMS were more than three times greater than those deposited by DCMS under the same sputtering circumstances [37]. Cu and Ag were sputtered on textiles by Scholz et al. [44]. Cu's antibacterial capabilities outperformed Ag only on a few types of bacteria, such as *Staphylococcus aureus* and *Escherichia coli*, when compared Cu and Ag coated textiles.

Rtimi et al. coated polyester textiles with TiON and TiON-Ag coatings to improve the antibacterial action [45]. *Escherichia coli* was completely killed in 120 minutes when the TiON coating thickness was 70 nm. On the TiON-Ag coating, *Escherichia coli* was killed much quicker (within 55 minutes) when Ag was added to the coating. Rtimi et al. also used polyester textiles to deposit TiN and TiN-Ag coatings [46]. They discovered that

when Ag-doped (TiN-Ag) coatings were compared to TiN coatings, the rate of bacteria deactivation increased.

The sputtering deposition of TiO₂ coating on textiles improves their UV resistance and antimicrobial properties [47,48]. In another work, Rtimi et al. also deposited Cu, TiO₂ film, and TiO₂/Cu coatings [49]. They discovered that TiO₂/Cu coating had a considerably greater antibacterial impact than the others. TiO₂ was said to have a synergistic impact on Cu[50]. Furthermore, the antibacterial effectiveness of the Cu/CuO coating deposited on polyester textile against *E. coli* was more than 3 times that of the deposited Cu coating [51].

On the other hand, Subramanian et al. deposited CuO coatings on polyester nonwoven textiles. The coated textiles revealed a strong antibiotic effect on *Staphylococcus aureus* and *Escherichia coli*[52]. When deposited ZnO coatings on textiles, the coated textiles could also get favorable anti-ultraviolet and antimicrobial properties[53,54].

Because of its antibacterial characteristics, Ag has been widely utilized in the functionalization of textiles. Hegemann et al. deposited Ag on fabrics by magnetron sputtering process [36]. They were able to achieve good antibacterial activity with modest quantities of deposited Ag while maintaining the fabric's characteristics. Scholz et al. used the magnetron sputtering technique to create textiles containing SiO₂ fibers covered with precious metal PVD layers. The antibacterial efficacy of platinum, silver, copper, gold, and platinum/rhodium layers was determined. Copper was presented to be the more efficient against fungus and bacteria. Silver was also efficient against bacteria, although its activity against fungus was found to be limited. The efficacy of the other metals tested was not achieved [44,55]. Shahidi's objective was to improve the fastness and antibacterial characteristics of colored cotton samples. Cotton textiles were dyed using a variety of dyes, and the dyed samples were then sputtered with Ag and Co for 15 seconds using a plasma sputtering apparatus. For the production of a metal nano-layer on the surface of samples, he employed a DCMS method. He noticed that the differences in characteristics caused by sputtering might improve the performance of some textiles. As a result, the sputtering approach might be a unique way to improve the washability and lightfastness of colored cotton samples [56]. The textiles' antimicrobial activity lasted for at least 30 cycles after laundering [57,58]. Using HiPIMS, Chen et al. deposited Ag on poly(ethylene terephthalate) fabric. Antimicrobial activity against *Staphylococcus aureus* and *Escherichia coli* was discovered in the samples. Rtimi et al. deposited ZrNO and Ag on PET textiles to create antimicrobial textiles with ZrNO-Ag composite coatings. The antimicrobial effect of the composite coating on *Escherichia coli* was significantly improved when compared to the single-layer coating[60].

4. Diamond-like carbon

The hydrophobicity, high hardness, transparency, excellent thermal conductivity, chemical stability, and biocompatibility of diamond-like carbon (DLC) coatings are well-known.

Deposition techniques for DLC coatings include radio frequency, plasma-enhanced chemical vapor deposition, ion beam deposition, ion plating, plasma immersion ion implantation and deposition, filtered cathodic vacuum arc, pulsed laser deposition, ion beam sputtering, and mass-selected ion beam deposition [61-69].

The magnetron sputtering process, in particular, is a very promising and versatile technique for performing DLC coatings because it allows carbon coating growth even at low substrate temperatures and delivers ion bombardment of the surface, which has the benefit of increasing coating adhesion to the substrate and thus improving coating quality.

For their role as outstanding protective coatings in bio-applications, DLC characteristics have been widely investigated. In vitro, diamond-like carbon coatings have antibacterial and anti-biofouling properties against bacteria such as *S. aureus*, *S. epidermidis*, and *P. aeruginosa* [70,71]. Bacterial adherence to the diamond-like carbon film is linked to their

sp^2 and sp^3 hybridization, and lowering the sp^3/sp^2 ratio improves antimicrobial efficacy significantly [72]. Because of their strong interaction with human cells and improved corrosion resistance and wear, DLC coatings having a large proportion (>80%) of sp^3 bonds are often used for biomaterial films [73]. Some methods have been proposed in order to better understand the bactericidal efficacy of DLC films. One mechanism is the direct physical damage to microorganisms caused by interaction with pure diamond-like carbon films, which results in severe membrane degradation and the release of microbial internal compounds [74]. Other researchers hypothesized that diamond-like carbon films' antibacterial action stems from their chemical inertness as a result of the weakening of the chemical contact during the bacterial adhesion process [75]. The mechanism of DLC coatings can be altered depending on the microbiological species in a variety of circumstances. DLC and DLC doped with germanium, for example, had a significant anti-biofouling impact against gram-negative bacteria but did not inhibit gram-positive bacteria [76]. It's worth noting that there's some evidence that DLC films have extremely poor or non-existent antibacterial action against *Staphylococcus epidermidis* and *Staphylococcus aureus* [77-79]. DLC coatings' bactericidal activity is closely connected to their surface profile, which includes a strong dispersive component of surface energy, hydrophobicity, and smoothness [80].

The high hydrophobicity of DLC coatings, in particular, can induce changes in bacterial cell membranes, leading to biological death [81]. Furthermore, the surface free energy is a key factor influencing DLC antibacterial efficacy. The surface energy value of DLC coatings is frequently carefully chosen for specific purposes. Many elements can be added to DLC coatings with the goal of changing the value of surface energy. The addition of fluorine groups, for example, causes bonding changes in DLC coatings by lowering C–CF bonds and increasing CF and CF₂ bonds, enhancing antibacterial effectiveness by raising the work of adhesion of the coatings for bacteria [82]. Fluorine has the capacity to change the wettability of diamond-like carbon coatings by lowering the surface free energy and increasing the contact angle [83]. The initial attachment of microorganisms is known to be significantly connected to the total surface energy of the coatings, as the number of adherent cells decreases as the total surface energy of the coatings decreases [84]. As a result, considering the surface characteristics of DLC films will aid in the design of bactericidal films by optimizing the surface energy.

Nanoparticles are commonly added to DLC coatings in order to activate or enhance their antibacterial characteristics. Incorporating a metal particle into the DLC structure can function as a catalyst for the formation of sp^2 -rich boundary sites [85,86]. It has been discovered that a low silver concentration can reduce the number of carbon atoms bound in sp^2 configuration, which promotes sp^3 bonding, but a greater Ag content raises the sp^2/sp^3 ratio [87]. Cu nanoparticles, on the other hand, are well recognized for improving the bactericidal activity of DLC coatings. Experiments revealed that adding Cu to a-C:H enhanced its antibacterial activity by up to 99.9% (>58.76 wt. percent) [85]. Furthermore, Cu has the ability to alter the wetting characteristics of DLC coatings, affecting bacterial adhesion considerably [88,89]. Metallic nanoparticles may have disadvantages over the DLC matrix in a variety of scenarios. For example, adding Ag to a-C:H coatings improved their antibacterial and hydrophobic properties, but it came at the cost of decreased hardness. Additional increases in Ag content did not help to improve antibacterial ability, but they did result in a significant loss in surface flatness and hardness [90]. Whether the mechanism of nanoparticles embedded into DLC films is identical to that of free particles or whether these particles function differently is unknown [76]. Nonetheless, due to their ability to control the release of antimicrobial nanoparticles, DLC/composite coatings are used effectively as tailored antimicrobial films [91].

4.1 DLC coating with Nanoparticles

Because of their small sizes, unique chemical and physical properties, and high specific surface, materials for instance metal nanoparticles, metal oxide nanoparticles, carbon

nanomaterials, and their composites have been extensively used as new antimicrobial agents. This enables them to dissolve more quickly in a given solution than bigger particles, releasing more metal ions [4,92]. Furthermore, these compounds are readily incorporated into the polymeric matrix of fibers, making them excellent for use in textiles [4].

Consequently, the incorporation of Au, CuO, ZnO, TiO₂, or Ag Nanoparticles to DLCs, with Ag being the element most likely used to obtain antimicrobial properties, could allow fabrics, including those used in masks, to have the two properties that are crucial in this study: antimicrobial and hydrophobic [93].

AgNPs are the most widely used antimicrobial nano agent because of their broad-spectrum antimicrobial properties and strong antimicrobial effectiveness against a large number of bacteria, viruses, and fungi, which is also higher when compared to particles made from other heavy metals such as Au and Zn [92]. The antimicrobial mode of action of metals, which may be triggered by the metal reduction potential, metal donor atom selectivity, and/or speciation, can trigger the biocidal effect of metals [4]. This mode of action may cause a variety of processes, such as the formation of reactive oxygen species, that have a significant impact on the integrity and functionality of bacteria and viruses, including cell wall synthesis damage or inhibition, cell membrane function inhibition, protein synthesis inhibition, nucleic acid synthesis inhibition, and inhibition of other metabolic processes [4]. The antibacterial activity of Ag, particularly, has been recognized as an oligodynamic effect, and in compounds exhibiting this oligodynamic effect, only very tiny amounts of the active substance are required for substantial antimicrobial activity, further supporting Ag's high efficiency [94].

In relation to the combination of DLC and Ag, there are several studies that show that silver-doped DLC (AgDLC) coatings have an excellent antimicrobial effect [93]. The biocidal action of AgDLC thin films is longer than other substrates with metallic NPs, as the film surface is continuously renewed with Ag due to its segregation through the carbon matrix. Concentration gradients attract Ag ions to the top layer of the surface, where most of the moisture and less Ag ions are present. The bacteria are also contained in this higher layer, allowing the silver ions to reach their target locations and impact microbial viability [94]. As bacteria only interact with surface' materials, AgDLC films exhibit improved and extended antimicrobial activity compared to films without silver segregation. This phenomenon shows the advantage of AgDLC films over AgNPs, as the Ag content can be reduced while maintaining a high antimicrobial activity [93], opening the possibility of controlling the antimicrobial action of this type of coating. Therefore, a successful deposition of AgDLC coating in textiles may provide a wide range of possibilities in the biomedical sector, depending on the desired application.

5. Conclusions and Perspectives

With the advances made across all the fields, such as physics, chemistry, electronics, etc., more and more methods and tools are available to be tested and studied. The textile industry is not indifferent to this, and therefore there are all these new processes being studied in order to improve the effectiveness and performance of textiles, in particular medical textiles. There has been lingering some bacterial and infectious problems in healthcare environments, problems that have been augmented during the Covid-19 pandemic, and therefore the interest in antimicrobial textiles has intensified. The medical textiles available throughout healthcare environments all over the world are far from ideal, however the technology required to enhance some of those textile's performance is already available. Some of the methods that raise more interest are surface modification methods. Nowadays, there are a few surface modification methods, such as polymer coatings, that allow the implementation of finishing treatments in textiles in a way far more appealing to the textile industry sector, as they have the potential to reduce energy use and environmental impact while giving the desired finishing properties. The potential of

modified textiles is immense. Their use may facilitate some medical procedures, for example, as it is possible to give some textiles biocompatible characteristics, as well as use them as drug delivery systems. They can also prevent pathogens from spreading, as antimicrobial and hydrophobic properties may be given through finishing processes used in medical clothing or masks. The combination of DLC and AgNPs is one of the possibilities that are able to provide antimicrobial and hydrophobic characteristics to textiles. New methods and ideas to improve textiles performance keep being explored, as is the case with PVD techniques, and as more results and findings keep being shared throughout the scientific community, the performance of textiles can only improve.

Funding: This research is sponsored by national funds through FCT – Fundação para a Ciência e a Tecnologia, under the project UIDB/00285/2020 and On-SURF [co-financed via FEDER (PT2020) POCI-01-0247-FEDER-024521].

References

1. Chua, M.H.; Cheng, W.; Goh, S.S.; Kong, J.; Li, B.; Lim, J.Y.C.; Mao, L.; Wang, S.; Xue, K.; Yang, L.; et al. Face Masks in the New COVID-19 Normal: Materials, Testing, and Perspectives. *Research (Wash D C)* **2020**, *2020*, 7286735, doi:10.34133/2020/7286735.
2. Karim, N.; Afroj, S.; Lloyd, K.; Oaten, L.C.; Andreeva, D.V.; Carr, C.; Farmery, A.D.; Kim, I.D.; Novoselov, K.S. Sustainable Personal Protective Clothing for Healthcare Applications: A Review. *ACS Nano* **2020**, *14*, 12313–12340, doi:10.1021/acsnano.0c05537.
3. O'Dowd, K.; Nair, K.M.; Forouzandeh, P.; Mathew, S.; Grant, J.; Moran, R.; Bartlett, J.; Bird, J.; Pillai, S.C. Face Masks and Respirators in the Fight against the COVID-19 Pandemic: A Review of Current Materials, Advances and Future Perspectives. *Materials (Basel)* **2020**, *13*, doi:10.3390/ma13153363.
4. Morais, D.; Guedes, R.; Lopes, M. Antimicrobial Approaches for Textiles: From Research to Market. *Materials* **2016**, *9*, doi:10.3390/ma9060498.
5. Sousa-Pinto, B.; Fonte, A.P.; Lopes, A.A.; Oliveira, B.; Fonseca, J.A.; Costa-Pereira, A.; Correia, O. Face masks for community use: An awareness call to the differences in materials. *Respirology* **2020**, *25*, 894 – 895, doi:10.1111/resp.13891.
6. Tcharkhtchi, A.; Abbasnezhad, N.; Zarbini Seydani, M.; Zirak, N.; Farzaneh, S.; Shirinbayan, M. An overview of filtration efficiency through the masks: Mechanisms of the aerosols penetration. *Bioact Mater* **2021**, *6*, 106–122, doi:10.1016/j.bioactmat.2020.08.002.
7. Teesing, G.R.; van Straten, B.; de Man, P.; Horeman-Franse, T. Is there an adequate alternative to commercially manufactured face masks? A comparison of various materials and forms. *J Hosp Infect* **2020**, *106*, 246–253, doi:10.1016/j.jhin.2020.07.024.
8. Li, G.; Liu, H.; Li, T.; Wang, J. Surface modification and functionalisation of silk fibroin fibers/fabric toward high performance applications. *Materials Science & Engineering C-Materials For Biological Applications* **2012**, *32*, 627–636, doi:10.1016/j.msec.2011.12.013.
9. Wang, H.; Wei, Q.; Gao, W. Sputter Deposition of Antibacterial Nano-Silver on PLA Nonwoven Medical Dressings. *Aatcc Review* **2009**, *9*, 34–36.
10. Abd Jelil, R. A review of low-temperature plasma treatment of textile materials. *Journal of Materials Science* **2015**, *50*, 5913–5943, doi:10.1007/s10853-015-9152-4.

11. Shahidi, S.; Moazzenchi, B.; Ghoranneviss, M. A review-application of physical vapor deposition (PVD) and related methods in the textile industry. *Eur. Phys. J. Appl. Phys.* **2015**, *71*. 614
615
12. Peralta-Videa, J.R.; Zhao, L.; Lopez-Moreno, M.L.; de la Rosa, G.; Hong, J.; Gardea-Torresdey, J.L. Nanomaterials and the environment: a review for the biennium 2008-2010. *J Hazard Mater* **2011**, *186*, 1-15, doi:10.1016/j.jhazmat.2010.11.020. 616
617
618
13. Kitahara, N.; Sato, T.; Isogawa, H.; Ohgoe, Y.; Masuko, S.; Shizuku, F.; Hirakuri, K. Antibacterial property of DLC film coated on textile material. *Diamond and Related Materials* **2010**, *19*, 690-694, doi:10.1016/j.diamond.2010.03.013. 619
620
621
14. Carvalho, I.; Curado, M.; Palacio, C.; Carvalho, S.; Cavaleiro, A. Ag release from sputtered Ag/a:C nanocomposite films after immersion in pure water and NaCl solution. *Thin Solid Films* **2019**, *671*, 85-94, doi:10.1016/j.tsf.2018.12.010. 622
623
624
15. Aldalbahi, A.; El-Naggar, M.E.; El-Newehy, M.H.; Rahaman, M.; Hatshan, M.R.; Khattab, T.A. Effects of Technical Textiles and Synthetic Nanofibers on Environmental Pollution. *Polymers (Basel)* **2021**, *13*, doi:10.3390/polym13010155. 625
626
627
16. Gorberg, B.L.; Ivanov, A.A.; Mamontov, O.V.; Stegnin, V.A.; Titov, V.A. Modification of textile materials by the deposition of nanocoatings by magnetron ion-plasma sputtering. *Russian Journal of General Chemistry* **2013**, *83*, 157-163, doi:10.1134/S1070363213010350. 628
629
630
17. Brozena, A.; Oldham, C.; Parsons, G. Atomic layer deposition on polymer fibers and fabrics for multifunctional and electronic textiles. *Journal of Vacuum Science & Technology a* **2016**, *34*, doi:10.1116/1.4938104. 631
632
18. Peran, J.; Razic, S. Application of atmospheric pressure plasma technology for textile surface modification. *Textile Research Journal* **2020**, *90*, 1174-1197, doi:10.1177/0040517519883954. 633
634
19. Azam Ali, M.; Shavandi, A. 6 - Medical textiles testing and quality assurance. In *Performance Testing of Textiles*, Wang, L., Ed.; Woodhead Publishing: 2016; pp. 129-153. 635
636
20. Girijappa, Y.; Rangappa, S.; Parameswaranpillai, J.; Siengchin, S. Natural Fibers as Sustainable and Renewable Resource for Development of Eco-Friendly Composites: A Comprehensive Review. *Frontiers in Materials* **2019**, *6*, doi:10.3389/fmats.2019.00226. 637
638
639
21. Nadi, A.; Boukhriss, A.; Bentis, A.; Jabrane, E.; Gmouh, S. Evolution in the surface modification of textiles: a review. *Textile Progress* **2018**, *50*, 67-108, doi:10.1080/00405167.2018.1533659. 640
641
22. Nurhan Onar Camlibel and Buket, A. Sol-Gel Applications in Textile Finishing Processes. In *Recent Applications in Sol-Gel Synthesis*, Usha, C., Ed.; IntechOpen: Rijeka, 2017. 642
643
23. Gowri, S.; Almeida, L.; Amorim, T.; Carneiro, N.; Souto, A.; Esteves, M. Polymer Nanocomposites for Multifunctional Finishing of Textiles - a Review. *Textile Research Journal* **2010**, *80*, 1290-1306, doi:10.1177/0040517509357652. 644
645
646
24. Huang, Z.; Ghasemi, H. Hydrophilic polymer-based anti-biofouling coatings: Preparation, mechanism, and durability. *Adv Colloid Interface Sci* **2020**, *284*, 102264, doi:10.1016/j.cis.2020.102264. 647
648
25. Poshina, D.; Otsuka, I. Electrospun Polysaccharidic Textiles for Biomedical Applications. *Textiles* **2021**, *1*, doi:10.3390/textiles1020007. 649
650
26. Song, K.; Wu, Q.; Qi, Y.; Kärki, T. 20 - Electrospun nanofibers with antimicrobial properties. In *Electrospun Nanofibers*, Afshari, M., Ed.; Woodhead Publishing: 2017; pp. 551-569. 651
652
27. Liu, L.; Xu, W.; Ding, Y.; Agarwal, S.; Greiner, A.; Duan, G. A review of smart electrospun fibers toward textiles. *Composites Communications* **2020**, *22*, 100506, doi:<https://doi.org/10.1016/j.coco.2020.100506>. 653
654

28. Haoyi Li and Weimin, Y. Electrospinning Technology in Non-Woven Fabric Manufacturing. In *Non-woven Fabrics*, Han-Yong, J., Ed.; IntechOpen: Rijeka, 2016. 655-656
29. Vigneshwaran, N. 8 - Modification of textile surfaces using nanoparticles. In *Surface Modification of Textiles*, Wei, Q., Ed.; Woodhead Publishing: 2009; pp. 164-184. 657-658
30. Zhou, C.-E.; Kan, C.-w.; Matinlinna, J.P.; Tsoi, J.K. Regenerable Antibacterial Cotton Fabric by Plasma Treatment with Dimethylhydantoin: Antibacterial Activity against *S. aureus*. *Coatings* **2017**, *7*, doi:10.3390/coatings7010011. 659-661
31. Susan, A.I.; Widodo, M.; Nur, M. Corona Glow Discharge Plasma Treatment for Hydrophobicity Improvement of Polyester and Cotton Fabrics. *IOP Conference Series: Materials Science and Engineering* **2017**, *214*, 012031, doi:10.1088/1757-899x/214/1/012031. 662-664
32. Irfan, M.; Polonskyi, O.; Hinz, A.; Mollea, C.; Bosco, F.; Strunskus, T.; Balagna, C.; Perero, S.; Faupel, F.; Ferraris, M. Antibacterial, highly hydrophobic and semi transparent Ag/plasma polymer nanocomposite coating on cotton fabric obtained by plasma based co-deposition. *Cellulose* **2019**, *26*, 8877-8894, doi:10.1007/s10570-019-02685-6. 665-668
33. Shahidi, S.; Moazzenchi, B.; Ghoranneviss, M. A review-application of physical vapor deposition (PVD) and related methods in the textile industry. *European Physical Journal-Applied Physics* **2015**, *71*, doi:10.1051/epjap/2015140439. 669-671
34. IKEDA, T.; SATOH, H. PHASE FORMATION AND CHARACTERISATION OF HARD COATINGS IN THE Ti-AL-N SYSTEM PREPARED BY THE CATHODIC ARC ION PLATING METHOD. *Thin Solid Films* **1991**, *195*, 99-110. 672-674
35. Hegemann, D.; Hossain, M.; Balazs, D.J. Nanostructured plasma coatings to obtain multifunctional textile surfaces. *Progress in Organic Coatings* **2007**, *58*, 237-240. 675-676
36. Wei, Q.; Xu, Y.; Wang, Y. 3 - Textile surface functionalisation by physical vapor deposition (PVD). In *Surface Modification of Textiles*, Wei, Q., Ed.; Woodhead Publishing: 2009; pp. 58-90. 677-678
37. Ehiasarian, A.; Pulgarin C Fau - Kiwi, J.; Kiwi, J. Inactivation of bacteria under visible light and in the dark by Cu films. Advantages of Cu-HIPIMS-sputtered films. 679-680
38. Chodun, R.; Wicher, B.; Skowrński, Ł.; Nowakowska-Langier, K.; Okrasa, S.; Grabowski, A.; Minikayev, R.; Zdunek, K. Multi-sided metallization of textile fibres by using magnetron system with grounded cathode. *Materials Science-Poland* **2017**, *35*, 639-646, doi:doi:10.1515/msp-2017-0078. 681-683
39. Chen, Y.-H.; Wu, G.-W.; He, J.-L. Antimicrobial brass coatings prepared on poly(ethylene terephthalate) textile by high power impulse magnetron sputtering. *Materials Science and Engineering: C* **2015**, *48*, 41-47, doi:<https://doi.org/10.1016/j.msec.2014.11.017>. 684-686
40. Saffari, M.-R.; Kamali Miab, R. Antibacterial property of PLA textiles coated by nano-TiO₂ through eco-friendly low-temperature plasma. *International Journal of Clothing Science and Technology* **2016**, *28*, 830-840, doi:10.1108/IJCST-12-2015-0139. 687-689
41. Depla, D.; Segers, S.; Leroy, W.; Van Hove, T.; Van Parys, M. Smart textiles: an explorative study of the use of magnetron sputter deposition. *Textile Research Journal* **2011**, *81*, 1808-1817, doi:10.1177/0040517511411966. 690-691
42. Strategic Machines. <http://strategicmachines.com/new-presentation/metallised-fabrics.html>. 692
43. Liu, Y.; Leng, J.; Wu, Q.; Zhang, S.; Teng, X. Investigation on the properties of nano copper matrix composite via vacuum arc melting method. *Materials Research Express* **2017**, *4*, 106512, doi:10.1088/2053-1591/aa9096. 693-694

44. Scholz, J.; Nocke, G.; Hollstein, F.; Weissbach, A. Investigations on fabrics coated with precious metals using the magnetron sputter technique with regard to their antimicrobial properties. *Surface & Coatings Technology* **2005**, *192*, 252-256, doi:10.1016/j.surfcoat.2004.05.036. 695-697
45. Rtimi, S.; Baghriche, O.; Sanjinés, R.; Pulgarin, C.; Bensimon, M.; Kiwi, J. TiON and TiON-Ag sputtered surfaces leading to bacterial inactivation under indoor actinic light. *Journal of Photochemistry and Photobiology A-chemistry* **2013**, *256*, 52-63. 698-700
46. Rtimi, S.; Baghriche, O.; Sanjines, R.; Pulgarin, C.; Ben-Simon, M.; Lavanchy, J.C.; Houas, A.; Kiwi, J. Photocatalysis/catalysis by innovative TiN and TiN-Ag surfaces inactivate bacteria under visible light. *Applied Catalysis B: Environmental* **2012**, *123-124*, 306-315, doi:<https://doi.org/10.1016/j.apcatb.2012.04.047>. 701-703
47. Xu, Y.; Wang, H.; Wei, Q.; Liu, H.; Deng, B. Structures and properties of the polyester nonwovens coated with titanium dioxide by reactive sputtering. *Journal of Coatings Technology and Research* **2010**, *7*, 637-642, doi:10.1007/s11998-010-9243-8. 704-706
48. ZGURA, I.; FRUNZA, S.; FRUNZA, L.; ENCULESCU, M.; FLORICA, C.; GANEA, C.P.; NEGRILA, C.C.; DIAMANDESCU, L. Titanium dioxide layer deposited at low temperature upon polyester fabrics. *Journal of Optoelectronics and Advanced Materials* **2015**, *17*, 1055-1063. 707-709
49. Rtimi, S.; Baghriche, O.; Pulgarin, C.; Lavanchy, J.-C.; Kiwi, J. Growth of TiO₂/Cu films by HiPIMS for accelerated bacterial loss of viability. *Surface and Coatings Technology* **2013**, *232*, 804-813, doi:<https://doi.org/10.1016/j.surfcoat.2013.06.102>. 710-712
50. Rtimi, S.; Giannakis, S.; Pulgarin, C. Self-Sterilizing Sputtered Films for Applications in Hospital Facilities. *Molecules (Basel, Switzerland)* **2017**, *22*, 1074, doi:10.3390/molecules22071074. 713-714
51. Rtimi, S.; Sanjines, R.; Bensimon, M.; Pulgarin, C.; Kiwi, J. Accelerated Escherichia coli inactivation in the dark on uniform copper flexible surfaces. 715-716
52. Subramanian, B.; Anu Priya, K.; Thanka Rajan, S.; Dhandapani, P.; Jayachandran, M. Antimicrobial activity of sputtered nanocrystalline CuO impregnated fabrics. *Materials Letters* **2014**, *128*, 1-4, doi:<https://doi.org/10.1016/j.matlet.2014.04.056>. 717-719
53. Septiani, N.L.W.; Kaneti, Y.V.; Yuliarto, B.; Nugraha; Dipojono, H.K.; Takei, T.; You, J.; Yamauchi, Y. Hybrid nanoarchitecturing of hierarchical zinc oxide wool-ball-like nanostructures with multi-walled carbon nanotubes for achieving sensitive and selective detection of sulfur dioxide. *Sensors and Actuators B: Chemical* **2018**, *261*, 241-251, doi:<https://doi.org/10.1016/j.snb.2018.01.088>. 720-723
54. Ahmed, M.A.M.; Mwankemwa, B.S.; Carleschi, E.; Doyle, B.P.; Meyer, W.E.; Nel, J.M. Effect of Sm doping ZnO nanorods on structural optical and electrical properties of Schottky diodes prepared by chemical bath deposition. *Materials Science in Semiconductor Processing* **2018**, *79*, 53-60, doi:<https://doi.org/10.1016/j.mssp.2018.02.003>. 724-727
55. Vihodceva, S.; Kukle, S.; Barloti, J.; Blüms, J. Metal Deposition on Textile Fabrics from Natural Fibres by Magnetron Sputtering. In Proceedings of the 6th International Textile Clothing and Design Conference "Magic World of Textiles" (ITC&DC): Book of Proceedings, Zagreb, 2012. 728-730
56. Shahidi, S. Plasma sputtering as a novel method for improving fastness and antibacterial properties of dyed cotton fabrics. *The Journal of The Textile Institute* **2015**, *106*, 162-172, doi:10.1080/00405000.2014.906104. 731-732
57. Shahidi, S.; Ghoranneviss, M.; Moazzenchi, B.; Rashidi, A.; Mirjalili, M. Investigation of Antibacterial Activity on Cotton Fabrics with Cold Plasma in the Presence of a Magnetic Field. *Plasma Processes and Polymers* **2007**, *4*, S1098-S1103, doi:<https://doi.org/10.1002/ppap.200732412>. 733-735

58. Morent, R.; De Geyter, N.; Verschuren, J.; De Clerck, K.; Kiekens, P.; Leys, C. Non-thermal plasma treatment of textiles. *Surface & Coatings Technology* **2008**, *202*, 3427-3449, doi:10.1016/j.surfcoat.2007.12.027. 736
737
59. Chen, Y.-H.; Hsu, C.-C.; He, J.-L. Antibacterial silver coating on poly(ethylene terephthalate) fabric by using high power impulse magnetron sputtering. *Surface and Coatings Technology* **2013**, *232*, 868-875, doi:<https://doi.org/10.1016/j.surfcoat.2013.06.115>. 738
739
740
60. Rtimi, S.; Pascu, M.; Sanjines, R.; Pulgarin, C.; Ben-Simon, M.; Houas, A.; Lavanchy, J.C.; Kiwi, J. ZrNO–Ag co-sputtered surfaces leading to E. coli inactivation under actinic light: Evidence for the oligodynamic effect. *Applied Catalysis B: Environmental* **2013**, *138-139*, 113-121, doi:<https://doi.org/10.1016/j.apcatb.2013.01.066>. 741
742
743
61. Li, D.; Cui, F.; Gu, H. Studies of diamond-like carbon films coated on PMMA by ion beam assisted deposition. *Applied Surface Science* **1999**, *137*, 30-37, doi:10.1016/S0169-4332(98)00485-1. 744
745
62. Sanchez-Lopez, J.; Donnet, C.; Fontaine, J.; Belin, M.; Grill, A.; Patel, V.; Jahnes, C. Diamond-like carbon prepared by high density plasma. *Diamond and Related Materials* **2000**, *9*, 638-642, doi:10.1016/S0925-9635(99)00362-3. 746
747
748
63. Lee, C.; Lee, K.; Eun, K.; Yoon, K.; Han, J. Structure and properties of Si incorporated tetrahedral amorphous carbon films prepared by hybrid filtered vacuum arc process. *Diamond and Related Materials* **2002**, *11*, 198-203. 749
750
64. Zou, Y.; Wang, W.; Song, G.; Du, H.; Gong, J.; Huang, R.; Wen, L. Influence of the gas atmosphere on the microstructure and mechanical properties of diamond-like carbon films by arc ion plating. *Materials Letters* **2004**, *58*, 3271-3275, doi:10.1016/j.matlet.2004.06.017. 751
752
753
65. Thorwarth, G.; Hammerl, C.; Kuhn, M.; Assmann, W.; Schey, B.; Stritzker, B. Investigation of DLC synthesized by plasma immersion ion implantation and deposition. *Surface & Coatings Technology* **2005**, *193*, 206-212, doi:10.1016/j.surfcoat.2004.07.061. 754
755
756
66. Sanchez, N.; Rincon, C.; Zambrano, G.; Galindo, H.; Prieto, P. Characterization of diamond-like carbon (DLC) thin films prepared by r.f. magnetron sputtering. *Thin Solid Films* **2000**, *373*, 247-250, doi:10.1016/S0040-6090(00)01090-7. 757
758
759
67. HE, X.; LI, W.; LI, H. BONDING STRUCTURE AND TRIBOLOGICAL PROPERTIES OF DLC FILMS SYNTHESISED BY DUAL-ION BEAM SPUTTERING. *Vacuum* **1994**, *45*, 977-980. 760
761
68. Shim, K.; Kim, S.; Bac, S.; Lee, S.; Jung, H.; Park, H. Fabrication and characterisation of diamond-like carbon thin films by pulsed laser deposition. *Applied Surface Science* **2000**, *154*, 482-484, doi:10.1016/S0169-4332(99)00401-8. 762
763
764
69. HOFSSASS, H.; BINDER, H.; KLUMPP, T.; RECKNAGEL, E. DOPING AND GROWTH OF DIAMOND-LIKE CARBON-FILMS BY ION-BEAM DEPOSITION. *Diamond and Related Materials* **1994**, *3*, 137-142, doi:10.1016/0925-9635(94)90045-0. 765
766
767
70. Myllymaa, K.; Levon, J.; Tiainen, V.; Myllymaa, S.; Soininen, A.; Korhonen, H.; Kaivosoja, E.; Lappalainen, R.; Konttinen, Y. Formation and retention of staphylococcal biofilms on DLC and its hybrids compared to metals used as biomaterials. *Colloids and Surfaces B-Biointerfaces* **2013**, *101*, 290-297, doi:10.1016/j.colsurfb.2012.07.012. 768
769
770
71. Liu, C.; Zhao, Q.; Liu, Y.; Wang, S.; Abel, E. Reduction of bacterial adhesion on modified DLC coatings. *Colloids and Surfaces B-Biointerfaces* **2008**, *61*, 182-187, doi:10.1016/j.colsurfb.2007.08.008. 771
772
72. Wang, J.; Huang, N.; Pan, C.; Kwok, S.; Yang, P.; Leng, Y.; Chen, J.; Sun, H.; Wan, G.; Liu, Z.; et al. Bacterial repellence from polyethylene terephthalate surface modified by acetylene plasma immersion ion implantation-deposition. *Surface & Coatings Technology* **2004**, *186*, 299-304, doi:10.1016/j.surfcoat.2004.02.046. 773
774
775

73. Kinnari, T.; Soininen, A.; Esteban, J.; Zamora, N.; Alakoski, E.; Kouri, V.; Lappalainen, R.; Konttinen, Y.; Gomez-Barrena, E.; Tiainen, V. Adhesion of staphylococcal and Caco-2 cells on diamond-like carbon polymer hybrid coating. *Journal of Biomedical Materials Research Part a* **2008**, *86A*, 760-768, doi:10.1002/jbm.a.31643. 776-778
74. Marciano, F.R.; Bonetti, L.F.; Santos, L.V.; Da-Silva, N.S.; Corat, E.J.; Trava-Airoldi, V.J. Antibacterial activity of DLC and Ag-DLC films produced by PECVD technique. *Diamond and Related Materials* **2009**, *18*, 1010-1014, doi:<https://doi.org/10.1016/j.diamond.2009.02.014>. 779-781
75. Zhou, H.; Xu, L.; Ogino, A.; Nagatsu, M. Investigation into the antibacterial property of carbon films. *Diamond and Related Materials* **2008**, *17*, 1416-1419, doi:<https://doi.org/10.1016/j.diamond.2008.01.047>. 782-783
76. Robertson, S.; Gibson, D.; MacKay, W.; Reid, S.; Williams, C.; Birney, R. Investigation of the antimicrobial properties of modified multilayer diamond-like carbon coatings on 316 stainless steel. *Surface & Coatings Technology* **2017**, *314*, 72-78, doi:10.1016/j.surfcoat.2016.11.035. 784-786
77. Gorzelanny, C.; Kmeth, R.; Obermeier, A.; Bauer, A.; Halter, N.; Kumpel, K.; Schneider, M.; Wixforth, A.; Gollwitzer, H.; Burgkart, R.; et al. Silver nanoparticle-enriched diamond-like carbon implant modification as a mammalian cell compatible surface with anti-microbial properties. *Scientific Reports* **2016**, *6*, doi:10.1038/srep22849. 787-790
78. Endrino, J.L.; Anders, A.; Albella, J.M.; Horton, J.A.; Horton, T.H.; Ayyalasomayajula, P.R.; Allen, M. Antibacterial efficacy of advanced silver-amorphous carbon coatings deposited using the pulsed dual cathodic arc technique. *Journal of Physics: Conference Series* **2010**, *252*, 012012, doi:10.1088/1742-6596/252/1/012012. 791-793
79. Almaguer-Flores, A.; Olivares-Navarrete, R.; Lechuga-Bernal, A.; Ximenez-Fyvie, L.; Rodil, S. Oral bacterial adhesion on amorphous carbon films. *Diamond and Related Materials* **2009**, *18*, 1179-1185, doi:10.1016/j.diamond.2009.03.003. 794-796
80. Jelinek, M.; Voss, A.; Kocourek, T.; Mozafari, M.; Vymetalova, V.; Zezulova, M.; Pisarik, P.; Kotzianova, A.; Popov, C.; Miksovsky, J. Comparison of the surface properties of DLC and ultrananocrystalline diamond films with respect to their bio-applications. *Physica Status Solidi a-Applications and Materials Science* **2013**, *210*, 2106-2110, doi:10.1002/pssa.201228713. 797-800
81. Maas, M. Carbon Nanomaterials as Antibacterial Colloids. *Materials* **2016**, *9*, doi:10.3390/ma9080617. 801
82. Bendavid, A.; Martin, P.; Randeniya, L.; Amin, M. The properties of fluorine containing diamond-like carbon films prepared by plasma-enhanced chemical vapour deposition. *Diamond and Related Materials* **2009**, *18*, 66-71, doi:10.1016/j.diamond.2008.09.021. 802-804
83. Nobili, L.; Guglielmini, A. Thermal stability and mechanical properties of fluorinated diamond-like carbon coatings. *Surface & Coatings Technology* **2013**, *219*, 144-150, doi:10.1016/j.surfcoat.2013.01.018. 805-806
84. Su, X.; Zhao, Q.; Wang, S.; Bendavid, A. Modification of diamond-like carbon coatings with fluorine to reduce biofouling adhesion. *Surface & Coatings Technology* **2010**, *204*, 2454-2458, doi:10.1016/j.surfcoat.2010.01.022. 807-808
85. Chan, Y.; Huang, C.; Ou, K.; Peng, P. Mechanical properties and antibacterial activity of copper doped diamond-like carbon films. *Surface & Coatings Technology* **2011**, *206*, 1037-1040, doi:10.1016/j.surfcoat.2011.07.034. 809-810
86. Ji, L.; Li, H.; Zhao, F.; Chen, J.; Zhou, H. Microstructure and mechanical properties of Mo/DLC nanocomposite films. *Diamond and Related Materials* **2008**, *17*, 1949-1954, doi:10.1016/j.diamond.2008.04.018. 811-812
87. Bociaga, D.; Jakubowski, W.; Komorowski, P.; Sobczyk-Guzenda, A.; Jedrzejczak, A.; Batory, D.; Olejnik, A. Surface characterization and biological evaluation of silver-incorporated DLC coatings fabricated by hybrid RF PACVD/MS method. *Materials Science & Engineering C-Materials For Biological Applications* **2016**, *63*, 462-474, doi:10.1016/j.msec.2016.03.013. 813-816

-
88. Liu, Y.; Guo, P.; He, X.; Li, L.; Wang, A.; Li, H. Developing transparent copper-doped diamond-like carbon films for marine antifouling applications. *Diamond and Related Materials* **2016**, *69*, 144-151, doi:10.1016/j.diamond.2016.08.012. 817
818
89. Love, C.; Cook, R.; Harvey, T.; Dearnley, P.; Wood, R. Diamond like carbon coatings for potential application in biological implants-a review. *Tribology International* **2013**, *63*, 141-150, doi:10.1016/j.triboint.2012.09.006. 820
821
90. Lan, W.; Ou, S.; Lin, M.; Ou, K.; Tsai, M. Development of silver-containing diamond-like carbon for biomedical applications. Part I: Microstructure characteristics, mechanical properties and antibacterial mechanisms. *Ceramics International* **2013**, *39*, 4099-4104, doi:10.1016/j.ceramint.2012.10.264. 822
824
91. Cloutier, M.; Turgeon, S.; Busby, Y.; Tatoulian, M.; Pireaux, J.; Mantovani, D. Controlled Distribution and Clustering of Silver in Ag-DLC Nanocomposite Coatings Using a Hybrid Plasma Approach. *Acs Applied Materials & Interfaces* **2016**, *8*, 21020-21027, doi:10.1021/acsami.6b06614. 825
827
92. Crisan, C.; Mocan, T.; Manolea, M.; Lasca, L.; Tabaran, F.; Mocan, L. Review on Silver Nanoparticles as a Novel Class of Antibacterial Solutions. *Applied Sciences-Basel* **2021**, *11*, doi:10.3390/app11031120. 828
829
93. Sohbatzadeh, F.; Farhadi, M.; Shakerinasab, E. A new DBD apparatus for superhydrophobic coating deposition on cotton fabric. *Surface & Coatings Technology* **2019**, *374*, 944-956, doi:10.1016/j.surfcoat.2019.06.086. 830
831
94. Schneider, G. Antimicrobial silver nanoparticles – regulatory situation in the European Union. *Materials Today: Proceedings* **2017**, *4*, S200-S207, doi:<https://doi.org/10.1016/j.matpr.2017.09.187>. 832
833
834